Development of an Optimization Model for Design and Planning of a Decentralized District Energy System

Mohammad Sameti

A Thesis
in the Department
of
Building, Civil, and Environmental Engineering

Presented in Partial Fulfillment of the Requirements
For the Degree of
Doctor of Philosophy (Building Engineering) at
Concordia University
Montreal, Quebec, Canada

July 2018

CONCORDIA UNIVERSITY

SCHOOL OF GRADUATE STUDIES

This is to certify that the thesis prepared

By: Mohammad Sameti

Entitled: Development of an Optimization Model for Design and Planning of a Decentralized District Energy System

and submitted in partial fulfillment of the requirements for the degree of

Doctor Of Philosophy (Building Engineering)

complies with the regulations of the University and meets the accepted standards with respect to originality and quality.

Signed by the final examining committee:

_____ Chair
Dr. Nizar Bouguila

_____ External Examiner
Dr. Marco Perino

_____ External to Program
Dr. Shahin Hashtrudi Zad

_____ Examiner
Dr. Fuzhan Nasiri

_____ Examiner
Dr. Radu Zmeureanu

_____ Thesis Supervisor
Dr. Fariborz Haghighat

Approved by

Dr. Fariborz Haghighat, Graduate Program Director

Friday, September 21, 2018

_____

Dr. Amir Asif, Dean
Faculty of Engineering and Computer Science

ABSTRACT

Development of an Optimization Model for Design and Planning of a Decentralized District Energy System

Mohammad Sameti, Ph.D.

Concordia University, 2018

This dissertation reports the development of a optimization model to help designing a tri-generation system for a given newly-built district with its consumers to satisfy the heating, cooling, and hot water demands featuring 4th generation district energy characteristics. The aim is to find the best way to select the equipment among various candidates (capacities), the pipeline network among the buildings, and their electrical grid connections. The objective function includes the annualized overall capital and operation costs for the district along with the benefits of selling electricity to the grid. The distributed energy supply consists of heating, cooling, and power networks, different CHP technologies, solar array, chillers, auxiliary boilers, and thermal and electrical storage. The performance of the model was evaluated for designing two different case under various scenarios: (i) a combined heat and power design, and (ii) a combined cooling and power design both carried out for the new part of Suurstoffi district situated in Risch Rotkreuz, Switzerland with seven residential and office complexes. For the combined heat and power design, the scenarios are defined based on the existence or non-existence of the distribution network (both heat and electricity) and the effectiveness of the storage systems. Allowing heat exchange among the buildings leads to 25% reduction in the total annualized cost and 5% reduction in emission compared to the conventional districts. Simultaneous heat and electricity exchange results in a higher reduction equal to 40% of the base scenario. Adding storage systems opens up an opportunity to lower both costs and emission even more and turns the district to a net-zero energy and energy plus districts. For the combined cooling and power design, the effectiveness of the network is analyzed together with the potential of feeding absorption chillers using the heat from the solar and non-solar energy sources. More than 67% of CO_2 emission reduction is achieved through the hybrid heat and solar-driven arrangement.

ACKNOWLEDGMENTS

The doctoral journey is often described as an “independent research”, yet I would have never been able to reach the finishing line without the help and support of the most wonderful network of supervision committee, friends and family, to whom I am indebted with deepest gratitude. It is a great honor for me to have this opportunity to extend my appreciation and to acknowledge the contribution of the people who have helped me during this doctoral research.

First and foremost, I would like to express my deepest gratitude to my supervisor Prof. Fariborz Haghighat who has been very illuminating and supportive to me and provided excellent guidance and encouragement throughout the entire duration of my research. Without his continuous advice, constructive comments, and kind willingness to share his knowledge with me, I would not have reached where I am today with this work in its present form.

I am deeply indebted to my parents, my brother, Mahdi, my sister, Marsa, and her husband, Mohammad, for their patience, continuous support and encouragement. My deepest gratitude goes to my mother and father for their inspiration, encouragement, endless sacrifices and unconditional support. Without their love and understanding, I would not have been able to reach to where I am now.

I also would like to express my gratitude to Miss. Farinaz Haghighat for her valuable comments and suggestions.

Last but not least, I would also like to express my thanks to my friends and colleagues in energy and environment group for their unfailing support and expert advices.

TABLE OF CONTENTS

LIST OF FIGURES

LIST OF TABLES

SPECIAL SYMBOLS AND ABBREVIATIONS

Latin symbols

A	Surface area of the pipe, surface area of PV (m^2)	I	Income (US $), Carbon intensity (kg/kWh)
AF	Annuity factor	SOC	State of charge
C	Cost (€)	N	Lifetime (years)
CO_2	CO2 emission ($kg/year$)	p_{loss}	Pressure losses for a 1 meter long pipe (Pa)
d	Distance (m)	R	Consumption rate (W)
E	Power flow (kW)	r	Interest rate of a device *i*
p	Price of energy carrier	S	Solar irradiation (kW/m^2)
W	Binary variable for selling/purchasing power	T	Temperature (℃)
G	Nominal capacity (kW)	$X_{i,j}$	Binary variable to represent connection between the nodes
R	Binary variable for thermal storage	$Y_{i,j}$	Binary variable to represent the existing connections between the nodes
O	Binary variable for chiller	X	Binary variable for CHP
Q	Heat flow (kW)	Y	Binary variable for pipeline connection
CT	Carbon tax (€/kWh)	Z	Binary variable for (compression) chiller
B	Binary variable for battery bank	U	Binary variable for boiler
T	Binary variable for wire connection and absorption chiller	V	Visiting order

Greek symbols

κ	A constant	δ	Number of hours in each period
η	Efficiency	ζ	Heat to power ratio
σ	Percentage of heat loss	θ	Slope
α	Interest rate	Δ	Duration (hour)

Subscripts and superscripts

ac	Absorption chiller	TS	Thermal storage
ct	Carbon tax	tot	Total
cc	Compression chiller	inv	Investment
dem	Energy flow to cover building's demand	op	Operation
out	Discharged energy	max	Maximum capacity
pipe	pipleline	BB	Batter bank
power	Electricity demand	m	Number of chillers
q	Type of PV	Up	Upper bound
r	Type of solar thermal collector	loss	Energy loss in network
hs	Heat storage	max	Maximum capacity
l	Type of compression chiller	min	Minimum capacity
m	Type of absorption chiller	t	Period number
cold	Cooling energy	tech	Technology used
sto	Stored energy	ub	Upper bound
car	Carbon emission	n	Number of years, number of equipment
elec	Electricity	k	Type of CHP unit
pur	Purchased	sol	Solar
sel	Soled	chil	Chiller
i, j	Building number	s	Season
PV	Photovoltaic array	used	Self-used energy
B	Boiler	grid	Utility grid
CHP	Cogeneration unit	Gas	Fuel (natural gas)
heat	Heating demand	Lo	Lower bound

Abbreviations

HER	Heat to electricity ratio	DHS	District heating system
CHP	Combined heat and power	DCS	District cooling system
COP	Coefficient of performance	CRF	Capital recovery factor
TES	Thermal energy storage	EER	Energy efficiency ratio

Chapter 1

Motivation

1.1 introduction

In the past, buildings were typically designed singly because the energy had low price. Designers did address the extraction of energy sources situated far away from the consumer site and the environmental impacts of their depletion, utilization and transportation as major issues. Engineers did not put considerable effort into finding opportunities to save energy at both generation and consumption sides. Instead, engineers dealt with the issue of guaranteeing various services and to provide acceptable indoor environment both in term of thermal comfort and indoor air quality. Recent advances of efficient thermal prime movers along with their interactions with renewable energy sources for distributed generation are changing the approach of power and heat generation from conventional large centralized plants to local generation units scattered over the neighborhood. The design and planning of the future sustainable energy systems comprising 100% of renewable resources is studied in a number of recent papers and technical notes [1, 2]. These systems are basically designed as a combination of intermittent renewable energy resources such as solar, wind, and geothermal along with the fuel resources such as waste and biomass on which there are some environmental issues about their utilizations.

When there is a group of buildings, up to a whole city, with its heating, cooling, hot water, and electricity fulfilled by a piece of integrated energy generation equipment, there is a need for a distribution network. The existing utility grid may be utilized for supplying electricity, however, for heating, cooling, and hot water, a distribution pipeline network should be designed and implemented. In other words, the resulting system, called district energy system, is defined as a system made up of several integrated poly-generation plants (units), along with the required

distribution network and sub-networks, providing a number of buildings with their energy demands i.e. heating, cooling, hot water, and power as shown in Figure 1.1 [3].

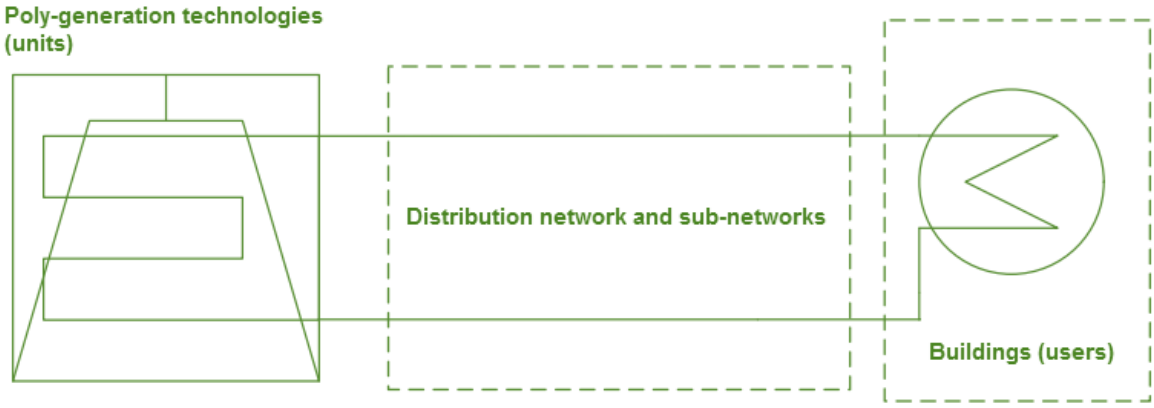

Figure 1.1: A typical schematics of a district energy system *[3]*

A district energy system may incorporate one or several micro-grids, which can operate autonomously or interact with the electricity grid. It comprises of three main constituents: production, storage and demand. The micro-grid supplies the buildings in a reliable and sustainable way and takes advantage of the environmental resources available in the area nearby to improve the overall efficiency of the system. Control and balance between generation sides and district demand is one of the main goals about the micro-grid. The production generally includes technologies such as solar thermal or electricity, wind turbines, fuel cells, gas engines, and micro turbines. These equipment can operate smoothly together in a way that provide the district with the required electrical and thermal energy demand. Various types of combinations of the technologies can be implemented to cover the energy demand for a group of industrial, residential and commercial buildings.

1.2 Why district energy systems?

The optimal design of a building is generally carried out by keeping the boundaries of the system under analysis within the single building. However, based on the boundaries considered, there may be major changes in level of comfort, efficiency and selection of the best system to supply the energy requirements. As a matter of fact, a building is hardly ever isolated from other buildings; instead, it is generally surrounded by other similar or different constructions with which it can interact. By extending the boundary of the analysis to the level of neighborhood or district, there

can be a chance to increase the level of sustainability and efficiency. Basically, merit of district energy systems can be expressed in three different categories:

Thermodynamic aspect: Reasonably low-temperature sources of less than 200℃ is required not only in residential and commercial buildings for the purpose of space heating but also various industrial applications calls for this range of temperature. Currently, a considerable portion of this heating demand is covered by combustion of oil, coal, natural gas or by electricity. However, combustion of those fossil fuels brings in temperatures far above those temperatures really required for residential heating or different process steam utilization [4]. From the thermodynamics point of view, the differences in temperature among combustion products and heat requirement provide the opportunity to carry out mechanical work or generate electricity. However, in the above-mentioned case, the low-temperature supply does not give such an opportunity. Moreover, utilization of electricity to generate low-temperature heat represents an inconsistency between high-quality and low-quality forms of energy supply and demand. A thermodynamically preferable idea is to take advantage of the temperature difference to generate electricity and utilize the waste heat from the condenser or turbine to cover low-temperature heat. As a result, using fuel through this process is improved drastically [5]. The overall thermal efficiency is defined as the ratio of the fuel converted to power together with the ratio of fuel converted to useful heat. Generally, cogeneration systems provide an overall efficiency in the range 65% to 90% as illustrated in Figure 1.2 [5].

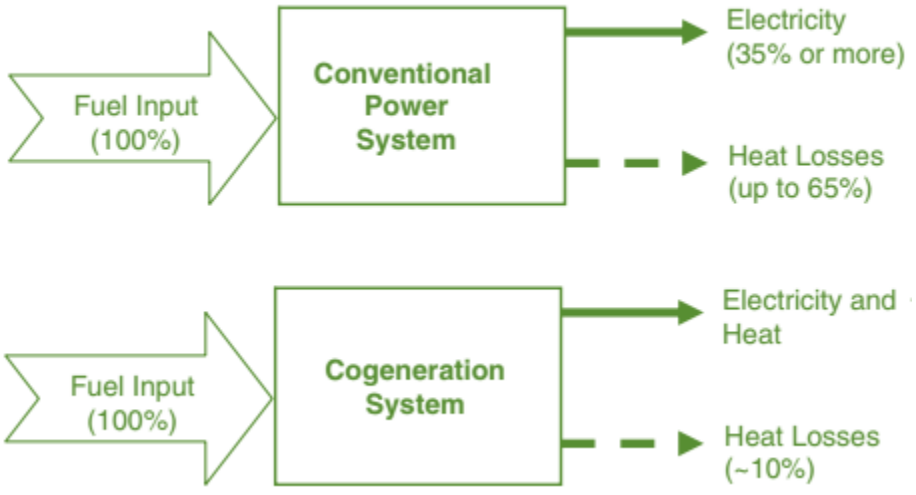

Figure 1.2: Primary thermodynamic advantage of district energy systems *[5]*

Economic aspect: The main economical merit of implementing a district energy system is its lower heating costs in a case of higher international fuel tariff or in a case of higher taxes or fees due to the consideration of environmental impacts as damage costs [6]. The costs associated with heat distribution are lower in dense areas with concentrated heat demands compared to suburban and rural areas with scattered heat demands in which the competitiveness decreases. The benefit of thermodynamically improved use of fuel and hence decreased fuel and operating costs happens at the expense of extra investment costs for supply and distribution infrastructure. In other words, the economic viability of district energy systems is usually a trade-off among higher initial investment but lower cost for fuel and operation versus lower upfront costs and higher cost for fuel in conventional energy systems. The economic benefits and limitations play a key role in the choice of implementing a decentralized or centralized district energy system. From an economic point of view, society can enjoy several advantages of decentralized poly-generation energy systems. Consumers may benefit the option of best cost effective configuration that matches their site perfectly [5]. In remote or rural areas an autonomous micro grid could be a more cost efficient alternative instead of extending the traditional main grid. The implementation of a poly-generation system in developing countries cannot only increase the average standard of living but can also result in new business opportunities for the community [7]. It is reported that 1.2 billion people around the world did not get access to electricity in the year 2012 [8]. To provide a number of those houses without access to the traditional electricity grid, various micro-grid plans has been carried out at these local areas. It also leads to generate income among many deprived areas.

Environmental aspect: When large combustion power plants are substituted for several smaller boilers inside or outside the buildings, the quality of air will drastically increase. Moreover, the mortality risk from very low and high ambient temperatures, which is common among all kinds of district heating and cooling systems [9]. Recycling of heat according to the notion of co-generation results in no or very small peripheral emission of CO_2. Therefore, substantial lower emissions are generated when conventional fossil primary energy system replaces recycling heat supply, which prevents waste of heat [10]. Beside heat recycling, utilization of green energy resources, such as solar and wind, in district energy system results in reduction of environmental damage and achievement of sustainable goals.

1.3 Current status

The total number of district energy systems all over the world is about 80 000 where 6000 systems operate in Europe [11]. Annual global amount of heat injected into district heating systems are illustrated by several supply categories in Figure 1.3 [12]. A reduction in heat deliveries can be seen in the middle of 1990s because many industrial consumers in Russia were disconnected from the network due to the changes in economic policy. The annual heat supply starts to increase from 2000 with a mean growth rate around 1%, due to the China's expansion plan for district heating system [12, 10]. However, European Union shows a nearly unchanging annual heat delivery since 1990. Removing some consumers and hence reduction in heat supply due to the former economic policy in Eastern Europe were balanced and compensated by new consumers in other parts of the world. It is concluded that the heat supply through district heating systems has not changed significantly and it has not shown the same growth rate for the entire expansion of energy systems around the world [12, 6]. Regarding different ways of heat deliveries, the European Union recycles more heat (72%) and extract more renewable heat (27%) in comparison with the global proportions in which the proportions of recycled heat and renewable heat are around 56% and 9%, respectively. The explanation is that the proportion of CHP units in China and Russia (almost 50%) affects the low global volume of recycled heat [10]. The above numbers for recycled heat shows that the heat supply is primarily provided in large boilers by direct utilization of fossil fuels. In other words, the basic idea of implementation of district heating is not fully addressed in those large countries [12, 6]. Thermal energy storage is sometimes implemented to smooth daily variations in heat demand. The seasonal thermal storage virtually never had the chance to play role in district energy systems; however, new solar district energy systems in small towns and villages in Denmark recently implemented relatively high-capacity thermal storages in combination with their systems [13].

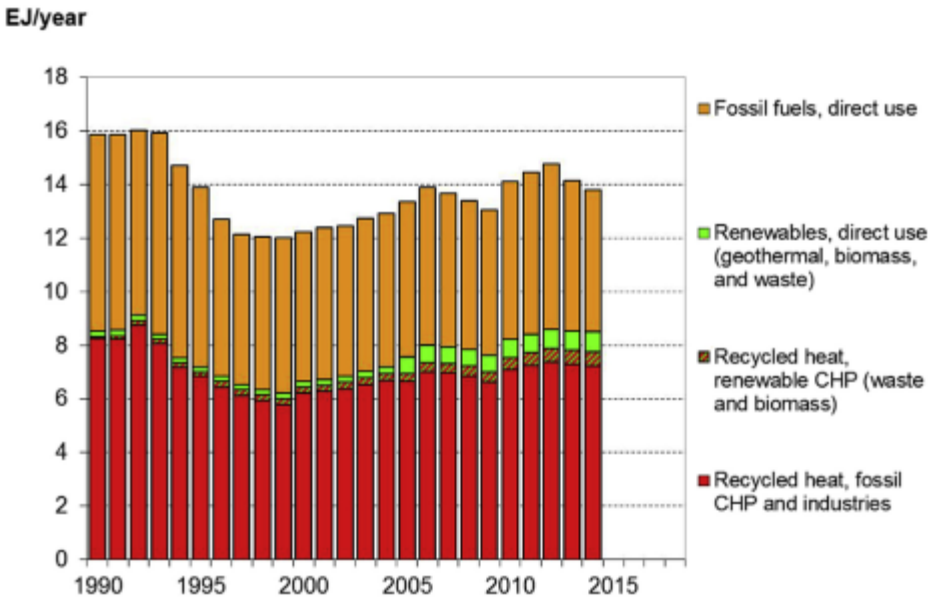

Figure 1.3: Global heat delivery into all district heating systems based on supply approach *[12, 10]*

The types of energy resource utilized in district heating are illustrated in Figure 1.4 with no description of heat delivery approach as discussed earlier in Figure 1.3. It is still obvious that the percentage of heat delivery through fossil fuels still remains very high. The proportions for the world and European Union are around 90% and 70%, respectively, because fossil fuels continue to be the primary group of energy supply for both boilers and CHP units. For example, Natural gas and coal are the primary fuels in Russia and in China, respectively. To achieve a future reduction in CO_2 emissions from boilers and CHP plants, current plants should substitute with modern heat resources independent from fossil fuels. An example of such new sources is the recovered heat by waste incineration, called waste-to-energy, which has been implemented in several district systems around the world [14]. In 2014, waste-to-energy application provided 400 PJ in the world where European Union contributed 208 PJ heat [12]. Industrial processes give a great opportunity for heat recycling when they produce excess heat. The idea requires a systematic heat cascading procedure to be integrated in a district and has been successfully implemented in some countries such as Germany, Sweden, and Russia [15].

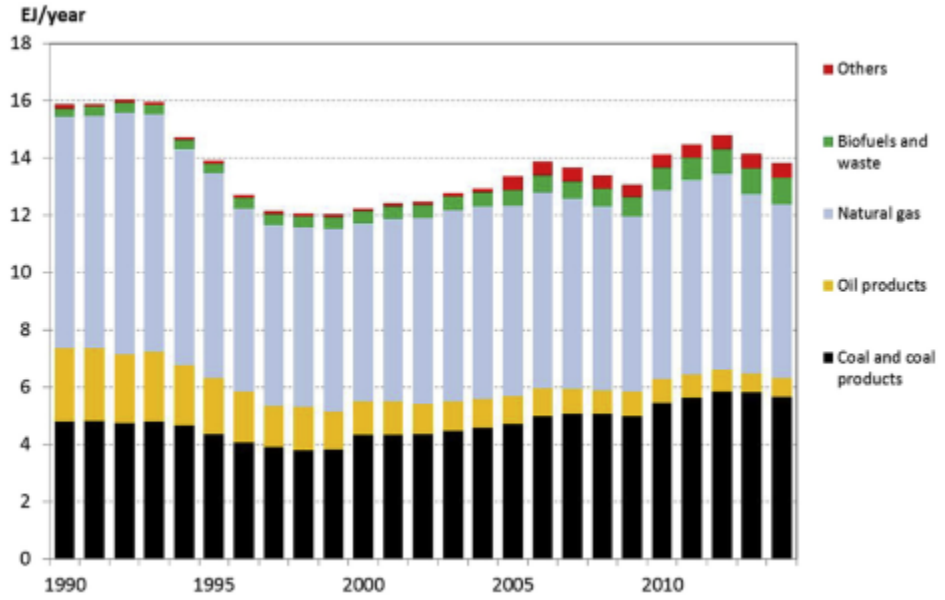

Figure 1.4: Global heat delivery into all district heating systems based on fuel type *[12, 10]*

The estimated specific CO_2 emissions per year caused by operation of district heating systems are expressed in Figure 1.5 separately for the world and European Union [12]. In the analysis, it is assumed that each 1 MJ heat from natural gas, fuel oil, and coal release 56, 76, and 95 grams of CO_2, respectively [16]. Analysis of Figure 1.5 leads to two main conclusions:

(1) One of the findings is that since 1990, the specific CO_2 emissions in the world stay nearly fixed on a level of 55 grams per each 1 MJ heat supplied. The total annual CO_2 emission in 2014 was estimated to be 604 million tons, which is almost 15% lower than the emissions released by combustion of only natural gas as the heat source. However, this large volume of emissions is a result of the low share of CHP units of almost 50% in both China and Russia [10]. In the few past years, China expanded several district heating with coal as a fuel, which counteracted the lower emission strategies in other countries. Russia also did not adopt any approach to increase the share of CHP units in it future heat supply plan [17].

(2) Currently, European Union releases 40% CO_2 emission less than the average emission in the world. In 2014, the average specific CO_2 emission accounted for 31 grams per 1 MJ of supplied heat resulting in 59 million tons CO_2 as total emission. The European Union accomplished to decrease its specific emissions by 35% during 24 years (from 1990 to 2014). The explanation for

this achievement is increasing the share of CHP units and renewable sources in the heat delivery plan. This brief analysis shows how the European Union fulfil the goal for expansion of district heating systems to higher level compared to other parts of the world.

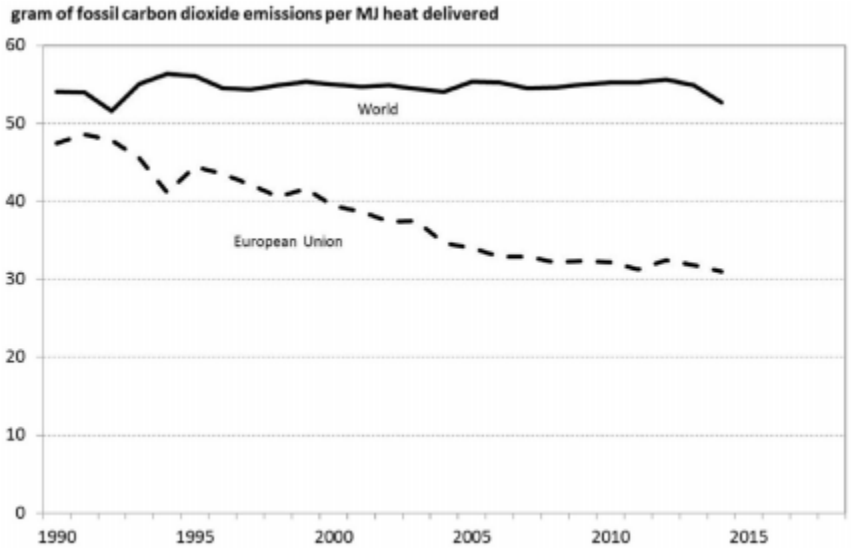

Figure 1.5: Trend for global specific CO_2 emissions *[12, 10]*

In Figure 1.6, the combinations of the specific CO_2 emissions and the total share of recycled heat and non-fossil sources are illustrated for the world and European Union together with 47 countries with considerable annual heat supplies with more than 1 PJ per annum [12]. The high level of specific CO_2 emission in China arose from utilization of coal as the primary fuel as well as the low share of CHP units in the heat supply plan which is analyzed by Yu et al. in a study focusing on the current and future status of CO_2 emissions in the urban area of Beijing [18]. Iceland takes the greatest position in European Union with no CO_2 emission since geothermal energy is their dominating heat supply. Both Norway and Sweden are very close to the Iceland.

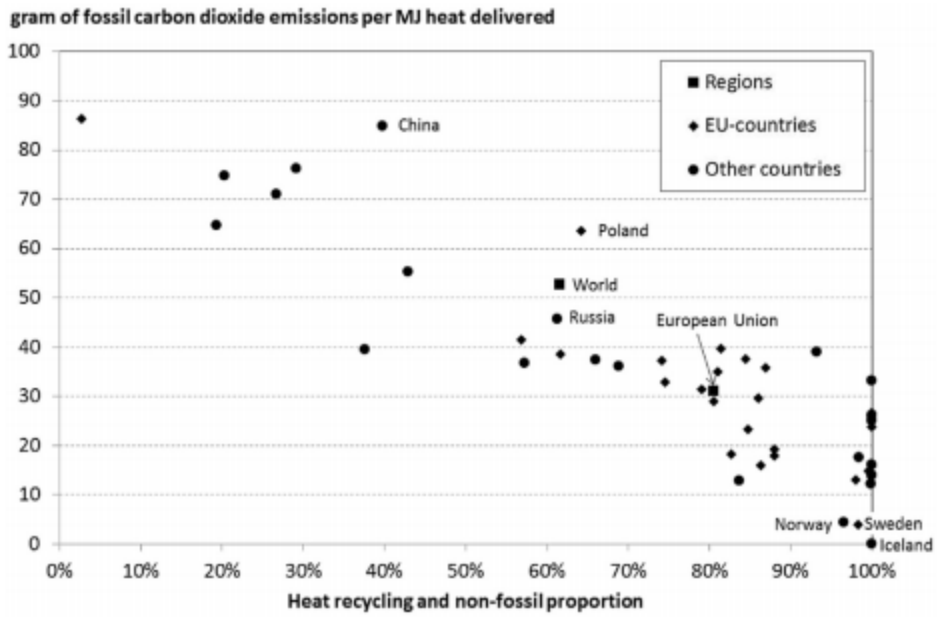

Figure 1.6 Global specific CO_2 emissions for several countries *[12, 10]*

1.4 Design consideration

In the planning step to design a sustainable district, a key factor to consider is associated with the sustainable way of energy supply. Buildings in the district require energy to maintain a favorable indoor environment condition through space heating, cooling, and ventilation, and hot water for domestic purposes, or provision of facilities such as electric lighting. It is important to mention that to achieve a successful design of new district energy systems, especially when power requirement is also included, the following considerations need to be taken into account. The size of the technologies has great importance since the district energy system is a combination of different technologies and units where the technologies should operate together to satisfy the demand. To achieve that goal in the most efficient way, the energy requirements of the consumers need to be consistent with the design size of the combination of the technologies and plants. Assurance of the best scheduling ad co-operation of the supply side of the district energy system should be provided to attain best operation with respect to the desired objective(s).

1.5 Objective and contribution

The centralized or decentralized energy source and the energy distribution network(s) comprises the two major intensive components of the district energy systems. Therefore, it is of upmost importance to identify the role and structure of these two elements in the design especially when future district energy systems are investigated. The goal of this research is to find the best combination of technologies or related capacities to satisfy the energy requirements in a sustainable (lower emission) and economically feasible way while the energy demands of the buildings making up a district. This gives the decision makers the ability to select the mix of technologies or their sizes to further analyze the design stage.

Current study shows novelty in several aspects: first, it is remarkable to mention that very few papers deal with the issue of the design of the heating, cooling, and power distribution among the consumers i.e. the way that buildings are connected to each other in a district is not fully addressed. In other words, the layout of the network and the heating, cooling, and power units are usually predefined in the literature for the operation optimization. The configuration of the network plays an important role in designing future districts because of two main reasons: (1) high investment in pipelines, especially in cold water pipelines, and (2) indirect effect on the operation and costs. This part of the model also includes the selection of the technologies. In other words, district energy systems can show to be inefficient when the required energy density is too low. However, no earlier work could be found that compute the optimal energy system for a district by comparing district energy systems versus individual energy systems. Second, simultaneous optimization of design and operation of a district has not been well studied. It means that literature focuses on only the network or the operation of the equipment in a district without noticing that these two are in fact interconnected and affects each other. Finally, the network analysis in this study considers all the terms related to costs. For example, pumping cost and costs corresponds to the network design are also taken into account.

It is important to mention that most of the earlier studies concentrate on matching supply and demands without considering any storage medium in their design or model. Moreover, energy storage in decentralized district energy systems have not been studied well especially when the design and operation of the storage system are accompanied by sizing, locating, and load allocation of other technologies implemented on the site. Current research addresses the aforementioned issues by presenting a comprehensive economic and environmental multi-objective optimization model for the investment planning of heat and power district energy systems emphasizing on thermal and electrical storage. The set of optimal solutions opens up an

opportunity to analyze the optimal design of a net-zero energy district and a stand-alone district and investigate the effects of storage and energy exchange on cost and CO_2 emissions. Definition and analysis of net-zero energy district are totally new fields in the area of future sustainable districts where its simulation and optimization is carried out for the first time in the current study.

Moreover small number of the earlier research dealt with the issue of the optimal combination of heating and cooling sides to achieve the best performance of the overall system in terms of cost, emission, or efficiency. In other words, by considering several heating and power sources to supply the chiller units, their integration must take into account their characteristics, operating costs and technical constraints. As a consequence, even with a limited number of plants, the best solution to the location, type and size of the hybrid technologies as well as the optimal control strategy in which the district plants operate to incur the lowest cost or exploit the highest available share of renewable sources, or other desirable goals. The current work concentrate on finding a solution to the following issues by proposing a mathematical approach: (1) optimal integration of heating technologies into district cooling, (2) optimal layout of the cooling grid, and (3) optimal control of the chilled water flow and storage media.

1.6 Organization of the current thesis

This thesis is organized into six chapters. Chapter 2 presents different types of optimization problems, constraints and techniques as well as the optimization tools used in district energy systems, and provides a comprehensive literature review. Objective functions at the district level are typically: carbon emission, production, revenue, operation costs, investment, fuel costs, and renewables exploitation. Contradiction of the objective functions is presented as a multi-objective problem. Then the effects of the distribution networks (both thermal and electrical) on overall cost are studied in Chapter 3 on a real case study. In other words, chapter 3 presents a mathematical programming procedure to model the optimal design and planning of a new district focusing on the energy exchange among the buildings. The aim of the computational model is to find the best way to select the equipment among various candidates (capacities), the pipeline network among the buildings, and their electrical connections. Chapter 4 presents the findings for comparative analysis among different scenarios with and without thermal and/or electrical storage to study the effects of load shifting on the total cost and emission of a new design. Both thermal and battery storage are considered in decentralized implementations and a set of optimal solutions are

illustrated as a Pareto front. Two important solutions showing net-zero energy districts are analyzed as well as a stand-alone district.

In chapter 5, a mathematical optimization model is tailor-designed for design of a new district cooling energy system fed by the combination of heating supply equipment, which takes into account the scheduling at the same time. An optimization methodology is proposed and tested on a real district cooling system with seven buildings.

Chapter 6 concludes this thesis with a summary of the key findings reported in all preceding chapters, and is followed by some recommendations for further research for better optimization models to include more details and results in more efficient design.

1.7 Type of the current thesis

This dissertation is a manuscript-based thesis in which the contents of the chapters 2 to 5 are part of the published journal papers in high-quality journals in the area of energy engineering as:

- Chapter 2:
  Sameti, Mohammad, and Fariborz Haghighat. "Optimization approaches in district heating and cooling thermal network." *Energy and Buildings* 140 (2017): 121-130.
- Chapter 3:
  Sameti, Mohammad, and Fariborz Haghighat. "Optimization of 4th generation distributed district heating system: Design and planning of combined heat and power." *Renewable Energy*130 (2019): 371-387.
- Chapter 4:
  Sameti, Mohammad, and Fariborz Haghighat. "Integration of distributed energy storage into net-zero energy district systems: Optimum design and operation." *Energy* 153 (2018): 575-591.
- Chapter 5:
  Sameti, Mohammad, and Fariborz Haghighat. “Hybrid solar and heat-driven district cooling system: Optimal integration and control strategy.” Solar *Energy* Under Review.

Chapter 2

Optimization approaches in district heating and cooling thermal network

2.1 Introduction

Modelling, simulation and optimization of an isolated building separated from the district in which they operate is no longer of interest as a viewpoint of improved efficiency, economic benefits and exploitation of renewable energy resources. Instead, district energy systems have the capacity to obtain several benefits, regarding the practical, environmental and safety by taking advantage of large poly-generation energy conversion technologies. The use of optimization techniques to design such high-efficient systems is strongly motivated by minimizing of the cost for the required infrastructures, minimizing emission, and maximizing the generation or efficiency but is particularly challenging because of the technical characteristics and the size of the real world applications. In this chapter, different types of optimization problems, constraints and techniques as well as the optimization tools used in district energy systems are discussed.

2.2 Optimization in district energy systems

A district energy system is able to simultaneously satisfy the demands of local buildings by providing on-site electricity, heating, and cooling [19]. The adoption of district energy systems exhibits several benefits. It allows for a reduced transmission losses through on-site generation, increased conversion efficiency, utilization of waste heat, reduction in constructing large generation plants, mitigation of emission problem and associated economic profits, and exploitation of renewables [20] [3] [21]. These systems may split into two categories:

decentralized and centralized [22]. In the former, which is most suitable for large-scale areas, energy conversion technologies are integrated in almost every building, and then are distributed among various buildings in an area. In the latter, which is better for relatively small, energy conversion technology is adopted outside the buildings and then the energy flows towards the buildings via a distribution network [23]. The rational design and planning of district energy systems have a pivotal role to achieve maximum energy saving/efficiency and maximum economic benefits of implementation of such systems [24]. However, as Figure 2.1 shows, achieving these goals is a complex task for several reasons [25].

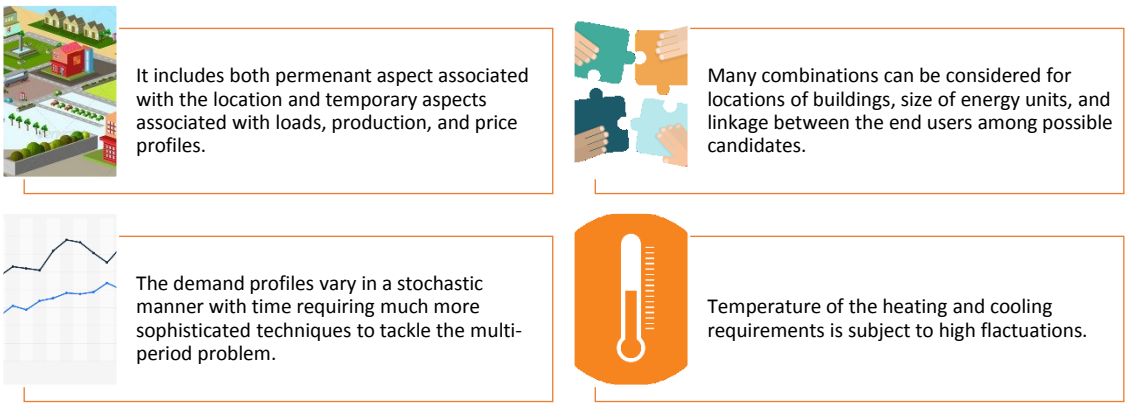

Figure 2.1 Four main challenges faced by optimization at district level

Allegrini et al. [26] presented a review on simulation approaches and tools for energy systems at district level. Olsthroom et al. [27] reviewed the integration of renewable energies into district heating and storage technology. Lake et al. [28] reviewed the implementation of district heating and cooling in real case studies. Lund et al. proposed the concept of 4th generation district based on integration of smart thermal grid and its role in future networks [29, 30]. In contrast to previous reviews on district heating and cooling, current study deals with the optimization of such systems. This chapter first gives an overview of the mathematical approaches of the problem, and it then discusses different areas of applications at district level, and the constraints used in the formulation of the problem. Finally, it briefly discusses the existing optimization tools used in this area.

2.3 Overview on the mathematical approach

Considering more than one objective function at the same time may result in conflict between them. For example, minimization of the cost and pollutant emissions is usually conflicting [31]. Table 2.1 shows most popular types of optimization objectives used at district level and their conflicts. Mathematical programming methods have been employed in wide range to make decision regarding the optimum design, planning and operation of district energy systems. Mathematical models for optimization usually lead to structured programming such as Linear Programming (LP), Mixed Integer Linear Programming (MILP), Non-Linear Programming (NLP), and Mixed Integer Non-Linear Programming (MINLP) [32] [33] [34].

Table 2.1. Conflict of popular objectives at district level (C: contrast, S: supporting, D: dependent)

Objective functions	Maximum revenue	Minimum emission	Maximum production	Minimum operation costs	Minimum investment	Minimum fuel cost	Maximum renewables
Maximum revenue	*	C	D	C	D	C	D
Minimum emission	C	*	D	C	C	C	S
Maximum production	D	D	*	C	C	C	D
Minimum operation costs	C	C	C	*	C	S	C
Minimum investment	D	C	C	C	*	S	C
Minimum fuel cost	C	C	C	S	S	*	C
Maximum renewables	D	S	D	C	C	C	*

If the objective function and the constraints are linear, the problem is said to be linear. Otherwise, the problem is called a nonlinear problem [35]. Mixed-integer linear and nonlinear programming involves both continuous and discrete variables arise in many applications of engineering design. Roy et al. [36] investigated the characteristics and details of each algorithm for engineering design. However, the detailed description of each algorithm is beyond the scope of the present

thesis. Direct search techniques choose the best solution at each iterative by comparing the results and move to the next step based on the current results [37, 35]. The techniques are typically efficient, however, they may find local solutions instead of the global one. In some cases, for example when the objective function (cost function) is not convex and not smooth in terms of the decision variables [38], typical gradient-based optimization methods fail to solve the problem. Therefore, evolutionary algorithms are required which are based on the Darwinian principle to remove the poorest solutions in each generation. Common operators are employed to make new generations of solutions. Genetic Algorithms (GA) [38, 33, 39, 40, 41] are widely used especially to optimize subsystem building blocks of a district. The most popular implementation for multi-objective problems is NSGA-II [42]. It is a popular option to establish the optimal heating/cooling distribution configuration by randomly generating many network designs for the entire district. Other popular method within the optimization of energy systems is to employ more than one technique in a hybrid optimization [43, 44]. A near optimal solution is found by applying a global-search technique and the result helps another technique to find the local optimum solution. Both single and multi-objective studies are included in the literature [45, 46]. A well-known method to tackle the multi-objective problems is to rewrite the several objectives in the form of only one function using constant weights [47] [48]. One main drawback of the method is that the solution to the optimization problem is not uniform. Another drawback is that the method fails in non-convex regions [49]. As the engineering viewpoint, the weighted sum approach is an efficient and easy-to-use method, however it calls for an expert in the field to identify the weight factors and compromise between the functions [50].

Within the time frame, district optimization problems may be split into two groups: (1) short-term problems which the operational management of the system is analyzed within a given period (typically one day/week/year); (2) long-term problems in which the formulation and analysis is carried out over the whole life cycle [51]. Decision variables represent the degrees of freedom in the optimization model. They include both binary and continuous variables. Binary variables define existence of a component or its operation status (on/off) [52]. A general framework of the optimization procedure at district level is given in Figure 2.2. This overview is applicable to a wide range of district configurations and framework conditions which can be represented by a group of input parameters.

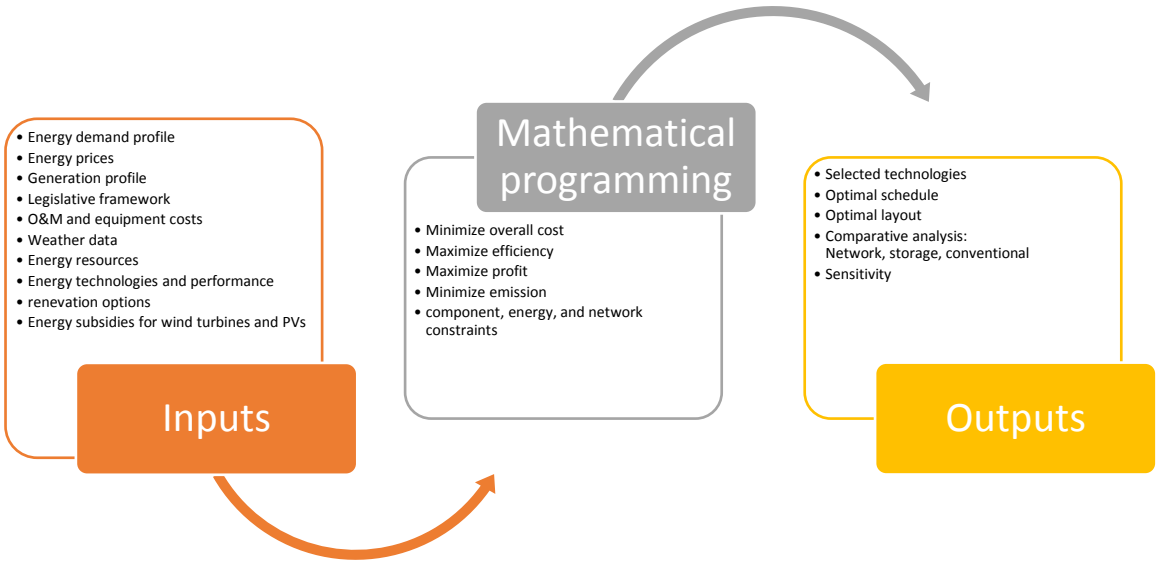

Figure 2.2 A framework for optimization at neighborhood level

2.4 Recent optimization studies at district level

The scientific literature for optimization approaches at district level can be classified into four main topics as illustrated in Figure 2.3. In the following sections, the most recent publications regarding each category are discussed.

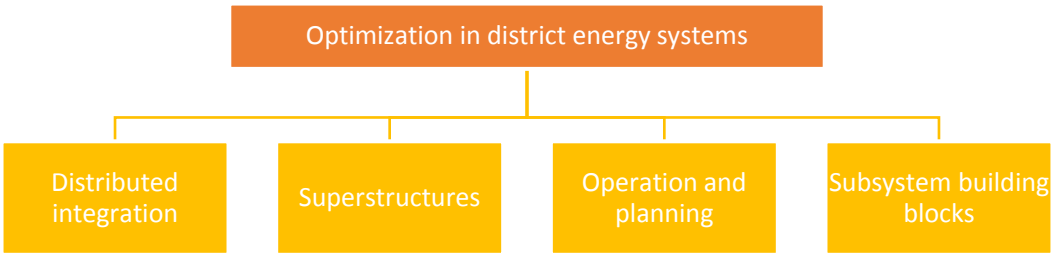

Figure 2.3 Classification of research papers in district optimization

2.4.1 Distributed integration

Distributed integration deals with the connection of energy resources to the district energy system to provide reliable, sufficient, economic and environmental-friendly power generation. The complexity of the integrated system associated such as CHP or heat pump [53] with the energy planning within the district calls for optimization analysis. Two major aspects recently draw attentions for economic optimization of CHP systems: developing accurate models and providing effective mathematical solvers [54]. Sartor et al. [55] developed a nonlinear programming (NLP) and proposed a quasi-steady state model based on thermodynamics, combustion processes and heat transfer intended to accurately estimate the performances of a biomass CHP plant integrated with a district heating system. The authors used optimization to calibrate their model based on an existing plant. Wang et al. [56] employed a linear programming (LP) technique and studied a CHP based DH system with RES and developed a modelling and optimization method for planning and operating such CHP-DH systems. The objective of the optimization was to minimize the overall costs of the net acquisition for heat and power in deregulated power market. The optimization model for the CHP-DH system was efficiently simulated in larger time scale (monthly horizon) rather than typical days of the years. In a study by Ondeck et al. [57], the authors adopted MILP and investigated the optimal integration of a CHP plant as a utility producer at a neighborhood level. The optimum operation for combination of CHP with PV is also investigated for predominantly cold climates. The authors considered fluctuations in energy rates, ambient conditions, and demand level as well as the day-ahead price in their economic study. Falke et al. [33] proposed a decomposed optimization solution to a multi-objective problem with an integrated economic and ecological objective function to reduce computation complexity of similar problems. The authors used Kruskal and Genetics Algorithms to tackle the problem. The optimization model comprises of three stages: (i) heating network design, (ii) generation plants, storage systems and renovation measures, and (iii) operation of the generation plants and storage systems. Weber and Shah [58] took MILP and proposed a tool, called DESDOP, to find the optimal combination of technologies to meet the energy demands of an eco-town under different scenarios. The authors did not consider uncertainty of the energy sources (especially wind) in their models. With a different methodology, Sameti et al. [59] presented a techno-economic model and multi-objective optimization taking Pareto approach and genetics algorithm to analyze a CHP system integrated with gas turbine to be used in a low-energy community. Uris et al. [60] studied the optimal sizing of a cogeneration unit with ORC (organic Rankine cycle) supplied by biomass taking NLP approach. The authors tried to achieve maximum profits when the system is integrated to an existing district system. Operation of the co- and tri- generation systems were considered

under full and partial loads and climatic severity. A similar simulation work including thermal storage was presented in a study by Noussan et al. [61], without considering optimization, in which the exergetic and economic criteria were studied. However, as the authors stated, the optimal results are different from existing configuration. Maatallah et al. [44] employed HOMER and its hybrid optimization feature to get the optimal share of a hybrid PV/wind/diesel with and without battery storage. Similar study to electrify a rural area was carried out with HOMER without considering storage but including hydropower in the analysis [43].

2.4.2 Superstructures

The main output for optimization problem in this category includes the existence and size of each component/technology based on suggested scenarios. This is usually followed by an optimal operation for a case study in which the goal is to decide which engines, chillers, CHP etc. at which capacity and at which point during the time horizon should operate. In this section, a review on the most recent studies is carried out. In a study by Mehleri et al. [62] a mixed-integer linear programming (MILP) model by Genetics Algorithm (GA) is presented where the objective is to find the optimal selection of the system components among several candidate technologies (micro combined heat and power units, photovoltaic arrays, boilers, central power grid), including the optimal design of a heating pipeline network, that allows heat exchange among the different nodes. A similar work was carried out by Wu et al. [48] in which they proposed a MILP model allowing determination of the energy generation components among various candidates, the site and size of each selected technology, optimal running schedule, as well as optimal layout of heating pipelines. They made a comparison between three different scenarios: CON (conventional), DES + HSN, DES + TES. Li et al. [47] proposed a model in which the objectives were to minimize the total annual cost and CO_2 (carbon dioxide) emission and achieve the optimal design and operation to meet the yearly energy demands for heating, cooling, and power. Bordin et al. [63] optimized selection of the set of new users that were connected to an existing district network during time horizons of five and ten years. They adopted Opti-TLR to build a MILP model. The model tried to maximize revenues and minimize operating and investment costs using fundamental of graph theory. Ameri and Besharati [64] compared four separate scenarios (conventional, CCHP without network, CCHP with network, and CCHP/PV with network) among several components candidates to achieve the minimum equivalent CO_2 emission and cost saving. Rivarolo et al. [65] used their own developed software (W-ECoMP) and performed a thermo-economic analysis for a smart micro-grid in time-dependent conditions and carried out a

hierarchical optimization using penalty method for both the sizing and the planning of all plant units. Two different co-generation and two different tri-generation layouts were considered to find the best solution. In another optimization study by Buoro et al. [52], a MILP model was proposed in commercial software Xpress for a distributed supply system included both centralized (CHP, boiler, and solar) and decentralized (CHP, chiller and boiler) technologies focusing on the solar power plant. They considered four different types of thermal storage including tank, pit, borehole, and aquifer. Karschin and Geldermann [66] adopted MILP approach in Xpress and focused on maximizing local bioenergy production of biomass system considering different ways of connecting customers to the supply grid as well as the design of the heating network and plants, cost, heat loss, and the legislation of the country. They compared five different scenarios.

2.4.3 Operation and planning

Even with a limited number of units, the definition of a planning strategy controlling the district plants to run at minimum cost or exploit the maximum possible share of renewables is not a simple task. Vesterlund and Dahl [67] employed ReMIND and CPLEX to tackle the MILP problem of the hydraulic performance of a district distribution system. They introduced a new process integration technique which allows the modeling of DHSs with loops (closed path for a fluid flow), without introducing any simplification or modification to their physical structure, modeling of DHSs containing of multiple sources of thermal energy production and redesign of the DHS structure, in particular to add or remove consumers. In an LP model proposed by Wang et al. [68], an energy integration system was studied named smart hybrid renewable energy for communities (SHREC). Their model took into account non-sudden starting and shutting down of CHP. Carpaneto et al. [69] developed an optimization procedure in MATLAB and investigated different scenarios for using renewable energies in district heating networks. The focus of the study was on solar energy, however, CHP, boiler, and storage were also considered. Wang et al. [70] employed Newton's method for a NLP problem to minimize the cost of a district heating system (an N-floor building) based on separate mass flow rate (pumping cost) and thermal conductance (heat exchanger cost). One drawback of their modelling is that it requires very long computational time when large networks are taken into account. Therefore, a tool is required for the model to be applicable in larger districts. Next, the temperature drop along the feed line for users in each floor results in non-uniform distribution of thermal energy, which is not favorable. Khir and Haouari [71] presented computational experiment for a MINLP model to optimize the design of a district cooling system based on the size of chiller units, cold thermal storage, and layout of the main piping network.

Besides the usual technical and operational constraints, the authors considered temperature and pressure drop in their model. Zhou et al. [72] proposed and compared two mathematical models to minimize the total annual cost of a combined cooling, heating and power system (CCHP) based on two assumptions: constant efficiency and off-design characteristics of different components. Powell et al. [73] presented a dynamic optimization to find the optimal charging/discharging time for thermal storage, which is used to shift cooling and electrical loads. Three scenarios were considered for costs: fuel-only, fuel with revenue from selling excess power, and fuel with both purchasing and selling. Jie et al. [74] introduced an optimization model to minimize the sum of pumping and heat loss costs for an existing district heating system. Four different strategies were considered and compared based on considering constant or variable flow rates for primary and secondary sides of the district. The best solution is when both the primary and secondary mass flow rates are under controlled. Jiang et al. [75] proposed a model considering wind turbine as one of the energy sources for electric water heater besides using solar water heater and gas-fire boiler. The authors minimized fuels consumption (kilogram coal equivalent) based on boiler's set-point temperature and flow rate of the variable speed pumps. Ren et al. [76] developed an optimization for optimal planning of a grid-connected hybrid PV/fuel cell/battery district energy system to minimize both annual CO_2 emission and running costs. An extra constraint the authors considered is that the simultaneous buy-back and selling electricity is prohibited as a policy. The dynamic grid price, as a pivotal role, was neglected in the simulation. Fang et al. [38] proposed a static model to find the optimal plant supply temperatures and load allocation among the plants based on the real-time end-user measurements to optimize heat production planning. Automated meter reading data was employed to approximate the heat losses, flow rates, and nodal temperatures within the network. Kim et al. [77] considered several district systems simultaneously. They tackled the problem of combining and optimization of eleven real-world district heating systems to achieve minimum total cost and maximum profits. But their model did not include any pumping cost and storage and network losses for the sake of simplicity.

2.4.4 Subsystem building blocks

Other optimization studies have been conducted focusing on specific technical aspects of the components or building blocks of the district system. Jie et al. [78] proposed an analytical model

to find the optimal pressure drop and related minimum annual cost for the distribution network in district heating based on operating variables and different strategies. Wang et al. [79] used optimization (genetics algorithm) to calibrate their model for steady-state distribution of thermal energy through pipes in a network. Their mathematical model was simple, however, taking advantage of temperature and flow measurements for three cases resulted in reduced uncertain parameters (aggregated heat conduction coefficient) and more accurate model. Barberis et al. [40] proposed a thermo-economic approach to investigate the integration of different thermal (both hot and cold) and electrical energy storage systems for optimal management strategy in a real smart district. The battery operation was considered in both off-grid and islanded operations. The author considered virtual term in their objective function as a penalty to represent the energy exchange between the plant and the environment. Zeng et al. [41] optimized the annual cost of a piping network based on the diameter for two scenarios for one typical day: conventional central circulating pumps and distributed pumps with variable speed. The latter operates associated with the electricity price. Diangelakis et al. [80] proposed a dynamic analytical optimization model for a CHP in a hypothetical district consisting of 10 buildings. The decision variable was the displacement volume of the internal combustion engine to minimize the operational cost. Li et al. [47] focused on the optimal economic design of the distribution network of a seawater-source heat pump for commercial district bay. However, their study did not consider the demand change throughout the year resulting in variable flow speed and temperature. A number of the previous studies are summarized in Table 2.2 based on the optimization method/approach, objective function, decision variables, district type, and the tool used by the researcher.

Table 2.2 Summary of optimization approaches in some recent studies

Study	Optimization type	Method/ Algorithm	Objective(s)	DH type	Solver
Superstructures					
Mehleri et al. [62]	Single-objective	MILP	Total annualized cost of micro-grid	Centralized	GAMS CPLEX
Wu et al. [48]	Multi-objective	MILP	Both economic and environmental aspects	Decentralized	Not mentioned
Li et al. [47]	Single-objective Multi-objective	MILP	Annual cost and carbon dioxide emission	Decentralized	MATLAB Gurobi
Bordin et al. [63]	Single-objective	MILP	Selection of new users	Centralized	Opti-TLR CPLEX
Ameri et al. [64]	Single-objective	MILP	Costs savings and reduction in CO_2 emissions	Decentralized	CPLEX AIMMS
Rivarolo et al. [65]	Single-objective	NLP	Sum of annual variable costs	Centralized	W-ECoMP
Buoro et al. [52]	Single-objective	MILP	Annual investment, operating and maintenance costs	Combined	Xpress
Karschin and Geldermann [66]	Single-objective	MILP	Cost-efficient heating network	Centralized	Xpress
Operation and planning					
Vesterlund et al. [67]	Single-objective	MILP	operating costs for heat production	Centralized	CPLEX
Wang et al. [56]	Single-objective	LP	costs of the net acquisition for heat and power in deregulated power market	Centralized	LP2
Carpaneto et al. [69]	Single-objective	MILP	dispatching strategy for the different power sources	Centralized	MATLAB
Wang et al. [70]	Single-objective	Newton's method	total mass flow rate total thermal conductance	Centralized	Not mentioned
Khir and Haouari [71]	Single-objective	MINLP/MILP	capital and operating costs	Centralized	CPLEX
Zhou et al. [72]	Single-objective	MILP/MINP	annual capital, operation and maintenance cost of CCHP	Centralized	GAMS CPLEX
Powell et al. [73]	Single-objective	MILP/MINLP	system operating costs (fuel and grid)	Centralized	MATLAB BONMIN
Jie et al. [74]	Single-objective	NLP	pumping cost and heat loss cost	Centralized	MATLAB
Jiang et al. [75]	Single-objective	GSO	Energy consumption	Centralized	MATLAB
Ren et al. [76]	Single-objective	MILP	CO_2 emission and running cost	Centralized	Not mentioned

Fang et al. [38]	Single-objective	Genetics Algorithm	sum of fuel and pumping cost	Centralized	MATLAB C++
Kim et al. [77]	Single-objective	MILP	overall operation costs	Integration of Centralized systems	CPLEX
Distributed integration					
Sartor et al. [55]	Single-objective	NLP	cost per unit of thermal energy used	Centralized	Not mentioned
Wang et al. [68]	Single-objective	LP	overall net acquisition cost for energy	Centralized	LP2 EnergyPro
Ondeck et al. [57]	Single-objective	MILP	profit of CHP plant by selling electricity	Centralized	GAMS CPLEX
Falke et al. [33]	Multi-objective	Kruskal and Genetics Algorithms	costs of power and heat supply and CO_2 emission equivalents	Decentralized	Not mentioned
Weber and Shah [58]	Single-objective	MILP	Total annual costs including investment and operating	Centralized	GAMS CPLEX
Sameti et al. [59]	Multi-objective	NLP	total exergetic efficiency and the net power	Decentralized	MATLAB
Maatallah et al. [44]	Single-objective	Hybrid optimization	Total net present cost	Centralized	HOMER
Amutha et al. [43]	Single-objective	Hybrid optimization	Total net present cost	Centralized	HOMER
Subsystem building blocks					
Jie et al. [78]	Single-objective	Calculus-based	pipe investment cost	Centralized & Decentralized	Not used
Wang et al. [79]	Single-objective	Genetics Algorithm	Calibration	Centralized	MATLAB
Barberis et al. [40]	Single-objective	Genetics Algorithm	Annual variable cost	Centralized	W-ECoMP
Zeng et al. [41]	Single-objective	Genetics Algorithm	investment, depreciation, maintenance, heat loss, and operational cost of circulating pumps	Centralized	Not mentioned
Diangelakis et al. [80]	Single-objective	control vector parameterization (CVP) algorithm	Operation cost	Centralized & Decentralized	gPROMS gOPT
Xiang-l et al. [39]	Single-objective	Genetics Algorithm	Annualized price of distribution network	Centralized	Not mentioned

2.5 Formulation of constraints

In the optimization of district energy models, there are usually three groups of constraints [23, 64] as illustrated in Figure 2.4. Component constraints usually state input-output energy for each module. Constraints for energy balances insure that the amount of input energy is equal to the output, for each time interval and for each node (site) including supply and demand sides. Some common inequality constraints for different components are reviewed in Table 2.3. Equality constraints are highly dependent to the model, however, for some components such as thermal energy storage similar modeling are typically employed. Table 2.4 summarizes the constraints used in recent studies for optimization of district energy systems.

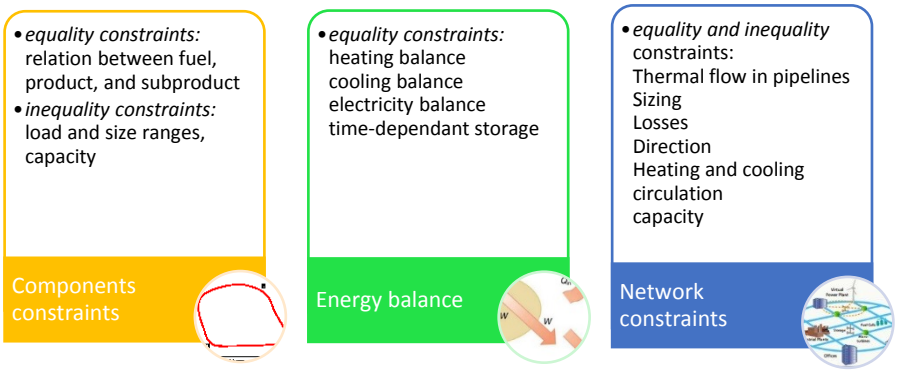

Figure 2.4 Classification of constraints in programming district energy optimization

Table 2.3 Formulation for some common inequality constraints at district level

Constraint	Formulation	Description
Number of components	$y_i \le n_i \le n_{max} y_i$	Number of that component n_i should be lower than a maximum value n_{max} where y_i is a binary variable
Power and heat generation	$P_{GT} \le P_{GT}^{max} y_{GT}$ $Q_B \le Q_B^{max} y_B$	The generated power by gas turbines P_{GT} and the produced heat of boilers Q_B are less than their maximum capacity at each point of the operation time. Where y_{GT} and y_B are binary variables showing "on" and "off" modes
Supply heat and flowrate	$G_{SA}^{min} y_{SA} \le G_{SA} \le G_{SA}^{max} y_{SA}$ $P_{EC}^{min} y_{EC} \le P_{EC} \le P_{EC}^{min} y_{EC}$	Steam flowrate is G_{SA} and supplied electricity is P_{EC}
Energy storage	$S_{TES,min} \le S_{TES} \le S_{TES,max}$ $S_{EES,min} \le S_{EES} \le S_{EES,max}$	TES: thermal energy storage EES: electrical energy storage
Power ramping	$\frac{P_{CHP}^t - P_{CHP}^{t-1}}{P_{CHP}^{t-1}} \le \epsilon$	Power by the plant between two successive time points are P_{CHP}^t and P_{CHP}^{t-1}.
Charging and discharging	$y_{in} + y_{out} \le 1$	Battery or TES cannot charge and discharge at the same time. By introducing two binary variables y_{in} and y_{out} for charging and discharging, respectively.
Charging supply	$\sum_{i=1}^{n} E_{sto,i} \le M y_{in}$	The storage may be charged from certain systems. $E_{sto,i}$ is the energy flow delivered by component i among n allowable units.
Grid interaction	$y_{in} + y_{out} \le 1$	Injection of electrical energy to the grid or its withdrawal cannot be implemented at the same time.
PV area on the roof	$\sum_{i=1}^{n} n_i A_{pv,i} \le A_{roof}$	Total PV area (n_i number of $A_{pv,i}$) is another constraint which cannot violate the available roof surface A_{roof}.
Solar absorption chiller	$\frac{P_{abs}}{COP} \le P_{solar}$	P_{abs} is the chiller requires energy with COP as the coefficient of performance and P_{solar} is the generated solar heat.
Up-time **Down-time**	$y_{on,t+1} = \begin{cases} 0 & T_{up,t} \ge T_{up} \\ 1 & T_{down,t} \le T_{down} \end{cases}$	The running time of a power or heat generation unit can be controlled by a binary variable $y_{on,t+1}$ at instant $t+1$ based on the instant t.
Priority operation	$P_{i,t} \le P_{i,t+1}$	Priority for the operation of the power or heating engines $P_{i,t}$ at point t may be considered to prevent generation of multiple solutions.
Allowable modes	$y_{tr,t} + y_{tr,t+1} = 1$	In case of successive permitted and unpermitted operation modes of a component, especially a CHP, a binary transition variable is defined as y_{tr}.
Energy flow direction	$y_{i,j} + y_{j,i} \le 1$	Binary variables $y_{i,j}$ and $y_{j,i}$ for two buildings
Delivery capacity	$E_{j,i} \le M y_{j,i}$	Maximum delivery capacity is M for energy flow $E_{j,i}$
Thermal energy circulation	$OR_j = OR_i + 1 - \lvert i \rvert (1 - y_{i,j})$	Creation of a loop results in production and circulation of energy that is not demanded. For example, CHP can operate at a higher rate in order to sell electricity while the actual demand of buildings is lower. OR is the order of a building.

All the non-linear terms in constraints can be approximated by piecewise-linear functions. For example, this linear approximation approach is adopted by Bordin et al. [63] to represent the nonlinear pressure drop in the network. Another method used by Khir et al. [71] is called the Reformulation-Linearization Technique (RLT). The technique includes two steps: reformation and linearization. The former step adds some nonlinear constraints to the problem introducing binary variables into the problem. Substitution of continuous variables are made in the linearization step. Other source of non-linearity corresponds to the efficiencies of the components. Energy production efficiency of the components depends on some factors such as the capacity, ambient temperature, and operation temperature. These introduce nonlinearity to the model and constraints, therefore it is a widely-adopted assumption with low optimization error in studies that conversion efficiencies are constants [64]. In a study by Zhou et al. [72], the nonlinear terms are assumed to be separable into summations and differences of some linear functions with single variables.

2.6 Smart grids and districts

Load shifting through effective thermal energy storage or electricity storage is a major part of smart grids and already exploited by various studies for generation–consumption matching and zero energy targeting. Gaiser et al. [81] investigated the change in electricity demand based on the net energy metering and the time of use rate for a smart apartment community. The authors employed smart scheduling to achieve peak load shaving in off-peak period by using different household appliances. Photovoltaic system supplies each apartment therefore it is desirable to maximize generation and sell it to the grid during peak hours. Zhang et al. [82] investigated energy generation taking advantage of photovoltaic, batteries and compressed-air storage, building demand response, passive cooling technologies along with the assessment of microclimate and landscape. Kolokotsa et al. [83] proposed an advanced energy scheduling to minimize the cost of the micro-grid using genetics algorithm for the operation a micro-grid district. The author adopted artificial neural network to support the optimization technique by prediction of energy load and forecasting energy generation (by the photovoltaic and hydroelectric plant). Similar studies besides the genetic algorithms [84] includes using of fuzzy logic and Particle Swarm Optimization (PSO) methods along with the non-linear constrain multi-objective optimization technique [85]. The second possible application of smart grids in district level includes the multiple operational characteristics ranging from office buildings, retail, industrial, with various energy trends and demands [86].

Table 2.4 Some common constraints employed in recent district optimization studies

Study	Number of each/all equipment	CHP/Boiler/Chiller capacity (min/max)	Storage capacity	PV area	PV rated capacity	Storage flow capacity	One-direction energy flow	Maximum pipeline capacity	Heating/ cooling circulation	Electricity balance	Heating balance	Storage balance	CHP/PGU/Boiler relationship	Grid interaction	Pipe heat interchange (capacity)	Input energy limitations	Up time/ Down time
Li et al. [47]	*	*	*	*	*	*	*	*	*	*	*	*	*				
Wu et al. [48]		*		*	*		*		*			*		*	*		
Ameri et al. [64]		*		*	*		*			*	*		*	*	*	*	
Mehleri et al. [24]	*	*		*	*		*		*					*			
Wang et al. [56]		*				*											
Carpaneto et al. [69]		*	*								*	*	*	*			*
Mehleri et al. [24]	*	*			*				*	*	*			*			
Yang et al. [19]	*																
Zhou et al. [72]	*	*	*							*	*	*					
Wang et al. [79]		*	*							*	*	*	*				
Ren et al. [76]			*							*	*	*		*			
Wang et al. [79]		*	*			*				*	*	*	*				

2.7 Optimization tools for solving district-level problems

Some popular optimization tools and their abilities are briefly introduced in Table 2.5. Most tools used in district energy optimization consist of algebraic modeling language (AML) i.e. they are high-level languages and usually have similar mathematical notation to describe optimization problems. Besides the aforementioned tools, some energy analysis software have features to both model and optimize a district energy system. EnergyPRO provides techno-economic optimization of poly-generation energy system in both thermal and electrical aspects. Technical parameters and preferences order are considered to calculate the unit operation, and the cash flow is reported as output [87]. HOMER allows modeling, optimization and parametric sensitivity grid-connected and standalone renewable energy technologies focusing on electrical energy conversion. Storage technologies include batteries, flywheels and hydrogen without any thermal energy storage. The tool has a limited number of thermal units that are typically simplified: CHP, boiler, and biomass are included. Different kinds of electrical and thermal demand profile/data can be used as input to show daily or seasonal variations [7]. SynCity adopts the same approach for mathematical programming in GAMS to optimize carbon emission, required energy, and total cost of a district. The tool includes built-in models, which take neighborhood layout as the input. Time and location demands for electricity, fuel consumption for transportation, and heating are calculated based on the simulated daily activities of people. The tool proposes optimal solution for configuration of network, activity locations and transportation map. Epic-hub takes the concept of “energy hub” for design, operation, and energy consumption optimization at site and district levels [88]. Neplan is used in designing, modelling, optimization of distribution network of water, electricity, gas, and thermal piping. The tool is able to carry out analysis regarding energy flow, energy loss, and hydraulics for the district to size the heating units, circulating pump, and heat exchangers. Another major advantage of the tool is its interface for GIS [89].

Table 2.5 Optimization programming tools in recent district optimization studies

Developer	Tool	Remark	Some solvers
AIMMS BV	AIMMS	Uncertainty can be taken into consideration in deterministic linear and mixed integer models	CPLEX, Gurobi, MOSEK, CBC, Conopt, MINOS, IPOPT, SNOPT, KNITRO, CP
AMPL Optimization	AMPL	AMPL is an AML tool used to handle linear and nonlinear convex quadratic problems with both integer and continuous variables. The tool supports variety of optimization problems such as	CBC, CPLEX, FortMP, Gurobi, MINOS, IPOPT, SNOPT, KNITRO, LGO

		semidefinite programming and is suitable for large scale linear and nonlinear programming	
GAMS development Corporation	GAMS	The tool is used to model and solve linear, nonlinear, and mixed-integer linear and nonlinear problems [90].	BARON, COIN-OR, CONOPT, CPLEX, DICOPT, Gurobi, MOSEK, SNOPT, SULUM, XPRESS
Math-Works	MATLAB	MATLAB is able to solve all kinds of linear, nonlinear, mixed-integer, and quadratic problems using Optimization Toolbox [91]	Gurobi
IBM	ILOG CPLEX Studio	CPLEX is able to solve linear and mixed-integer linear problems. CPLEX may also deal with certain types of problems where the objective function is nonlinear but quadratic whether the problem is constrained or not.	ILOG CPLEX optimizer solvers
FICO	FICO Xpress Suite	The tool can tackle linear and mixed integer problems, convex quadratic constrained and unconstrained problems, and second-order cone problems as well as the mixed integer counterparts.	Xpress-Mosel language
LINDO Systems	LINGO	A comprehensive optimization AML tool for building models and solving linear, mixed-integer linear, nonlinear (both convex & nonconvex problems), mixed-integer nonlinear, constrained and unconstrained quadratic problems, stochastic, second-order cone, semi-definite problems.	A set of fast built-in solvers are used but not mentioned

2.8 Conclusions

- Objective functions at the district level are typically: carbon emission, production, revenue, operation costs, investment, fuel costs, and renewables exploitation. Contradiction of the objective functions was presented in this review.
- Multi-objective optimization is widely tackled by weighted-sum function, which converts the original objectives into a single objective. However, choosing the weight factors requires previous knowledge of the problem. It is also, time-consuming and may result in non-uniform curves.

- MILP is taken as the most widely applicable approach for optimization of district energy systems. Branch & Bound is the most effective technique used by the researcher.
- Genetics algorithm can be used to find the optimum layout of a district system in a multi-level optimization approach. Therefore, the operation and planning can be followed by other technique as a hybrid optimization.
- Binary variables are introduced in the model to check the status (on/off) of the equipment and its running time during operation as well as its installation during the design stage. It can also be used to specify transition between modes of operations.
- Several linearization techniques were employed by the researchers to linearize constraints. Three different methods were discussed in this thesis used in districts: piecewise function, and sum/difference method. The piecewise approximation is the most applicable method.
- Linearization of constraints and adoption of constant efficiency were proved to introduce small error into the optimization problem.
- The implementation stage of most of the researches includes small number of buildings to save in optimization time and computational effort. However, a real-world community contains hundreds of buildings. Therefor more powerful algorithms and modelling techniques are required.
- Potential of new sources of energy such as ocean energy for future district systems and integration of mechanical energy storage are suggested as new topics in the area of district energy optimization. Moreover, multi-stage optimization is an interesting subject, which is able to both reduce the computation time and separate the design and operation steps.
- Most models suffer from very long computational time when large networks are taken into account. Therefore, a special tool is required for the model to be applicable in larger districts.
- Interaction of smart thermal grid and smart electrical grid is a new concept proposed for 4^{th} generation district energy system. Economic, environmental, and efficiency optimization models are necessary in this new area.

Chapter 3

Optimization of 4th generation distributed district heating system: Design and planning of combined heat and power

3.1 Introduction

This study applies a mathematical programming procedure to model the optimal design and planning of a new district which satisfies two features of the 4th generation district heating systems: energy reciprocity and on-site generation. The aim of the computational model is to investigate the effect of energy reciprocity (energy exchange among the buildings) as well as to find the best way to select the equipment among various candidates (capacities), the pipeline network among the buildings, and their electrical connections. The objective function includes the annualized overall capital and operation costs for the district along with the benefits of selling electricity to the grid. The distributed energy supply consists of heating, cooling, and power networks, several CHP technologies, solar array, chillers, and auxiliary boilers. The performance of the model for poly-generation was evaluated for designing the new part of Suurstoffi district situated in Risch Rotkreuz, Switzerland with seven residential and office complexes under four different scenarios.

3.2 Formulation of the problem

Energy reciprocity in district energy system, a concept investigated in this thesis, is defined as the ability of the buildings to share their heating effect, cooling effect, and power output to flatten the fluctuations and provides a smooth operational plan. The overall effect leads to a reduced design and operation cost of the supply system. As it is demonstrated in this thesis, the thermal and power distribution network do not follow the superposition rule. In this section, the optimal

design of a new distributed district is modeled to provides the best configuration of the district energy system and investigate the effect of energy reciprocity as well as the design of the heat and power distribution network. The optimization problem described above can be expressed as a mixed-integer linear programming (MILP) model. The MILP model includes an objective function as well as the design, operation, and planning constraints. As Figure 3.1 shows, the model considers on the optimal shape of the pipeline network to provide best heat exchange among the buildings. However, in order to provide best energy supply system, it also takes into account auxiliary boilers, photovoltaic (PV) arrays, various CHP technologies, solar thermal collectors, and chillers. Number of each technology to be placed in every building can be considered as constraint. Photovoltaic array may be installed in all buildings, however, according to the shape and dimensions of the buildings along with the national regulations, their sizes are restricted by an upper bound. Considering the available sizes in the market, the auxiliary boilers capacities are also bounded. The computational model introduced in this study assumes there is no a pre-existing heating or cooling network (no pre-existing connections among the buildings). Heat exchange among the buildings is allowed as one of the features of 4th generation districts however heat circulation is avoided to prevent erroneous. The district optimal design and operation takes advantage of the consumers' different demand, flatten the fluctuations and gives a smooth operational plan. It is assumed that the whole year has been split into different seasons and time periods.

3.2.1 Objective function

The total cost is the objective function which includes the technology and network capital and investment cost, operating cost, selling and purchasing grid electricity, and the total environmental cost as:

$$C_{total} = C_{inv} + C_{op} + C_{car} + C_{elec,pur} - C_{elec,sel} \quad (1)$$

The total capital cost consists of the costs for the PV and collector arrays, the gas-fired boilers, the (micro-) CHP technologies, chillers, and the pipeline connections among the buildings, which is amortized by multiplying the cost of each technology by its related capital recovery factor (CRF) as:

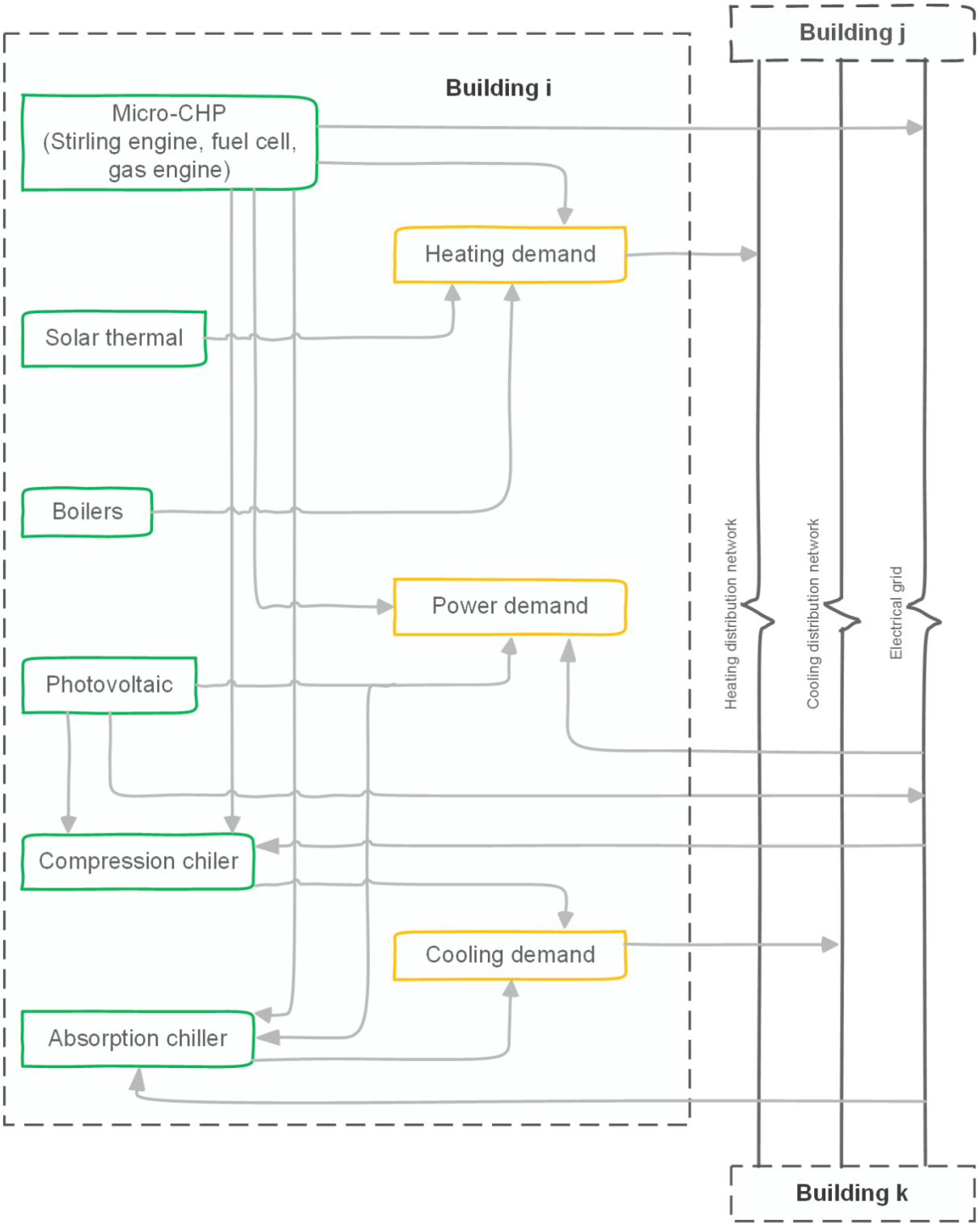

Figure 3.1 Schematics of the in-building supply and demand system and energy exchange among buildings in a district

$$C_{inv} = CRF^{PV} C^{PV} G^{PV} \sum_i A_i^{PV} + CRF^B C^B \sum_i G_i^B + \sum_k \sum_i CRF_k^{CHP} C_k^{CHP} G_k^{CHP} X_{i,k} + CRF^{pipe} \sum_i \sum_j C^{pipe} d_{i,j} Y_{i,j} + CRF^{sol} C^{sol} G^{sol} \sum_i A_i^{sol} + \sum_m \sum_i CRF_m^{chil} C_m^{chil} G_m^{chil} CRF_m^{chil} Z_{i,m} \quad (2)$$

where:

$$CRF = \frac{\alpha(1+\alpha)^n}{(1+\alpha)^n - 1} \quad (3)$$

and the decision design and operating variables corresponds to the equipment that will be installed in each building and the connection between the buildings:

- The optimal surface area of the PV array in each building;
- The optimal surface area of the solar thermal array in each building;
- The optimal capacity (maximum heat generation) of gas-fired boiler at each building;
- Optimal selection of CHP technologies among candidates;
- Optimal selection of cooling technologies among candidates;
- The optimal path for energy flow among buildings; and
- Decision concerning buying from/selling electricity to the grid.

The annual operating costs includes the fuel cost purchased to operate auxiliary boilers and the CHP technologies along with the electricity purchased to run the compression chillers. It is expressed by multiplying the sum of fuel/electricity consumption at each period with the corresponding price:

$$C_{op} = \sum_t \sum_s \sum_i \Delta_{s,t} \frac{Q_{i,s,t}^B p_{s,t}^{gas}}{\eta^B} + \sum_k \sum_t \sum_s \sum_i \Delta_{s,t} \frac{p_{s,t}^{gas} E_{i,s,t,k}^{CHP}}{\eta_k^{CHP}} + \sum_m \sum_t \sum_s \sum_i \Delta_{s,t} \frac{Q_{i,s,t,m}^{chil}}{\eta_m^{chil}} \quad (4)$$

where the electricity generated by the CHP unit is the sum of electricity consumed in the district and the one sold to the grid [62, 24, 92, 64, 48]:

$$E_{i,s,t,k}^{CHP} = E_{i,s,t,k}^{CHP,used} + E_{i,s,t,k}^{CHP,sel} \quad (5)$$

The annual cost for purchasing electricity is obtained by multiplying the aggregated amount of the electricity purchased by the utility electricity rate as [62, 24, 92, 64, 48]:

$$C_{elec,pur} = \sum_{t}\sum_{s}\sum_{i} \Delta_{s,t} E_{i,s,t}^{grid} p_{s,t}^{grid} \quad (6)$$

Backup boilers and CHP technologies burn fuel to produce heat and therefore emit carbon. Likewise, the carbon emissions generated from purchased electricity can be calculated by multiplying the total purchased amount by the related carbon intensity. The total cost for carbon emissions caused by the district annual operation is determined by multiplying the total emissions by carbon tax rate [62, 24, 92, 64, 48]:

$$\begin{aligned} C_{car} = {} & CT \sum_{t}\sum_{s}\sum_{i} \Delta_{s,t} E_{i,s,t}^{grid} I^{grid} + CT \sum_{t}\sum_{s}\sum_{i} \Delta_{s,t} \frac{Q_{i,s,p}^{B}}{\eta^{B}} I^{gas} \\ & + CT \sum_{k}\sum_{t}\sum_{s}\sum_{i} \Delta_{s,t} \frac{E_{i,s,t,k}^{CHP}}{\eta_{k}^{CHP}} I^{gas} \end{aligned} \quad (7)$$

The revenue generated from selling excess electricity back to the utility grid is computed based on the aggregated amount of electricity injected back to the grid. Present model has the option of considering periodic buy-back rates for electricity produced by cogeneration and PV arrays [62, 24, 92, 64, 48]:

$$C_{elec,sel} = \sum_{t}\sum_{s}\sum_{i} \Delta_{s,t} E_{i,s,t}^{PV,sel} p^{PV,sel} + \sum_{m}\sum_{t}\sum_{s}\sum_{i} \Delta_{s,t} E_{i,s,t,k}^{CHP,sel} p^{CHP,sel} \quad (8)$$

3.2.2 Design and planning constraints

This section presents the constraints implemented as part of the optimization model. Readers are encouraged to refer to section 2.6 and table 2.3 for more insights and a complete list of previous studies where these constraints are used. Capacity of the back-up boilers is restricted within

maximum and minimum bounds, i.e. availability of the boiler in the market determines bounds on its sizes [62, 24, 92, 64, 48]:

$$G_i^{B,lo} U_i \leq G_i^B \leq G_i^{B,up} U_i \tag{9}$$

where the binary variable represents whether the boiler is installed in the building i or not.

Maximum number of CHP units that can be installed in building $\boldsymbol{i}$ and its total capacity is given by the following constraints [62, 24, 92, 64, 48]:

$$G_i^{CHP,max} = \sum_k G_k^{CHP} X_{i,k} \tag{10}$$

$$\sum_k X_{i,k} \leq n^{CHP} \tag{11}$$

A constraint is required for PV to prevent its area from exceeding the available space for each building according to its dimensions, characteristics, and the local/national regulation [91, 45]:

$$A_i^{PV} \leq \frac{A_i^{PV,up}}{\cos\theta} \tag{12}$$

The same constraint is posed for solar thermal collector.

Only one direction of energy flow is allowed for each pair of buildings. It should also be mentioned that additional connections could be posed or relaxed in the design by this constraint [62, 24, 92, 64, 48]:

$$Y_{i,j} + Y_{j,i} \leq 1 \tag{13}$$

Electricity load of each building is met by the utility grid along with the energy generated by the PV arrays and the cogeneration as well as the power exchange among the buildings according to one of the features of 4th generation district:

$$E_{i,s,t}^{elec,tot} = E_{i,s,t}^{grid} + E_{i,s,t}^{PV,used} + \sum_{k} E_{i,s,t,k}^{CHP,used} + E_{j\rightarrow i,s,t} - E_{i\rightarrow j,s,t} \quad (14)$$

Heat demands can be met by the auxiliary boilers, the CHP technologies. Heat may be exchanged among the buildings which is referred to as two-way heating in 4th generation of district energy systems:

$$Q_{i,s,t}^{heat} = Q_{i,s,t}^{B} + \sum_{k} E_{i,s,t,k}^{CHP} \zeta_k + (1-\sigma) Q_{j\rightarrow i,s,t} - Q_{i\rightarrow j,s,t} \quad (15)$$

It is noteworthy to add that transmission heat losses are also taken into account in the above equation. The chillers provide the required cooling demands:

$$Q_{i,s,t}^{cool} = \sum_{m} Q_{i,s,t,m}^{chil} \quad (16)$$

Selling and purchasing electricity at the same time is not permitted for each building which is realized by [62, 24, 92, 64, 48]:

$$E_{i,s,t}^{grid} \leq E_{i,s,t}^{elec,tot} (1 - W_{i,s,t}) \quad (17)$$

At the same time, the amount of the injected electricity to the grid may be limited by regulations as [62, 24, 92, 64, 48]:

$$\sum_{k} E_{i,s,t,k}^{CHP,sel} + E_{i,s,t}^{PV,sel} \leq E_{i,s,t}^{sel,max} W_{i,s,t} \quad (18)$$

Electricity produced by the PV is limited by its nominal capacity and the available amount of solar energy radiated on it [62, 24, 92, 64, 48]:

$$E_{i,s,t}^{PV,sel} + E_{i,s,t}^{PV,used} \leq A_i^{PV} \eta^{PV} S_{s,p} \quad (19)$$

$$E_{i,s,t}^{PV,sel} + E_{i,s,t}^{PV,used} \leq A_i^{PV} G^{PV} \quad (20)$$

Equations (19) and (20) also hold for solar thermal collector in which the heat generated by the solar collector replaces the electricity generation by the PV units.

The heat generated by the boilers at each building is always less than its rated capacity [62, 24, 92, 64, 48]:

$$Q_{i,s,t}^{B} \leq G_{i}^{B} \tag{21}$$

Likewise, the following constraints indicate that the electricity produced from the CHP technology or the chillers should stay below its nominal capacity at any time [62, 24, 92, 64, 48]:

$$E_{i,s,t,k}^{CHP} \leq G_{k}^{CHP} X_{i,k} \tag{22}$$

$$Q_{i,s,t,m}^{chil} \leq G_{m}^{chil} O_{i,m} \tag{23}$$

The heat recovered by the CHP is calculated by its heat-to-power ratio and the nominal capacity as [62, 24, 92, 64, 48]:

$$Q_{i,s,t,k}^{CHP} = E_{i,s,t,k}^{CHP} \zeta_{k} \tag{24}$$

Heat exchange among the buildings is realized only if the corresponding pipeline linkage has been installed. Moreover, the capacity of transferred flow is restricted as:

$$Q_{i \rightarrow j,s,t} \leq Q_{i \rightarrow j,s,t}^{max} Y_{i,j} \tag{25}$$

Creation of directed loop (a closed path for fluid flow) in the network is not allowed due to waste of energy through unreasonable operation of units. In this case, heat produced in a building may circulate (in a closed loop) and gets back to the initial producer building. Another incorrect operation may happen when CHP works to sell more electricity but the heat is not used and circulate in the loop and causes heat losses. A constraint based on the Travelling Salesman Problem is considered in the model to exclude directed loops as [62, 24, 92, 64, 48]:

$$V_{j}^{O} - V_{i}^{O} \leq 1 - (1 - Y_{i,j}) \sum_{i} 1 \tag{26}$$

Electricity exchange between the sites may be limited by an upper bound as:

$$E_{i\to j,s,t} \leq E^{max}_{i\to j,s,t} T_{i,j} \quad (27)$$

The proposed optimization model is general and flexible. It provides a computational framework, which can be directly employed for various scales of districts with any climatic conditions. New energy policies may be added as extra constraints in the model.

3.3 Case study

In order to illustrative the model's applicability and evaluate its effectiveness, it was implemented for an urban area in Suurstoffi district located in Risch Rotkreuz, Switzerland. As shown in Figure 3.2, the new area under construction comprises of seven residential and office complexes. Table 3.1 lists distances among the buildings where the pipelines may be laid to establish the best distribution network.

Table 3.1. Distances between consumers in district (in meters) [93].

Building number	B1	B2	B3	B4	B5	B6	B7
B1	0	60	110	160	190	160	120
B2	60	0	40	90	170	160	120
B3	110	40	0	40	120	110	80
B4	160	90	40	0	40	70	70
B5	190	170	120	40	0	50	120
B6	160	160	110	70	50	0	40
B7	120	120	80	70	120	40	0

(a)

(b)

Figure 3.2 (a) Plan of the Suurstoffi district. White buildings are under construction. (b) Proposed model is applied to the sites with the labels shown. *[93]*

The area of the residential and office buildings is around 25000 m^2, comprising of 7 sites, which are all under construction and going to be completed by 2020. Heating and power demands are illustrated in Figure 3.3 and Figure 3.4, respectively, where the entire year is divided into three seasons including summer (from June to the end of September), mid-season (from March to the end of May as well as October), and winter (November, December, January, and February) [62]. In each day, 24 hours are divided into six periods. The heat and electricity demands are provided as the input data to the model. It should be noted that the heating demand reflects the space heating and equals zero all through the summer period for entire seven buildings, see Figure 3.3.

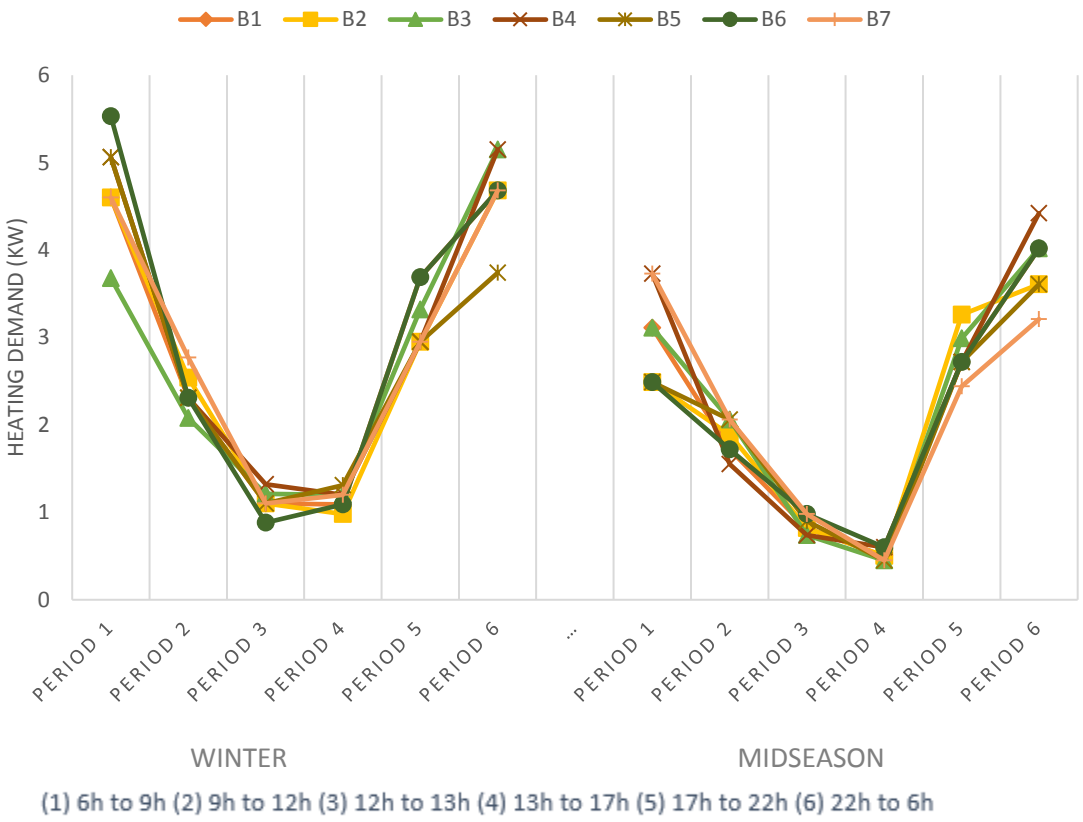

Figure 3.3 Heat demand of each building in district for each period and season

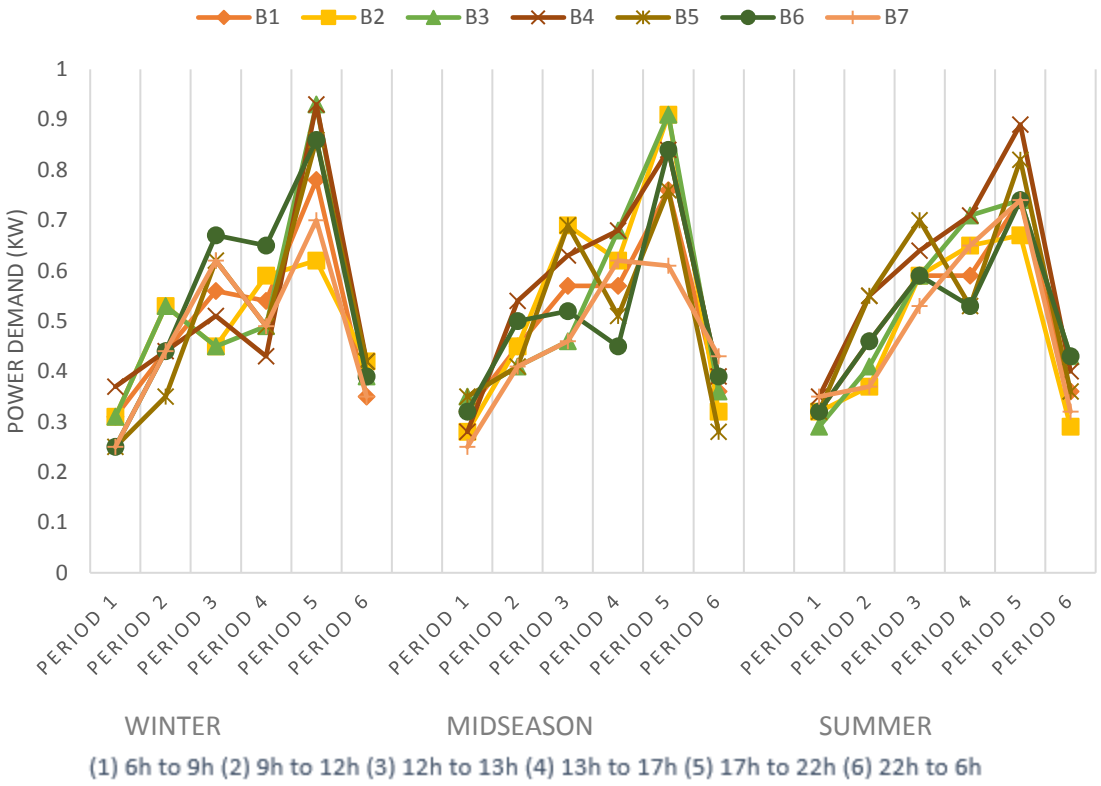

Figure 3.4 Power demand of each building in district for each period and season

The level of solar irradiation is a key factor in optimization of the PV installation area since the power produced by a PV array is basically proportional to the strength of radiation, however, secondary effects such as the precipitation, temperature extremes, wind, and humidity may restrict the power output. The hourly solar irradiation profiles for a typical day in three seasons for the location are shown in Figure 3.5 as well as its value for different periods. According to these curves, it can be seen that solar arrays are exposed to the highest irradiation around 11:00 AM in the morning. In Figure 3.5, the irradiation profiles are symmetric around 12:00 pm i.e. the intensity of solar radiation remains the same after and before 12:00 pm but the linearized curves are not, because the length of the time intervals (number of hours) used for calculation of average irradiation are different.

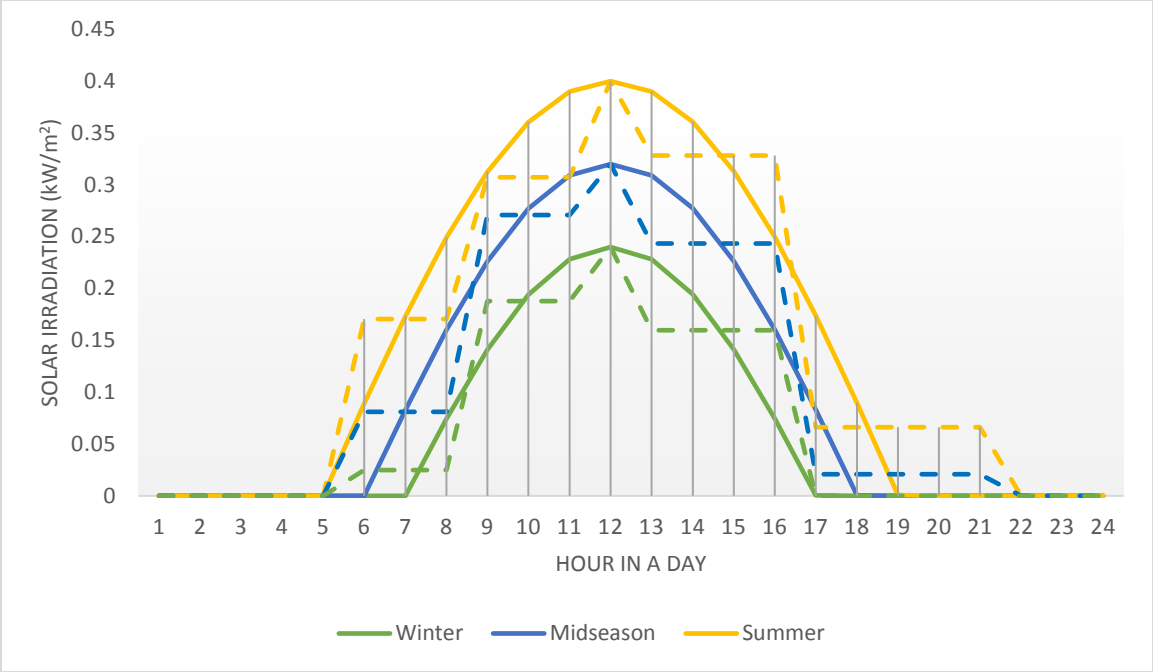

Figure 3.5 Hourly irradiation for typical day of each season and periodic linearization.

The basic technical characteristics and investment costs of the available choices are listed in Table 3.2. Six different candidates are put forward for the cogeneration including three gas engines, one fuel cell, one combustion engine, and one reciprocal engine with different production capacities. Electricity utility rate for selling excess energy and purchase as well as the fuel prices are given in Table 3.3 where both are assumed to be constant during all periods and seasons. The emission of CO_2 for the electricity or heat production as well as the carbon tax is given in Table 3.4. Carbon intensity for natural gas refers to the lower heating value of the fuel (natural gas) consumed [94]. The upper limit on the installed PV arrays area for each building along with its equivalent nominal power for each particular area is given in Table 5 based on the only PV candidate in Table 3.2. The simulation presented in this study assumes an annual interest rate of 6.0%. It is noteworthy to mention that inverters have a lifetime of 7.5 years (half of other technologies) i.e. the inverters should be replaced after 7.5 years indicating that the price for the inverters are doubled when analyzing the life cycle cost. It is also assumed that all the technologies are purchased at the beginning of the whole process. In this study, the maximum number of each component inside each building including CHP units (n^{CHP}) is assumed to be 1.

Table 4.2 Basic characteristics and capital costs of candidate equipment [95, 96, 97, 62, 92].

Candidate technology	Electrical capacity	Thermal capacity	Efficiency	Capital cost
PV array	200 W/m2	-	15%	2900 €/kW
Inverter	1 kW	-	100%	700 €
Boiler	-	0 to 35 kW	73%	100 €/kW
CHP (Gas engine)	1 kW	2.5 kW	26%	7 100 €
CHP (Combustion engine)	10.3 kW	21.6 kW	24%	15 000 €
CHP (Gas engine)	4.7 kW	12.2 kW	25%	11 750 €
CHP (Gas engine)	5.5 kW	12.7 kW	27%	13 750 €

Table 3.3 Price list for electricity and fuel ([62, 98, 92, 99]).

Item	Price
Electricity bought from grid	0.12 €/kWh
CHP electricity to grid	0.13 €/kWh
PV electricity to grid	0.55 €/kWh
Fuel for CHP (Natural gas)	0.049 €/kWh
Fuel for boiler (Natural gas)	0.042 €/kWh

Table 3.4 Carbon tax and carbon intensity [62, 98].

Item	Value
Carbon tax for CO_2	0.017 €/kg
Carbon intensity for gas	0.184 kg/kWh
Carbon intensity for electricity	0.781 kg/kWh

Table 3.5 Available area on the top of each building for PV arrays [93] (see **Table 3.2** for production).

Building	Available area (m^2)	Production (kW)
B1	50	7.5
B2	150	22.5
B3	200	30
B4	75	11.25
B5	100	15
B6	75	11.25
B7	200	30

Four different scenarios are considered to optimize to the effect of local technologies and also heat exchange among the buildings:

Scenario 1*:* The base scenario - a conventional system is simulated where the electrical demand is met by utility grid and gas-fired boilers provide the heating demand. No other technologies and distribution network is considered in this scenario. This is the reference scenario defined to evaluate any improvement gained by installation of new technologies or concept of energy exchange.

Scenario 2: Photovoltaic array and CHP technologies can be placed in each building but building interaction through the distribution network is not considered.

Scenario 3: All technologies (PV and CHPs) can be installed in the district and buildings are connected to each other to deliver and receive the required energy.

Scenario 4: All technologies (PV and CHPs) may be placed in the buildings and both heat and power can flow internally among the consumers.

It is assumed that all the buildings and the technologies in the district are operating under one management so that none of the buildings can benefits because of sending electricity or heat to other buildings or due to installation of generation plants.

The proposed MILP computational model is coded in GAMS CPLEX [90] and has been solved for the abovementioned scenarios to obtain the optimal solution with 5% optimality gap. Scenario 4 includes 4398 variables while 210 variables among them are discrete (binary) variables.

3.4 Computational results and discussion

In the optimal design for the base scenario (conventional district), all the buildings are equipped with the boilers in which their optimal capacity are close to 5 kW. The size of the back-up boiler in each building is determined by the optimization technique so that they can meet the peak heat load for each building, i.e. their sizes coincide the highest level of heat demand inside each building. Moreover, the electricity is purchased directly from the utility grid. For scenario 1, optimization results showed that the capital cost for installation of boilers is 7% of the total investment cost while majority of the cost (most of the rest 93%) includes the operation cost. In other words, buying fuel accounted for 64% of the total annual cost. Electricity purchased from the utility grid comprises 26% of the total annual cost and causes 23900 kg CO_2 emission. Figure 4.6 shows the optimal location of boilers inside the buildings and their capacities, which is selected based on the demand of each building separately.

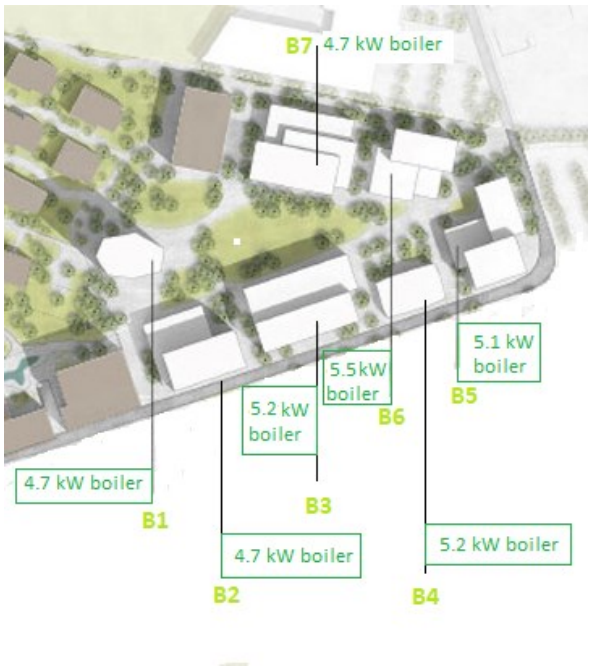

Figure 3.6 Optimal location of boilers (scenario 1)

Allowing the buildings to be equipped with other technologies (scenario 2) without connecting them results in less number of boilers (six boilers instead of seven), however, two more gas engine are chosen among CHP candidates (see Table 3.2) as combined heating and power units. The capacities of installed boilers are the same as the conventional district in scenario 1 except that B2 has lower capacity (1 kW instead of 4.7 kW) in which the gas turbine compensates the

energy deficiency. Roof of the sites B2, B3, and B7 are equipped completely with PV arrays to get the most advantage of buy-back electricity. Available surface area of the roof for these buildings are more than other sites: 150m^2, 200m^2, and 200m^2, respectively. 10% reduction in total annualized cost is observed with respect to the conventional district while 77% of the cost for the design is dedicated to capital cost. However, this high cost is covered by selling electricity generated by PV arrays on the top of three buildings B2, B3, and B7. Operational cost due to buying fuel accounts for 17% of the design cost leading to 21680 kg of CO_2. Figure 3.7 shows the optimal location of boilers, CHPs, and PV for each site and their capacities where two CHP units are identical; both are gas engines with the capacity of 4.7 kW.

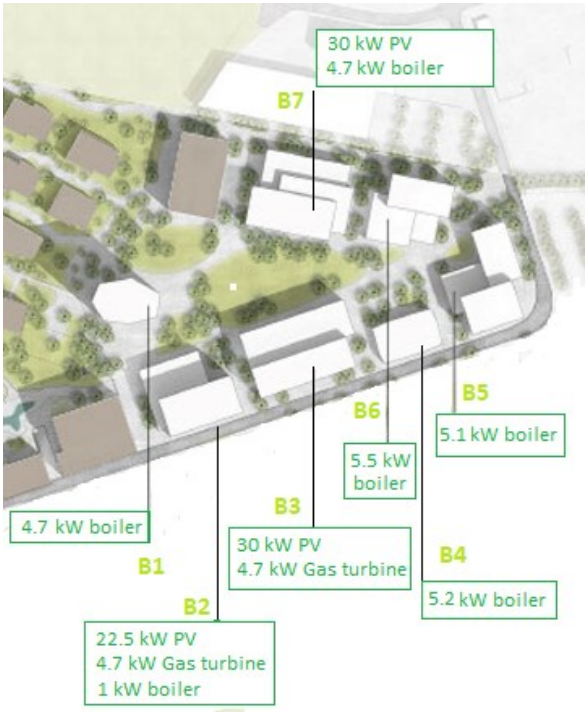

Figure 3.7 Optimal location of equipment (scenario 2)

Adding the pipeline network among the buildings to let the heat to be exchanged reduces the number of boilers to only one. This boiler with the capacity of 1.4 kW is installed in site B5. Other boilers are replaced with three CHP units (type: gas engine) where two of them have the capacity of 4.7 kW and one of them can produce 5.5 kW electricity. The configuration for PV array remains the same as in scenario 2, i.e. three sites with largest roof area are covered by PV to its maximum capacity to take the advantage of buy-back price. Figure 3.8 shows the optimal location of boilers,

CHPs, and PV for each site and their capacities as well as the optimal heat flow. It can easily be seen that the whole district is divided into three sub-networks where in each sub-network one building generates heat and /or power while the others are consumers. In other words, sites B1, B4 and B7 have no technologies installed on them, however, site B5 has a small boiler to compensate the rest of required heat produced by B3 and exported towards B4 and B5.

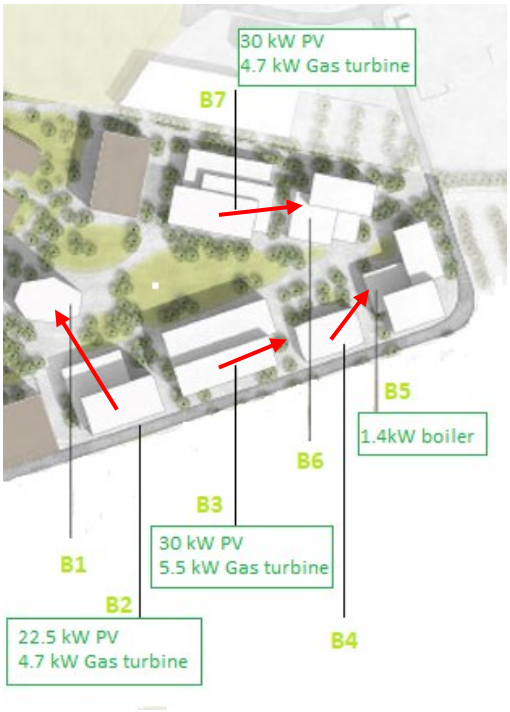

Figure 3.8 Optimal location of plants and directed heat flow (scenario 3)

It is interesting to study the benefits provided by the proposed design methodology which includes the potential of applying both heating and power networks at the same time to allow energy exchange between different sites defined as scenario 4. In this scenario, all the buildings are equipped with PV array to their maximum capacity except site B4, which is covered by 74 m^2 PV instead of 75 m^2 (available roof area). Due to the connection of buildings, they can compensate each other's power demand during the day; however, at night CHP units in site B1 and B4 are responsible to send extra electricity when it is available. Figures 3.9 and 3.10 illustrate the optimal connection and size of each equipment for scenario 4. The entire buildings are linked to each other to form only one heating sub-network. The direction is from B1 to B7 without creation of any loop as it is excluded by equation (26). Heat is produced in buildings B1 to B4 and then is

distributed to other buildings (B5 to B7). Although, shortage of electricity in site B7 is compensated by a **1** kW boiler in this building instead of drawing more heat from the neighbors. Site B3 and B7 has the highest capacity of installed PV, therefore, it is not surprising the B3 is connected to other sites to send them excess electricity. Moreover, there is a 4.7 kW gas turbine installed in B3 to strengthen the power generation. Another gas engine with higher capacity (5.5 kW) is placed in site B1 and make this building capable of exporting more electricity to the neighborhood. Therefore, this building is also connected to all other buildings in the district. Sites B3 and B7 are also interconnected indicating that in peak periods when, other buildings demand a lot of electricity, buildings B3 and B7 provide and receive electricity to balance their internal load. In total, 6 heating pipelines are built to connect the sites with the total length of 270 meters while 16 electrical connections are established. The new strategy for design and operation of the district results in 40% reduction in total annualized cost and 17% reduction in CO_2 emission compared to the conventional design.

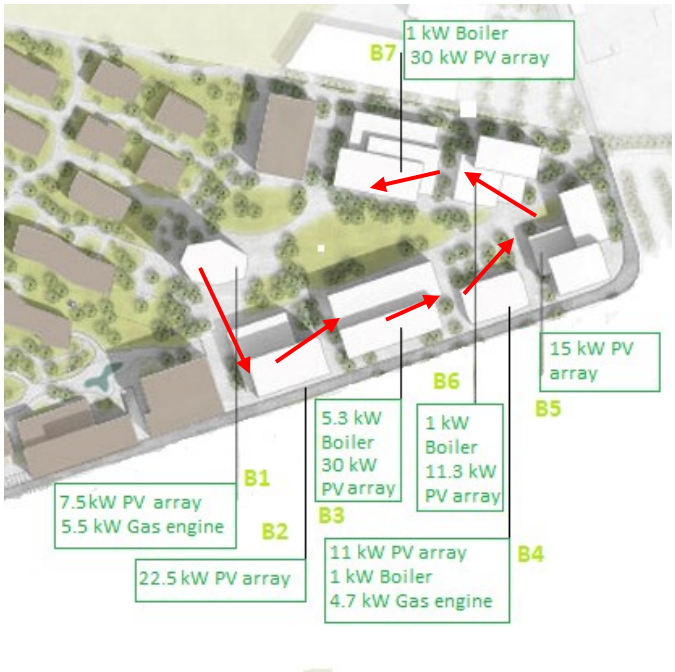

Figure 3.9 Optimal location of plants and directed heat flow (scenario 4)

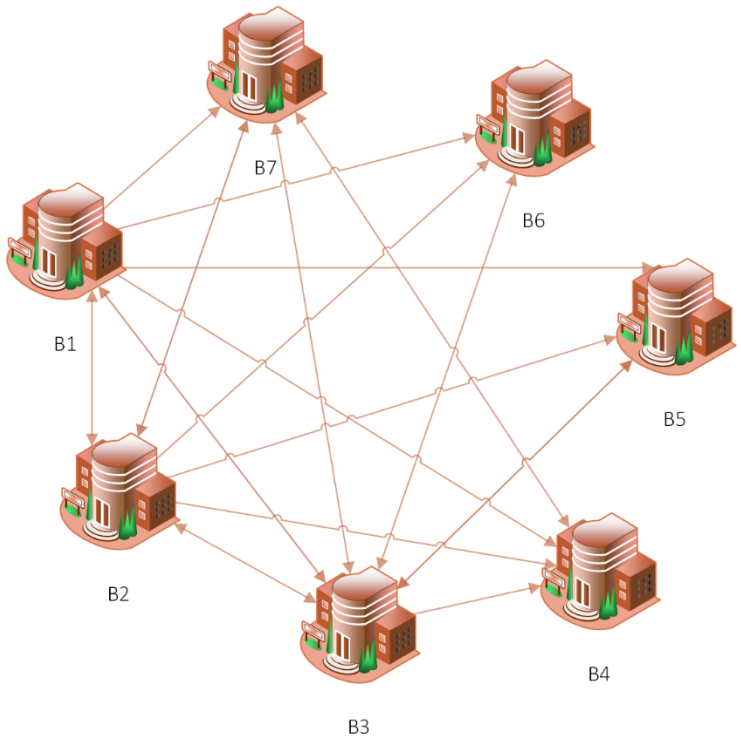

Figure 3.10 Power flow (wire connections) among the buildings in the district for scenario 4. Some energy flows are sideways and some of them are from side to side. (The scaled distances are ignored in this graph to clearly show the connections.)

By making a comparison between the objective functions for the optimal solutions, it can be seen that the adoption of the heat and power distribution networks along with the PV and gas turbines brings about the lowest total annualized cost and CO_2 emissions. However, its capital cost is higher compared to other scenarios basically because it involves installation of PV units in larger area. The results of this comparison are shown in Figure 3.11 for emission and in Table 3.6 for cost. When heat exchange is not allowed, as in scenarios 1 and 2, buildings should produce their thermal demands, and installation of CHP cannot be justified except in a case that leads to higher revenue by selling electricity to the utility grid. Therefore, the lowest CO_2 emission can be found in scenario 2 (installation of CHP in scenario 1 is not permitted) due to the two 4.7 kW gas engines installed at sites B2 and B3. However, in a case that heat exchange is possible among the sites, employing more CHP is more beneficial since the excess heat is transferred to other buildings and the electricity is exported to the utility grid to earn additional income. As Table 3.6 and Figure 3.11 show, the emission in scenario 2 is 8% more than scenario 3 because power exchange between the buildings results in taking advantage of covering all the available area with PV and

exports their electricity. It is more beneficial than investing on installation of CHP units to provide more electricity to sell. There are two gas engines installed in scenario 4, however, the three CHPs are placed in district for scenario 3. In fact, the third CHP in scenario 3 is replaced by three boilers in scenario 4 to satisfy the heating demand (see Figures 3.8 and 3.9). This conclusion can also be drawn by comparing the operation costs in Table 3.7 where the operation costs are almost the same (10 000 €), however, income from selling electricity produced by PV compensates the significant difference between the capital costs in scenarios 3 and 4.

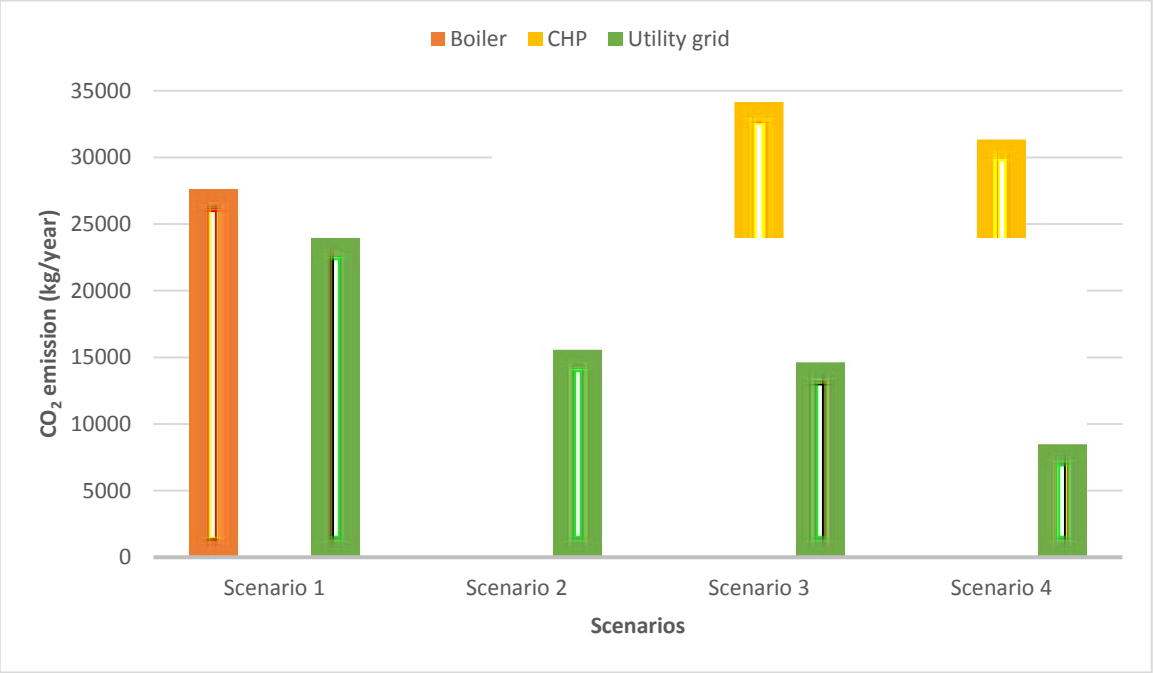

Figure 3.11 Comparison of CO2 emission between four scenarios

Table 3.6: Comparison of cost optimization for four scenarios.

Scenario	Capital cost (€)	Operation cost (€)	Emission cost (€)	Electricity purchased (€)	Electricity sold (€)	Total annualized cost (€)
1	349	8 100	875	3 365	0	12 688
2	38 127	8 633	794	2 186	38 384	11 326
3	39 975	10 130	835	2 058	43 546	9 452
4	58 561	10 023	725	1 195	62 784	7 720

Figure 3.12 shows the capability of each generation unit in each period for scenarios 3 and 4 to sell electricity to the utility grid. According to these graphs, the peak production for PV is changed significantly (51% increase), however, such a big difference cannot be seen for CHP production (only 12% reduction). This is a consequence of electricity exchange, which leads to much more PV area and more flexible power generation. Figure 3.13 illustrates the amount of electricity being used internally for scenario 3. Figures 3.14 and 3.15 show the total electrical energy bought from the grid for all buildings. It should be noted that for scenario 3, except for buildings B2, B3, and B7, all other buildings purchase electricity during all periods. The reason for this is that these sites are equipped with gas turbines so they can generate as much energy as needed and send the excess heat from cogeneration to other sites. However, in scenario 4, electricity is basically purchased when the radiation is low or when it is night. Although site B1 is connected to other sites, see Figure 3.10, its demand cannot be fully satisfied hence it needs to purchase the electricity shortage from the utility grid. Figures 3.16 and 3.17 compare the rate of heat exchange for scenarios 2 and 3. The lowest amount of transferred heat is between sites B6 and B7 because building B7 is equipped with a *1 kW* boiler while building B6 needs other building's support to meet its demand through the network. The highest rate of heat exchange is associated with the connection among sites B1 and B2, since building B2 can be considered as a "joint" which is able to transfer energy to other buildings. At the same time, building B2 is not equipped with any boiler and/or CHP unit. For connections B1→B2, B2→B3, and B3→B4 have two peaks representing they are acting as "joints" to fulfill the demands of other buildings namely B5, B6, and B7 where there is no heating plant installed. Figures 3.18 and 3.19 show the rate of heat generation from boilers and gas turbines for both scenarios. For scenario 3, boilers are operating at higher capacity since the total number of heating units in the district (4 units) is lower than that for scenario 4 (6

units). It should also be noted that boilers installed in B6 and B7 sites have the same schedule as in scenario 3 i.e. their operation profile in Figure 3.19 coincide. These boilers operate only on at the beginning and end of winter when they produce 1 kW heat i.e. they are running at their nominal capacity. Boilers in sites B3 and B4 also operate only for one period (period 6 in midseason) throughout the year. For both scenarios, the gas turbines of the B1, B2, B3, B4, and B7 site are always operating at partial load, and they supply their nominal electrical and thermal capacity when the buildings thermal demand is higher (see Figure 3.3). The boilers installed in buildings for scenario 3 are always operating at their partial load when they are on.

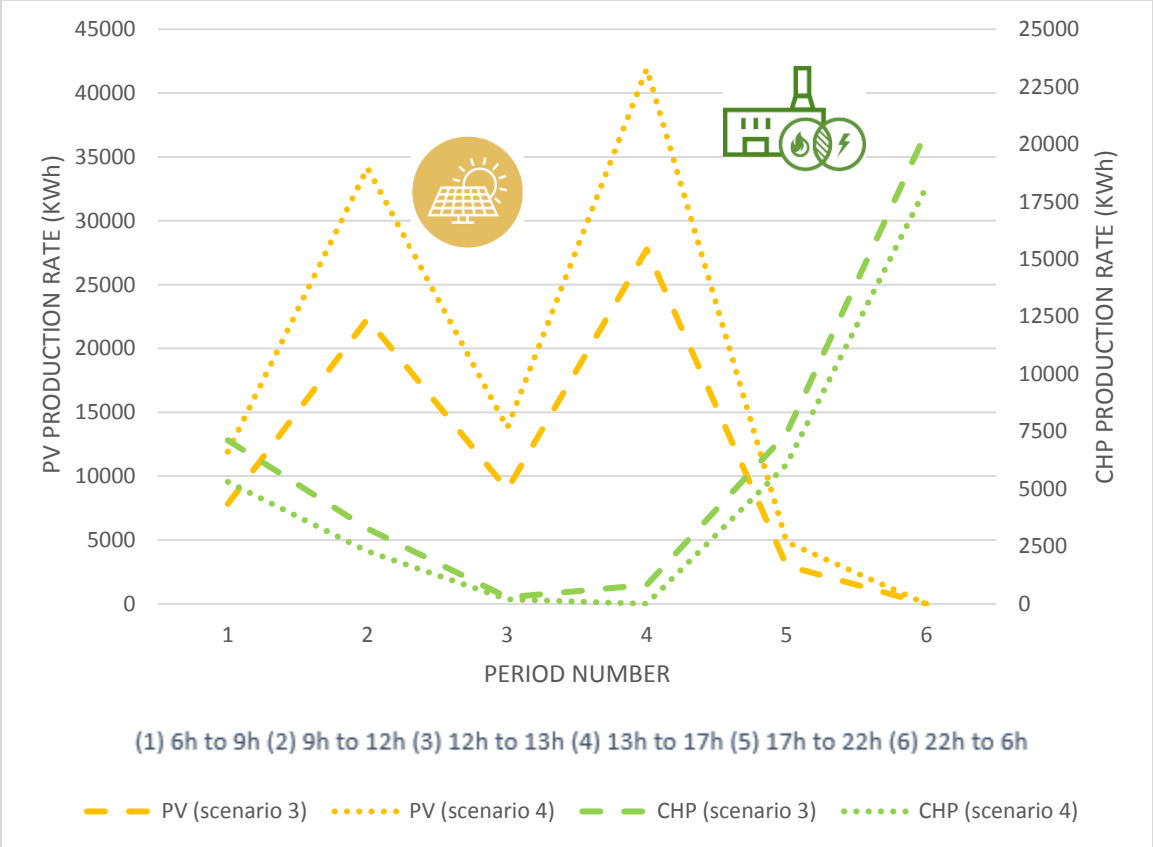

Figure 3.12 Periodic cumulative electricity sold to the grid by generation units

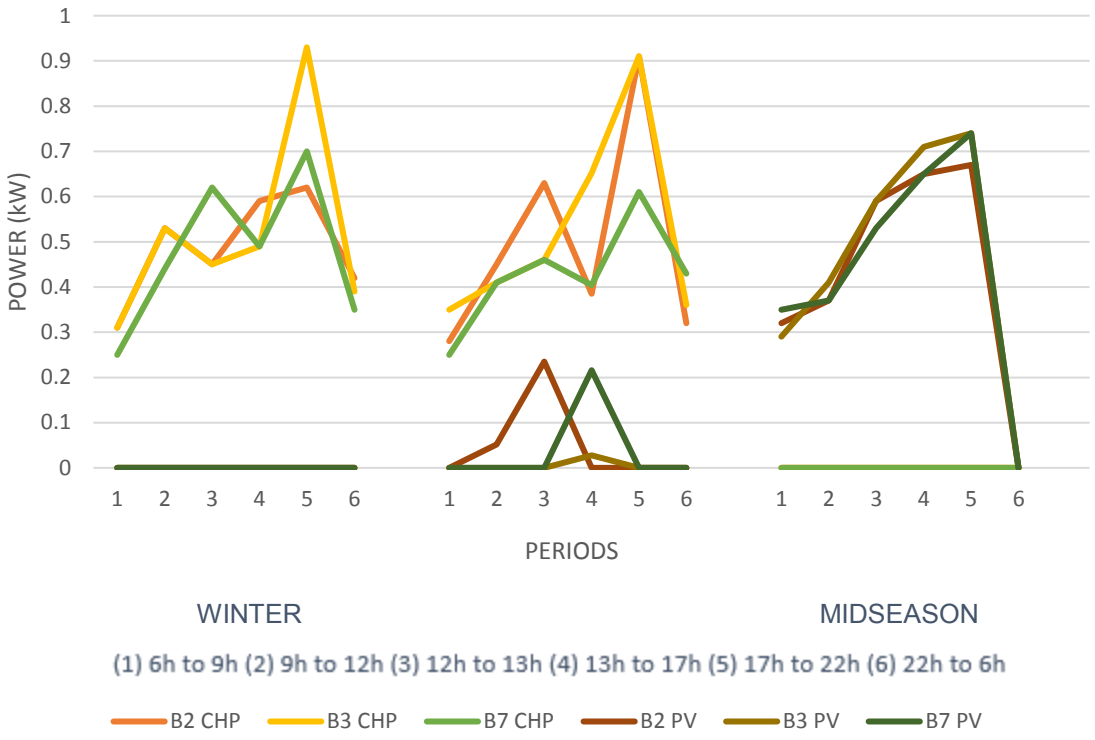

Figure 3.13 Self-used electricity produced by CHP and PV in each period (scenario 3)

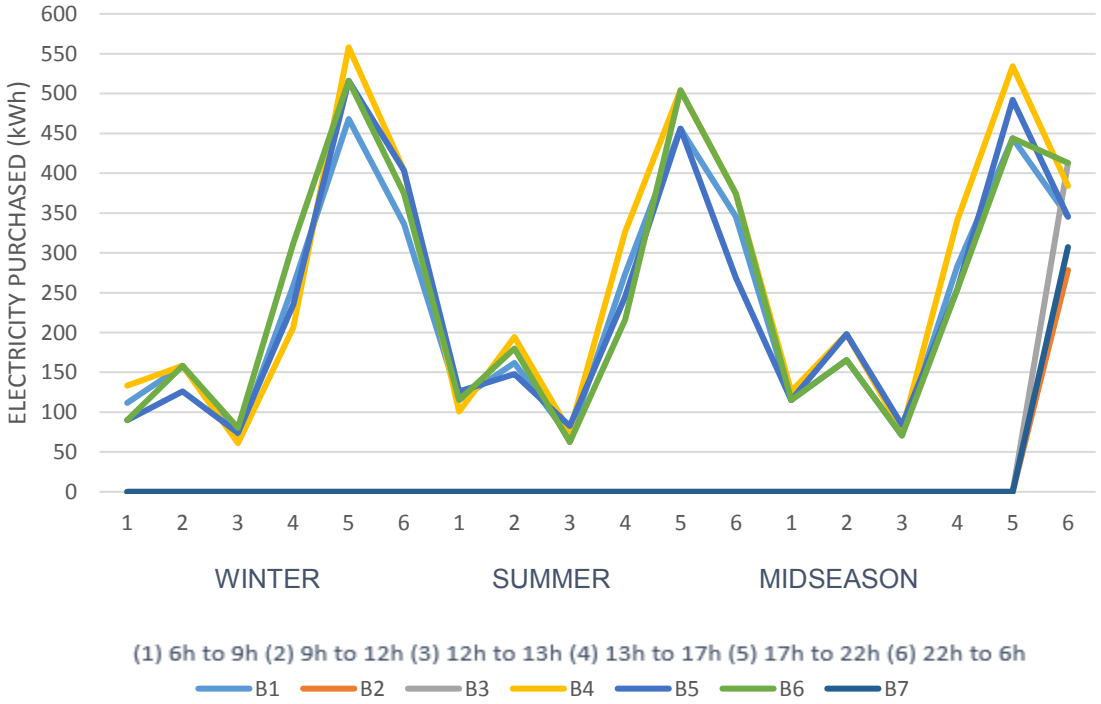

Figure 3.14 Total electricity purchased from the grid in each period (scenario 3)

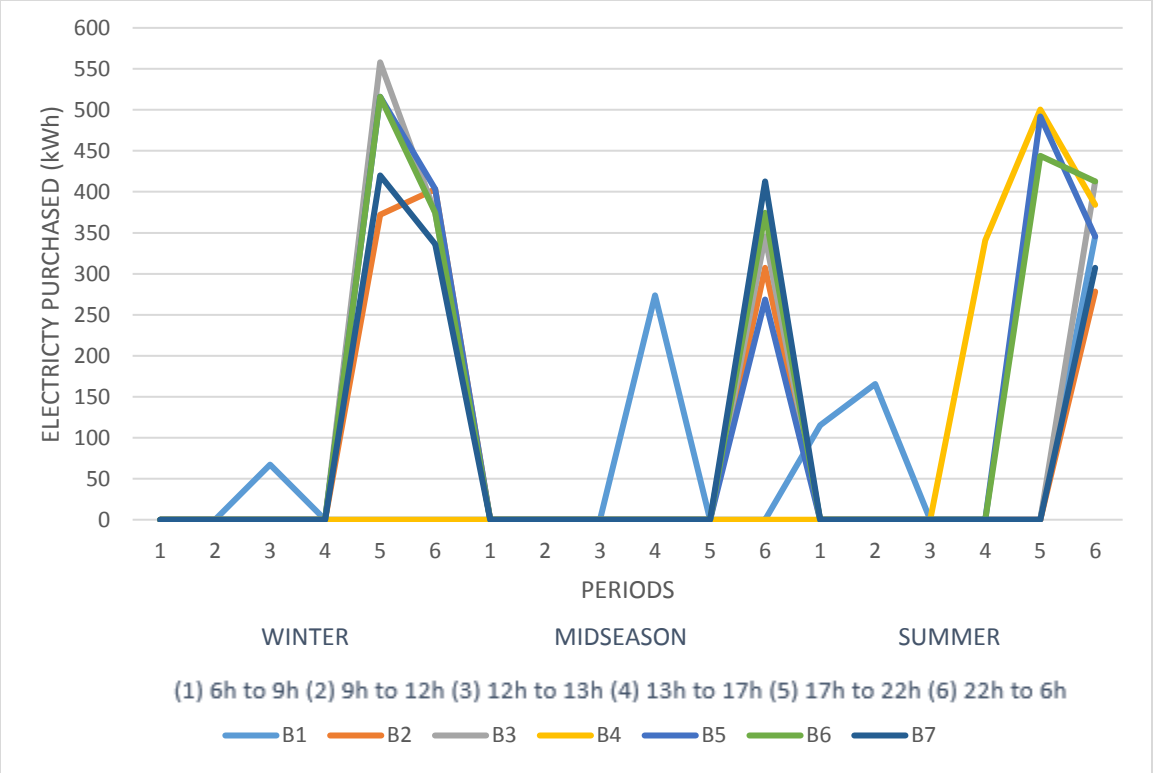

Figure 3.15 Total electricity purchased from the grid in each period (scenario 4

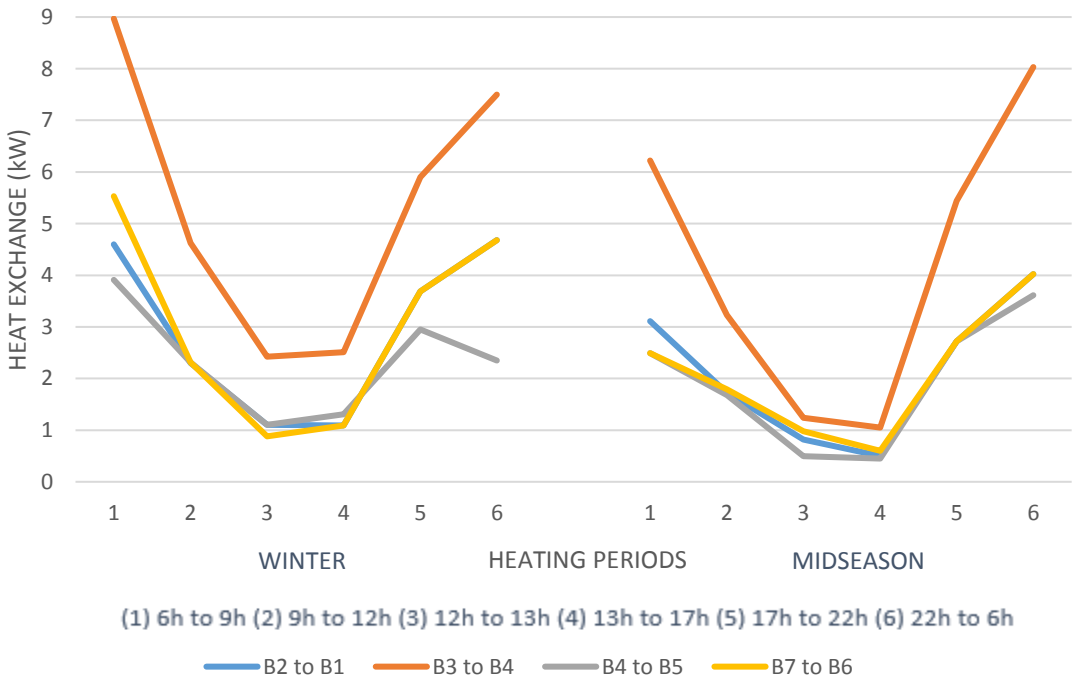

Figure 3.16 Rate of heat exchange among the buildings for each period (scenario 3)

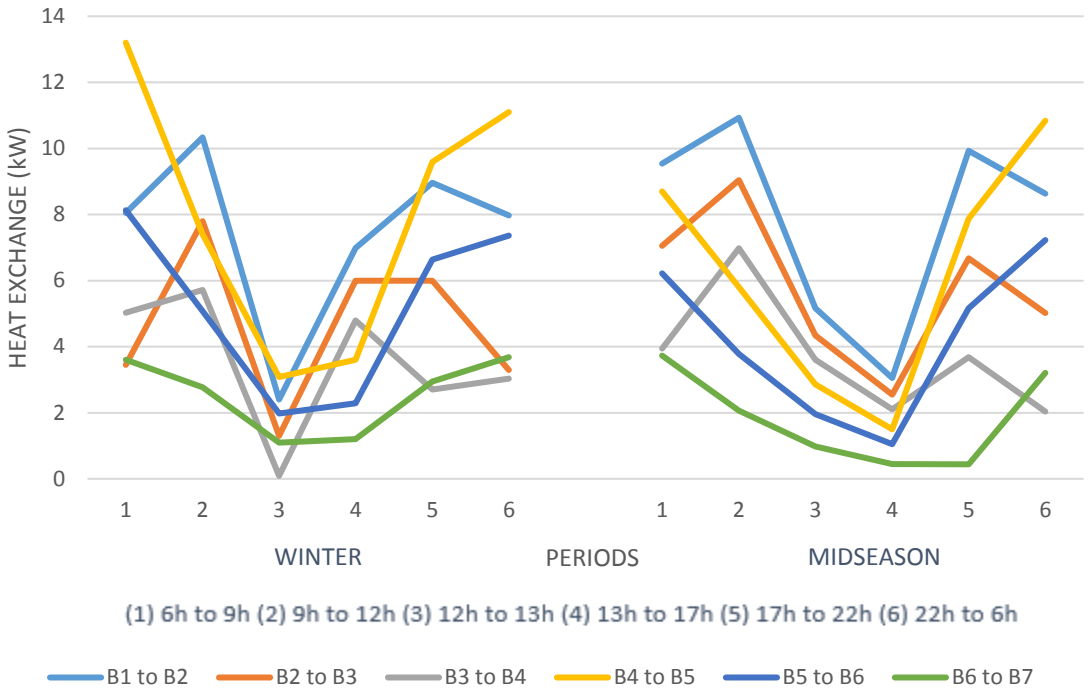

Figure 3.17 Rate of heat exchange among the buildings for each period (scenario 4)

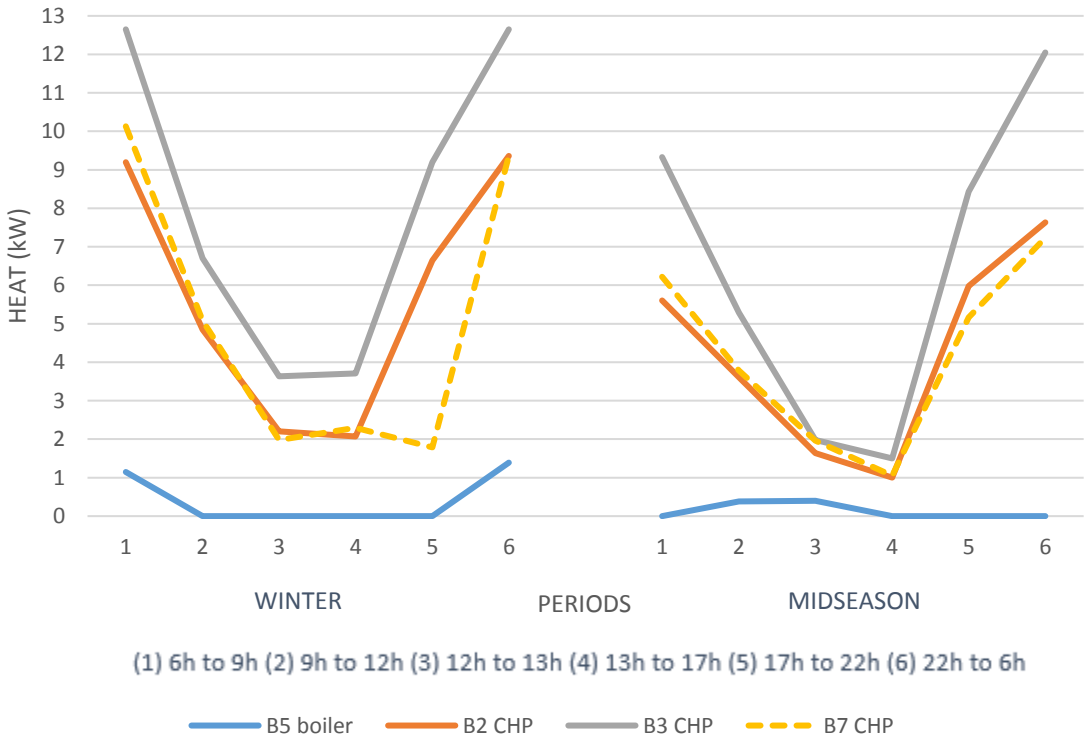

Figure 3.18 Sources of heat with their generation rates (scenario 3)

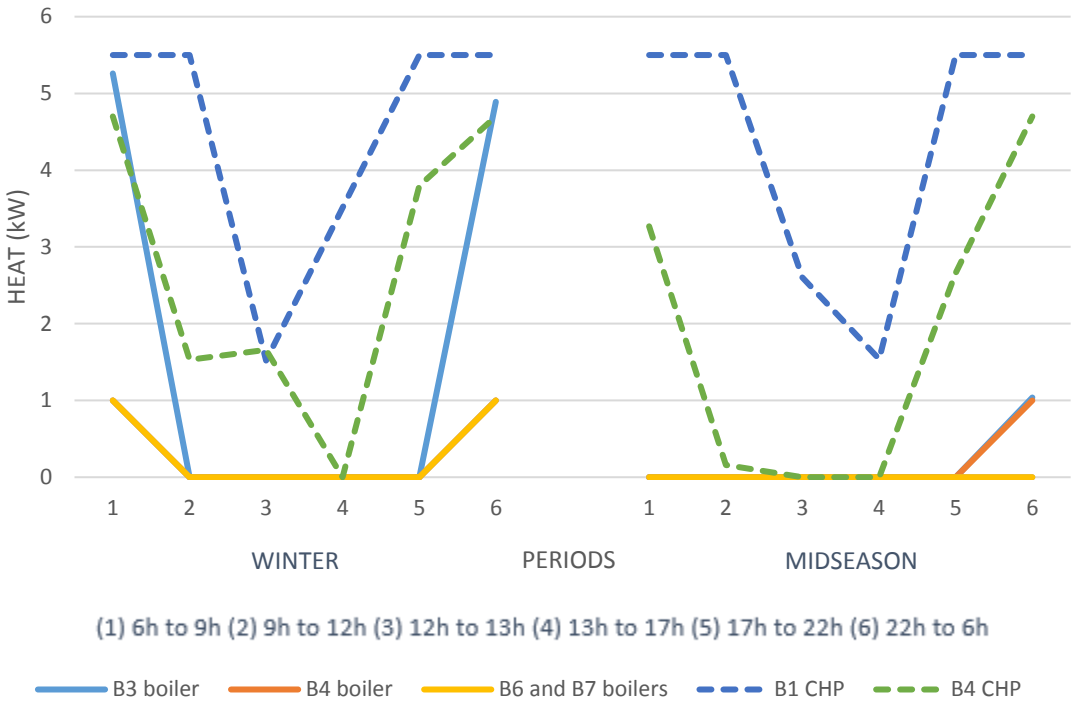

Figure 3.19 Sources of heat with their generation rates (scenario 4)

Figure 3.20 shows the effect of the maximum allowable power transfer (capacity) to the grid $E_{i,s,t}^{sel,max}$ as stated by equation (18). For lower capacities, the reciprocity effect is higher because the buildings send the extra power that they cannot sell to other buildings to be injected by them. Moreover, after a threshold which is 9 kW, the optimal cost is stabilized since the buildings cannot produce more than specific volume of electricity because of the technologies limitations.

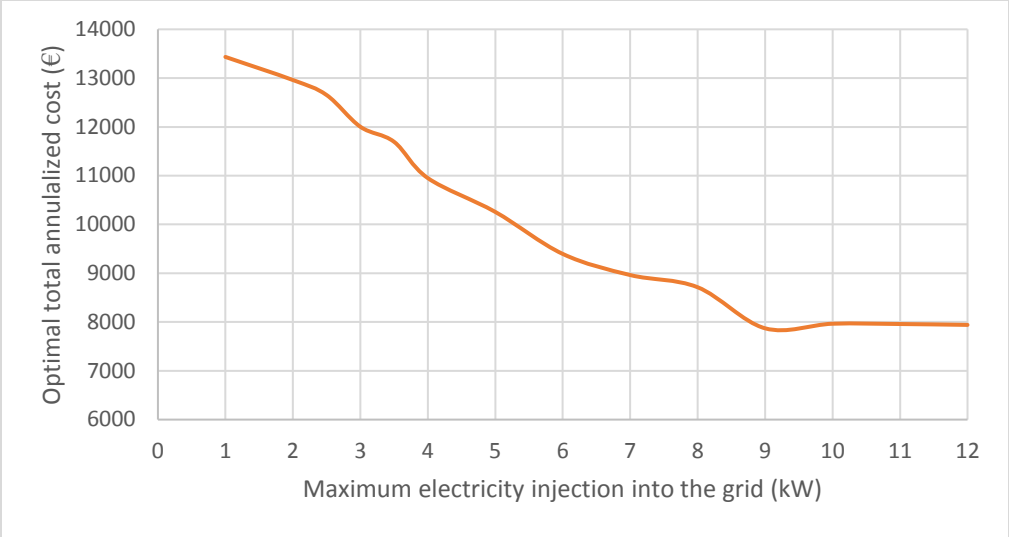

Figure 3.20 Effect of the electricity selling capacity (scenario 4).

3.5 Conclusions

In this chapter a computational optimization model has been introduced for designing a new decentralized energy generation system taking advantage of two features in 4th district generation. Specific interest has been taken in the design of the energy distribution network that facilitates heat exchange among the buildings. Effectiveness of the model is evaluated for a real district, which is under construction in Switzerland considering four different scenarios. Although laying the pipeline especially for long distances pose new operation and installation cost on the design but it was shown that heat exchange can reduce the total cost by more than 25% per year compared to the conventional district which burns fuel for boilers and buy electricity from the grid. Even more reduction was achieved with the idea of connecting all the buildings with both electrical wire and heating pipeline. This results in 40% reduction in total annualized cost and 17% reduction in CO_2 emission compared to the conventional design. Although the operation costs are almost the same for heat-exchange-only and dual-exchange districts, income from selling electricity produced by PV in the latter compensates the significant difference between the capital costs while the required electricity from the grid practically have halved. The idea presented in this thesis can be further developed to involve the impact of energy storage, which can shift the load and reduce the total cost even more. Moreover, a cost and emission comparison among centralized and decentralized system should be carried out to highlight the advantage of distributed generation.

Chapter 4

Integration of distributed energy storage into net-zero energy district systems: Optimum design and operation

4.1 Introduction

A net-zero energy district is any neighborhood in which the consumption of the buildings is offset by on-building generation on an annual basis. In this study, a net-zero energy district is identified among the set of optimal solutions and the effects of storage on its performance is investigated. It is assumed the model simultaneously optimizes the location of host buildings (energy generators), type of technologies and associated size, and the energy distribution network layout together with the optimal operating strategy. The optimization model addresses all technologies with special focus on the effect of application of energy storage. Two types of energy storage are considered inside each building: thermal energy storage (hot water tank) and electrical energy storage (battery bank). The model is applied to the new part of a district energy system located in Switzerland. The best integrated district energy systems are presented as a set of Pareto optimal solutions by minimizing both the total annualized cost and equivalent CO_2 emission while ensuring the reliable system operation to cover the demand. The results indicated that selection of the proposed optimal district energy system along with the storage brings great economic and environmental benefits in comparison to all other scenarios (conventional energy system, stand-alone system, and net zero-energy without storage).

4.2 Methodology

In this chapter, the optimal design of the district energy system has been established based on a trade-off between two objective functions: total annualized cost and annual CO_2 emission:

$$F_{pareto} = \min(F_{emi}, F_{cost}) \quad (1)$$

Hence, Bounded Objective Function (BOF) approach is employed to obtain the Pareto optimal solution. In this method the lowest and the highest acceptable achievement levels for annual CO_2 emission is specified as F_{emi}^{min} and F_{emi}^{max} and the minimum of the cost function is obtained subject to previous constraints together with a new constraint as:

$$F_{emi}^{min} \leq F_{emi} \leq F_{emi}^{max} \quad (2)$$

which indicates only one point on the Pareto optimal frontier for a specific given reasonable interval. For a specific solution, a decision maker or governmental incentives may prefer one objective function to other one. In Eq. (1), sometimes absolute values of both objective functions are normalized by reference cases to keep their order of magnitudes the same. The reference case is considered as the optimal total annualized cost of a conventional district in which the boilers inside every building covers the heat demand, and the utility grid provides the electrical load. However, in this study both environmental and economic objective functions are employed.

The optimization process is divided into four steps shown in Figure 4.1, which is solved iteratively within two different loops to constitute the Pareto optimal front. As illustrated in Figure 4.1, in the first step a value is assigned for upper and lower bounds to form the single objective function optimization. In the second step, the design of the district technologies and/or their rated capacities is determined. In the third step, the pattern of the distribution heating and power network is established. The design of the heating and power networks covers a wide range of connections among the buildings. It can consist of several smaller sub-networks as well as no distribution network at all. Moreover, selection of equipment is widely varied while each building has the potential of accepting any type of generation or storage unit. The fourth step takes care of the optimal operation and load allocation of all technologies and storage systems. Information regarding updated variables for selection of equipment is passed back to the second step to get values that are more close to the optimal solution.

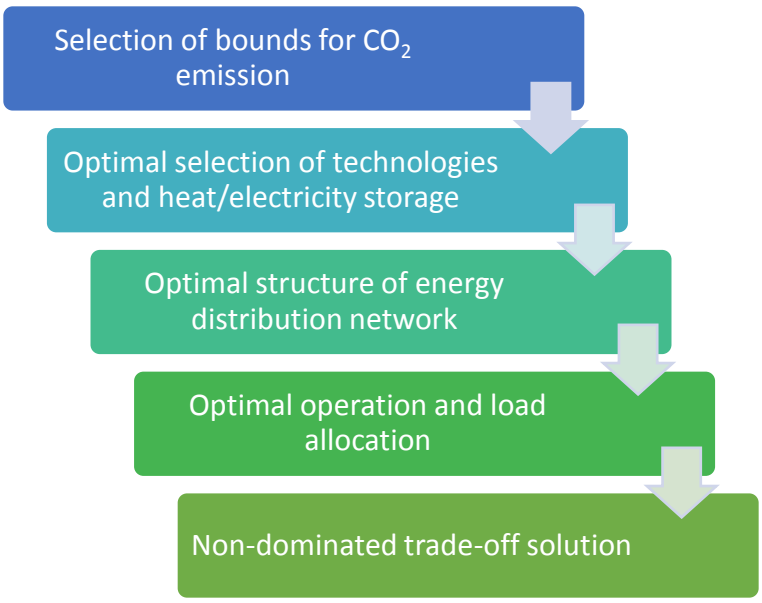

Figure 4.1 Process of the proposed optimization model

In this chapter, the energy performance of a neighborhood is examined in which several options are available to cover its power and thermal demands. The implementation of on-building equipment combined with heating and power distribution networks and storage systems are considered. The district is composed of a number of buildings with given power and thermal demand profiles as well as the distances among the buildings. Figure 4.2 shows that each building can meet its heat requirements by a CHP unit, an individual supplementary boiler, and a thermal storage tank. A thermal storage tank is used in the case of showing heat surplus, which is consumed in subsequent periods. Both back-up boiler and CHP unit are driven by natural gas. A PV array, a CHP unit, and a battery bank can satisfy the electricity load. The excess electricity may be delivered back to the utility grid to generate profits or can be stored in the battery bank for succeeding utilizations. The utility grid also plays a role in providing electricity to the district to eliminate deficit electricity when there is not enough generation or the generation is not beneficial in some periods. Heat and electricity exchanges are possible among the buildings in the neighborhood through thermal and power transmission networks. The utilization of a central controller provides the entire buildings with management of the balance on the energy supply and demand. In other words, the district electricity requirements are not billed up to a point where it is covered by local power generation inside the neighborhood otherwise the electricity consumption is billed. The input data to the optimization model and the outputs are given in Figure 4.3. All the decision variables listed in Figure 4.3 are optimized based on the objective function given in Eq. (1).

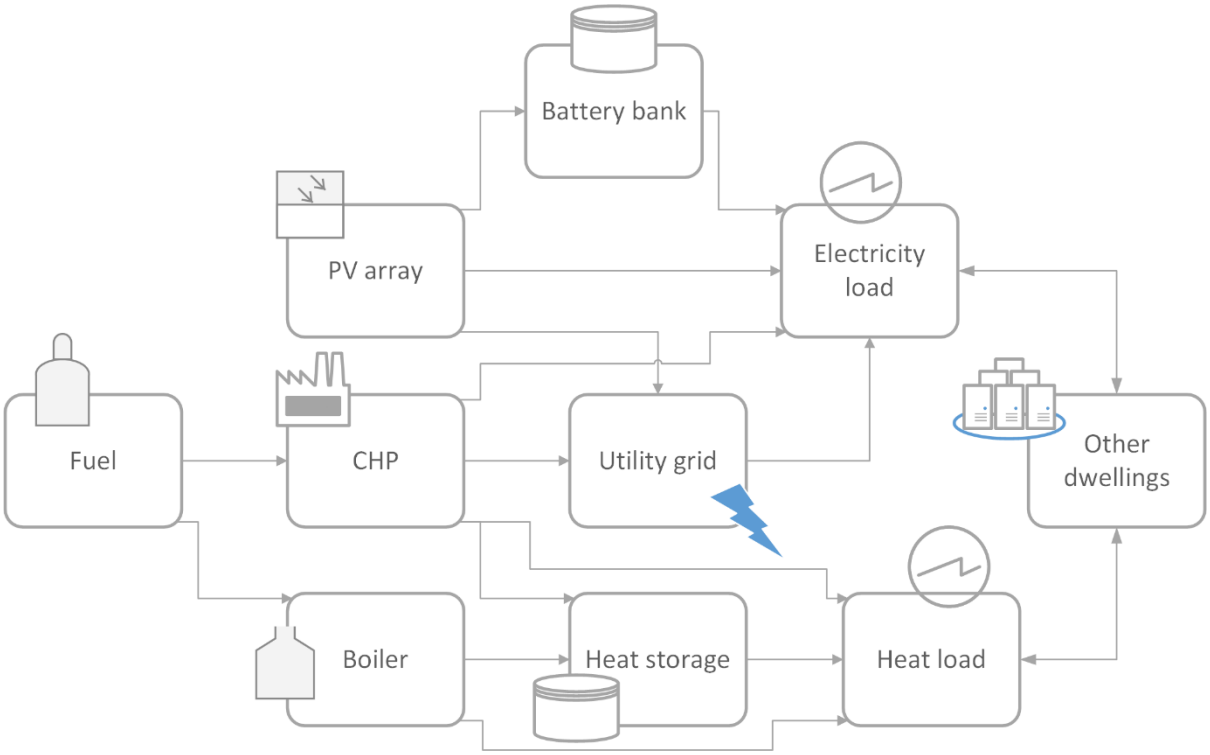

Figure 4.2 Proposed configuration of the neighborhood

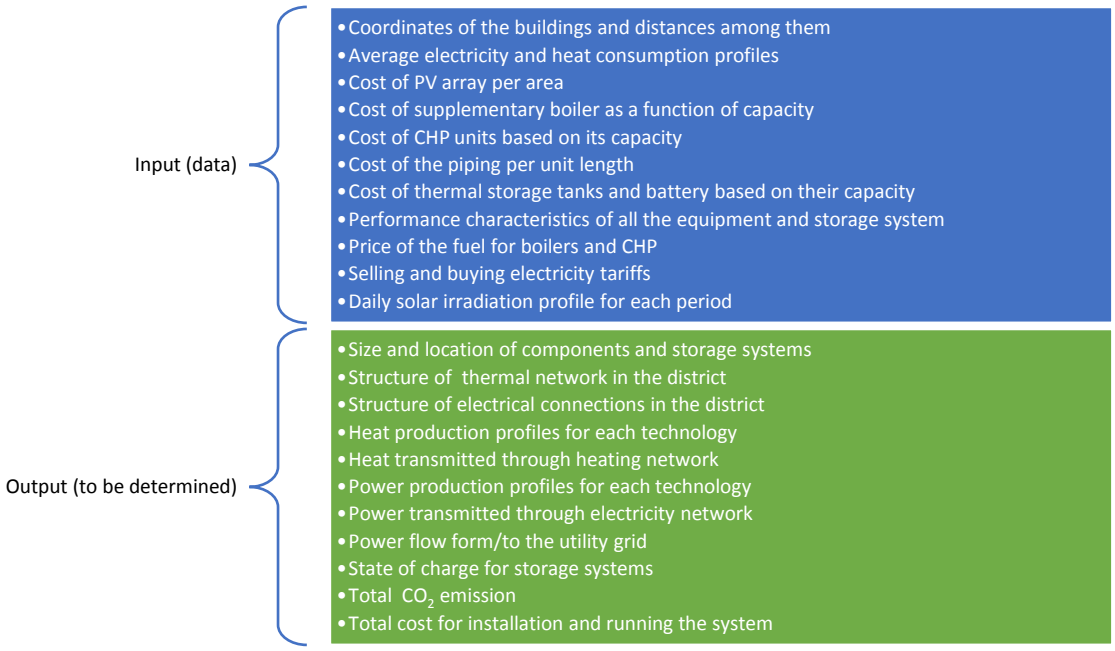

Figure 4.3 Overview of the required data in the model and its output

The total cost, F_{cost}, is the sum of annual investment cost, F_{cost}^{inv}, and the annual operating cost, F_{cost}^{op}, minus the income made by selling excess electricity to the grid, $F_{cost}^{grid,s}$, (purchase of electricity, $F_{cost}^{grid,p}$, is already included in annual operating cost). The total annual cost for purchasing electricity, $F_{cost}^{grid,p}$, from the grid is calculated by multiplying the accumulated amount of the electricity in each period by the electricity tariff in that period.

$$F_{cost} = F_{cost}^{inv} + F_{cost}^{op} - F_{cost}^{grid,s} + F_{cost}^{grid,p} \tag{3}$$

The total investment cost, F_{cost}^{inv}, is composed of the capital costs for the PV arrays, the supplementary boilers, the CHP plants, together with the cost of pipeline network among the buildings and storage systems, which are amortized by multiplying the cost of each component as:

$$\begin{aligned} F_{cost}^{inv} = {} & CRF^{PV} C^{PV} G^{PV} \sum_i A_i^{PV} + CRF^{B} C^{B} \sum_i G_i^{B} + \sum_k \sum_i CRF_k^{CHP} C_k^{CHP} G_k^{CHP} X_{i,k} \\ & + CRF^{pipe} \sum_i \sum_j C^{pipe} d_{i,j} Y_{i,j} + CRF^{HS} C^{HS} \sum_i G_i^{HS} \\ & + CRF^{BB} C^{BB} \sum_i G_i^{BB} \end{aligned} \tag{4}$$

In Eq. (4), the associated capital recovery factor (CRF) for each component is defined as:

$$CRF = r(1+r)^n ((1+r)^n - 1)^{-1} \tag{5}$$

The annual operating costs consider the cost of fuel purchased to operate back-up boilers and the CHP plants as well as the electricity purchased from the grid:

$$F_{cost}^{op} = \sum_t \sum_s \sum_i n_{s,t} \frac{Q_{i,s,t}^{B} p_{s,t}^{gas}}{\eta^{B}} + \sum_k \sum_t \sum_s \sum_i n_{s,t} \frac{p_{s,t}^{gas} E_{i,s,t,k}^{CHP}}{\eta_k^{CHP}} + F_{cost}^{grid,p} \tag{6}$$

The total electricity produced by the CHP technology is the sum of electricity used by the buildings and the electricity sold back to the grid to generate revenue.

Auxiliary boilers and CHP plants consume fuel to generate heat and power and therefore cause carbon emission. Moreover, the electricity purchased from the grid should be considered in the

environmental objective function because thermal power plants emit carbon dioxide. The total CO_2 emission, F_{emi}, can be obtained by adding them:

$$F_{emi} = \sum_t \sum_s \sum_i n_{s,t} E_{i,s,t}^{grid} I^{grid} + \sum_t \sum_s \sum_i n_{s,t} \frac{Q_{i,s,p}^{B}}{\eta^{B}} I^{gas} + \sum_k \sum_t \sum_s \sum_i n_{s,t} \frac{E_{i,s,t,k}^{CHP}}{\eta_k^{CHP}} I^{gas} \quad (7)$$

4.2.1 Optimization model

Annual operation of the installed equipment is divided into three seasons and each day is partitioned into six periods as illustrated in Table 4.1. The hourly load is assumed to be constant for each period, however, other parameters such as solar irradiation is deemed as hourly basis. The revenue is defined as the income by selling electricity to the utility grid. The overall annualized cost is composed of the capital cost of technologies (CHP units, back-up boilers, thermal storage, battery bank, and PV array), cost of purchased electricity from the utility grid, cost of establishing the distribution network, cost for operation and maintenance of the district energy system. The environmental function considers CO_2 equivalent emission caused by the operation of back-up boilers and CHP units as well as the electricity purchased from the grid. Assuming short distances among the buildings, required power for pumping and therefore associated cost are both negligible. The optimal solution of the distributed energy system described above insures that all constraints are satisfied i.e. all the installed technologies operate reliably and no reliability term is included in the objective functions.

Table 4.1 Definition of seasons and periods in the optimization model

Seasons																							
JAN		FEB		MAR		APR		MAY		JUN		JUL		AUG		SEP		OCT		NOV		DEC	
Winter				Mid-season						Summer										Winter			
Periods																							
1	2	3	4	5	6	7	8	9	10	11	12	13	14	15	16	17	18	19	20	21	22	23	24
VI				I					II			III	IV				V			VI			

Table 4.2 lists all the design constraints considered in the optimization model for all candidate technologies.

Electricity demand of each building is satisfied by sum of the electricity purchased from the utility grid, the electricity generated by the PV arrays and the cogeneration, electricity transfer among the buildings, and the battery bank:

$$E_{i,s,t}^{elec,tot} = E_{i,s,t}^{grid} + E_{i,s,t}^{PV,used} + \sum_{k} E_{i,s,t,k}^{CHP,used} + E_{i,j,s,t}^{EX} + E_{i,s,t}^{BB} \quad (8)$$

$$E_{i,j,s,t}^{EX} = E_{j\rightarrow i,s,t} - E_{i\rightarrow j,s,t} \quad (9)$$

Heat requirements can be supplied through the heat generated by back-up boilers and/or the CHP units, heat exchange among the buildings in the district, and the thermal energy storage as:

$$Q_{i,s,t}^{heat} = Q_{i,s,t}^{B} + \sum_{k} Q_{i,s,t,k}^{CHP} + Q_{i,j,s,t}^{EX} + Q_{i,s,t}^{HS} \quad (10)$$

$$Q_{i,s,t}^{EX} = (1-\sigma)Q_{j\rightarrow i,s,t} - Q_{i\rightarrow j,s,t} \quad (11)$$

In the both aforementioned heat and electricity balance equations, the power and heat flow for storage systems can be positive or negative, following the convention that negative flow implies charging and positive one means discharging, one can write:

$$Q_{i,s,t}^{HS} = Q_{i,s,t}^{HS,dis}/\eta_{dis}^{HS} - \eta_{ch}^{HS} Q_{i,s,t}^{HS,ch} \quad (12)$$

$$E_{i,s,t}^{BB} = E_{i,s,t}^{BB,dis}/\eta_{dis}^{BB} - \eta_{CH}^{BB} E_{i,s,t}^{BB,ch} \quad (13)$$

Table 4.2 Component and network constraints imposed in the optimization model

Remark	Formulation
Size of the auxiliary boilers is bounded according to market availability	$G_i^{B,lo} U_i \leq G_i^B \leq G_i^{B,up} U_i$
Maximum number of CHP to be installed in each building	$\sum_k X_{i,k} \leq n^{CHP}$
Maximum amount of heat production by CHP units in each building	$\sum_k G_k^{CHP} X_{i,k} \leq G_i^{CHP,max}$
Available roof space for each building to install PV array	$A_i^{PV} \leq \frac{A_i^{PV,up}}{\cos\theta}$
Heat can be exchanged between two buildings only in one direction	$Y_{i,j} + Y_{j,i} \leq 1$
Selling and purchasing electricity for buildings is not permitted at the same time	$E_{i,s,t}^{grid} \leq E_{i,s,t}^{elec,tot}(1 - W_{i,s,t})$
Selling electricity to the utility grid is bounded due to local/national regulations	$\sum_k E_{i,s,t,k}^{CHP,sel} + E_{i,s,t}^{PV,sel} \leq E_{i,s,t}^{sel,max} W_{i,s,t}$
Generation of electricity by PV array is limited by incoming solar irradiation	$E_{i,s,t}^{PV,sel} + E_{i,s,t}^{PV,used} \leq A_i^{PV} \eta^{PV} S_{s,p}$
Generation of electricity by PV array is limited by its capacity	$E_{i,s,t}^{PV,sel} + E_{i,s,t}^{PV,used} \leq A_i^{PV} G^{PV}$
Optimal size of the CHP units should be selected according to the market availability	See figure 6.
Heat produced by the boiler should be less than its rated capacity at any time	$Q_{i,s,t}^B \leq G_i^B$
Electricity produced by the CHP units should be less than its rated capacity at any time	$E_{i,s,t,k}^{CHP} \leq G_k^{CHP} X_{i,k}$
Heat and electricity generated by CHP units are interconnected using heat to electricity ratio	$Q_{i,s,t,k}^{CHP} = E_{i,s,t,k}^{CHP} \zeta_k$
Heat exchange among the buildings are restricted by the maximum capacity of pipeline	$Q_{i\to j,s,t} \leq Q_{i\to j,s,t}^{max} Y_{i,j}$
Electricity exchange among the buildings is bounded	$E_{i\to j,s,t} \leq E_{i\to j,s,t}^{max} T_{i,j}$
No heat circulation is allowed in the thermal distribution network	$V_j^O - V_i^O \leq 1 - (1 - Y_{i,j}) \sum_i 1$
Capacity of heat storage tank is bounded	$G_i^{HS,lo} R_i \leq G_i^{HS} \leq G_i^{HS,up} R_i$
Heat delivered by the heat storage is lower than its capacity	$Q_{i,s,t}^{HS} \leq G_i^{HS}$
Capacity of battery bank is bounded	$G_i^{BB,lo} B_i \leq G_i^{BB} \leq G_i^{BB,up} B_i$
Power delivered by the battery bank is lower than its capacity	$E_{i,s,t}^{BB} \leq G_i^{BB}$

The energy balance equation for the thermal storage system states that the total amount of available heat in the tank is equal to the amount of heat stored in the previous period plus the heat flow directed towards the tank in the current period minus the heat flow that is released to cover the demand:

$$SOC_{i,s,t}^{HS} = \eta^{HS} SOC_{i,s,t-1}^{HS} - Q_{i,s,t}^{HS} \quad (14)$$

The same description can be applied to the battery bank:

$$SOC_{i,s,t}^{BB} = \eta^{BB} SOC_{i,s,t-1}^{BB} - E_{i,s,t}^{BB} \quad (15)$$

The optimization model developed above is general, flexible, and applicable to any district with any size. In fact, for large districts and/or hourly input data the model can efficiently be solved by taking advantage of the decomposition technique (see Figure 4.3). Because both economic and environmental objective functions in Eq. (1) are convex and the linear combination is also convex, the weighting function approach can explore the whole Pareto front [100].

4.3 Illustrative example

A numerical study is illustrated in this section with seven residential and office buildings situated in Risch Rotkreuz, Switzerland. Schematic of the district energy system is illustrated in Figures 4.4 and 4.5. The area is under construction and is going to be completed by the year 2020. Therefore, the new district opens up an opportunity to investigate and evaluate various sustainable and beneficial designs and scenarios. Besides the topology of the district, other necessary input data for the optimization model is explained in the following sections:

Figure 4.4 Geographic layout of the buildings in Suurstoffi district *[93]*

4.3.1 Energy demand

Detailed information about energy requirements, for at least one year, is essential for an accurate optimal design and planning of a district energy system. Table 4.3 and Table 4.4 list the representative electricity and heating consumption profiles for the periods defined earlier in Table 4.1 for each of the seven buildings used in the case study [62]. It is important to mention that the electricity consumption profiles also include the electricity required by the compression chillers to provide cooling.

4.3.2 Electricity and fuel tariffs

Another essential input to the model is the market data for electricity buy-back price by the CHP plants and PV units together with the purchase price of electricity from the utility grid, which are all listed in Table 4.5 for each period. It is also assumed that natural gas is consumed both in the boiler and CHP plants where based on 1 kWh produced heat, the fuel tariff is 0.054 € [101] and the equivalent CO_2 emission is 0.184 kg considering the lower heating value of the fuel. Associated CO_2 emission for every 1 kWh of generated electricity in the conventional power plant, which is purchased from the grid is 0.781 kg [62, 98].

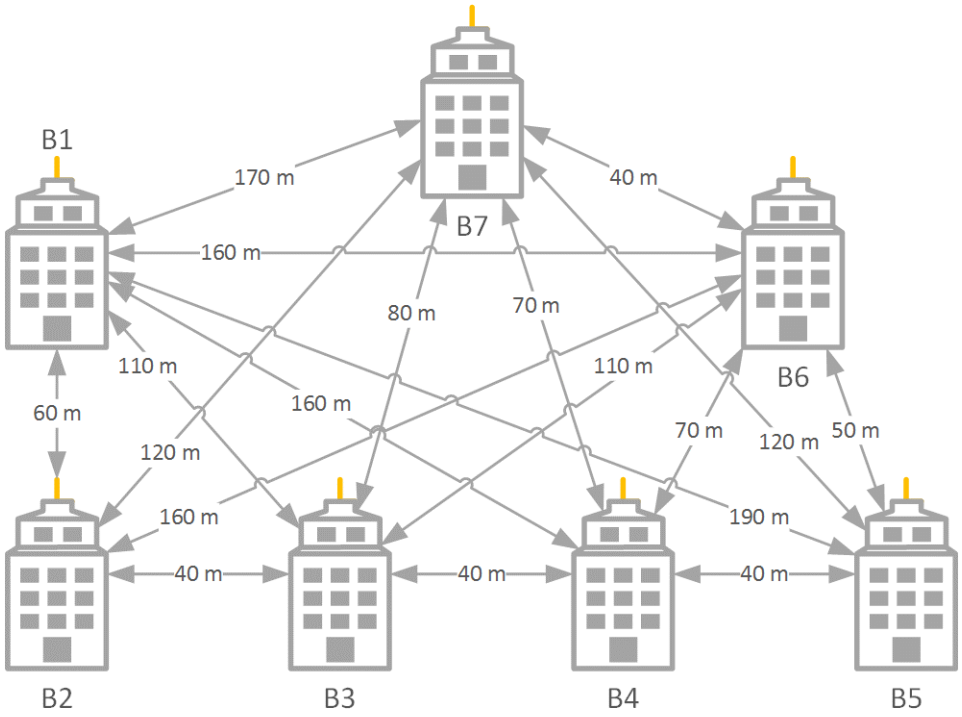

Figure 4.5 Relative coordinates and distances among of the buildings in Suurstoffi district

Table 4.3 Heat load of each building in the district for each period and season (kW)

	B7	B6	B5	B4	B3	B2	B1	
Winter	4.6	5.53	5.06	5.06	3.68	4.6	4.6	**Period 1**
	2.77	2.31	2.31	2.31	2.08	2.54	2.31	**Period 2**
	1.1	0.88	1.1	1.32	1.21	1.1	1.1	**Period 3**
	1.2	1.09	1.31	1.2	1.2	0.98	1.09	**Period 4**
	2.95	3.69	2.95	2.95	3.32	2.95	3.69	**Period 5**
	4.68	4.68	3.74	5.15	5.15	4.68	4.68	**Period 6**
Mid-season	3.73	2.49	2.49	3.73	3.11	2.49	3.11	**Period 1**
	2.06	1.72	2.06	1.55	2.06	1.89	1.72	**Period 2**
	0.98	0.98	0.9	0.74	0.74	0.82	0.82	**Period 3**
	0.45	0.6	0.45	0.6	0.45	0.5	0.5	**Period 4**
	2.44	2.72	2.72	2.72	2.99	3.26	2.72	**Period 5**
	3.21	4.02	3.61	4.42	4.02	3.61	4.02	**Period 6**

Table 4.4 Electricity load of each building in the district for each period and season (kW)

	B7	B6	B5	B4	B3	B2	B1	
Winter	0.25	0.25	0.25	0.37	0.31	0.31	0.31	**Period 1**
	0.44	0.44	0.35	0.44	0.53	0.53	0.44	**Period 2**
	0.62	0.67	0.62	0.51	0.45	0.45	0.56	**Period 3**
	0.49	0.65	0.49	0.43	0.49	0.59	0.54	**Period 4**
	0.7	0.86	0.86	0.93	0.93	0.62	0.78	**Period 5**
	0.35	0.39	0.42	0.42	0.39	0.42	0.35	**Period 6**
Mid-season	0.25	0.32	0.35	0.28	0.35	0.28	0.32	**Period 1**
	0.41	0.5	0.41	0.54	0.41	0.45	0.45	**Period 2**
	0.46	0.52	0.69	0.63	0.46	0.69	0.57	**Period 3**
	0.62	0.45	0.51	0.68	0.68	0.62	0.57	**Period 4**
	0.61	0.84	0.76	0.84	0.91	0.91	0.76	**Period 5**
	0.43	0.39	0.28	0.39	0.36	0.32	0.36	**Period 6**
Summer	0.35	0.32	0.32	0.35	0.29	0.32	0.32	**Period 1**
	0.37	0.46	0.55	0.55	0.41	0.37	0.46	**Period 2**
	0.53	0.59	0.7	0.64	0.59	0.59	0.59	**Period 3**
	0.65	0.53	0.53	0.71	0.71	0.65	0.59	**Period 4**
	0.74	0.74	0.82	0.89	0.74	0.67	0.74	**Period 5**
	0.32	0.43	0.36	0.4	0.43	0.29	0.36	**Period 6**

Table 4.5 Electricity selling and buying tariffs for each period and season (€/kWh) [33]

Periods	Period 1	Period 2	Period 3	Period 4	Period 5	Period 6
Purchase	0.1033	0.1230	0.1230	0.1230	0.1230	0.0659
Selling (PV)	0.55	0.55	0.55	0.55	0.55	0.55
Selling (CHP)	0.13	0.13	0.13	0.13	0.13	0.13

4.3.3 Available technologies

Various options for technologies and network design together with their technical characteristics and prices are listed in Table 4.6. There are six options for CHP in Figure 4.6 however all of them have the same electrical efficiency and heat-to-electricity ratio (HER). It should be mentioned that the size of the back-up boiler is a continuous decision variable and can get any value between 0

kWh and 30 kWh. The optimization model also assumes that all the conversion efficiencies for CHP plants, boiler, PV array, and storage systems are fixed, however, efficiency actually changes with load. The error introduced by considering constant efficiencies is negligible for model with high-level design [102]. Lifetime of all equipment is considered to be 20 years with the annual interest rate of 7.5% for capital costs.

Table 4.6 Basic characteristics and capital costs of candidate equipment [103, 104, 105]

Candidate technology	Capacity	Efficiency/Loss	Capital cost
PV array	0.15 kW/m^2	12%	4305 €/kW
Heat storage	0 - 30 kWh	Charge: 95% Discharge: 95%	25 €/kWh
Heating network	25 kW	Loss: 1%	40 €/kW
Battery bank	0 - 25 kWh	Charge: 95% Discharge: 95%	4000 €/kWh

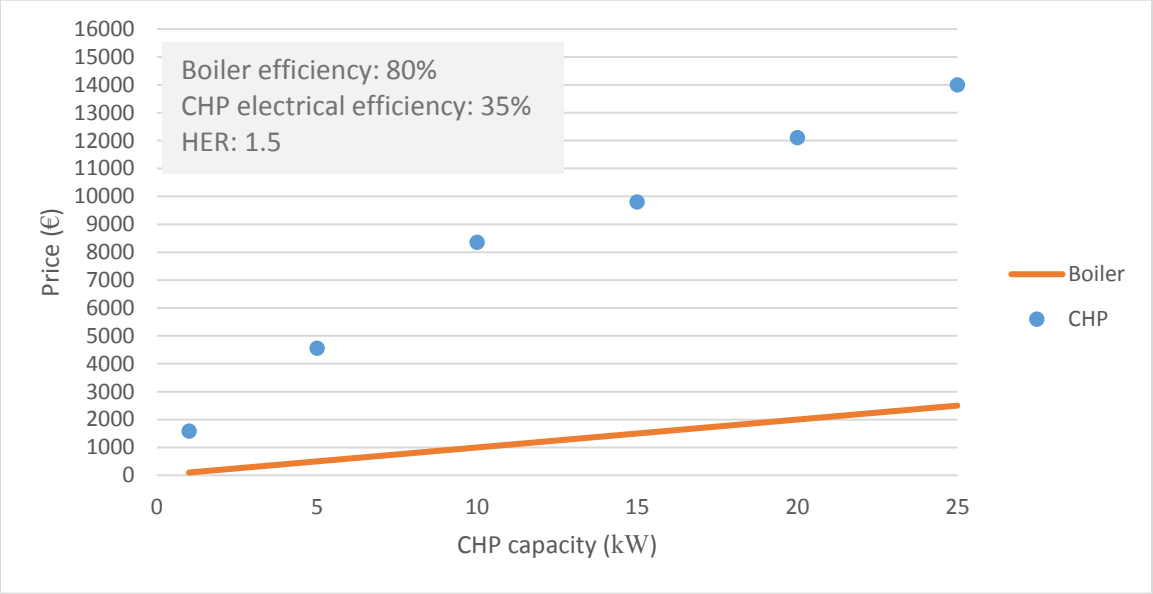

Figure 4.6 Capital cost and technical characteristics of CHP and back-up boiler *[103, 104, 105]*

4.3.4 Available PV area and solar irradiation

Figure 4.7 gives the available space to install the PV units on top of each building, while Figure 4.8 provides the hourly solar irradiation for three typical days in the periods defined earlier. It should also be mentioned that the solar radiation input to for the PV units is based on an hourly basis.

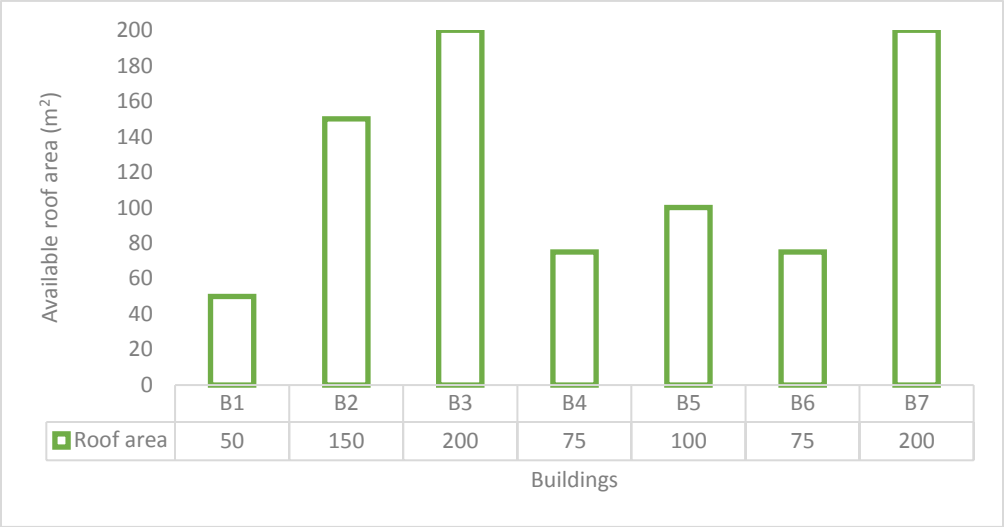

Figure 4.7 Available space in each building for PV installation

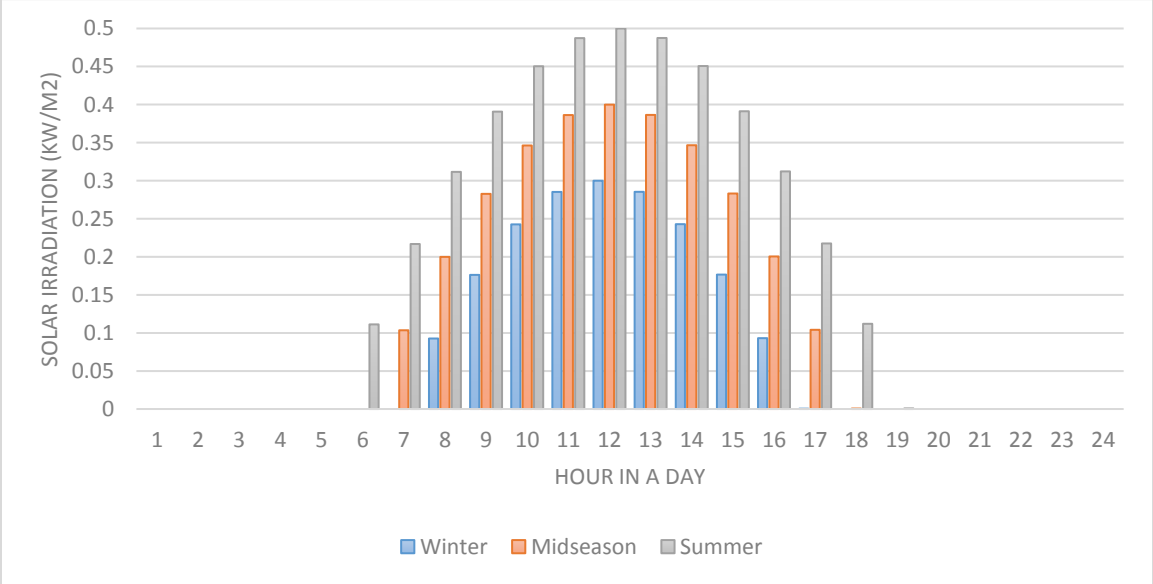

Figure 4.8: Hourly irradiation for typical days for each season

4.3.5 Setting of scenarios

Four different scenarios are envisaged and optimized to find a set of optimal solutions in which a net-zero energy district is recognized and the effect of storage is analyzed. A comparison is also made with a stand-alone district energy system:

Scenario 1 (conventional district): A conventional system is simulated where the utility grid meets the electrical demand and gas-fired boilers provide the heating demand. No other technologies including thermal storage systems and distribution network are considered in this scenario.

Scenario 2: All technologies (PV and CHPs) together with the back-up boilers but not storage systems can be installed in the district, and the buildings can interact with each other by electrical connections and heating pipelines to exchange energy and cover their loads when applicable. District is also connected to the utility grid to buy and sell electricity. A net zero-energy district can be recognized among the solutions.

Scenario 3: All technologies (PV, CHPs, boilers) including electrical and thermal storage can be installed in the district, and the buildings can exchange heat and electricity. Buildings may inject or withdraw electricity to/from the utility grid. A net zero-energy district can be recognized among the solutions.

Scenario 4 (stand-alone district): The district works as a stand-alone system and is not connected to the utility grid. PV units, CHP plants, supplementary boilers, thermal storage tank, and battery bank can be installed in the district, and the buildings may exchange heat and electricity.

The proposed MILP optimization model is coded in GAMS CPLEX and has been solved for the aforementioned scenarios to get optimal set of solutions.

4.4 Results and discussions

The simulation results showed that an optimized conventional district costs 12 000 € per year where significant portion of that is the operational cost (almost 70%). Such a system emit more than 52 300 kg CO_2 per year where 28 000 kg CO_2 is associated with the gas boiler and 24 300

kg CO_2 is from purchasing electricity from the utility grid and associated with the fuel burns in the large power plants. There is no Pareto front for the conventional district since the emission is fixed and cannot change to form a set of solutions. The result of optimization model for other scenarios is expressed as a number of feasible solutions which reflects the different capacities of the CHP, boiler, thermal storage, battery bank, and PV as well as the optimal network structure and operation of the generation units. For most of the solutions, the CO_2 emission interval is set to 1000 kg or 500 kg as it can be seen from the results in Figures 4.9 to 4.11.

For the grid connected district without any storage system installed (scenario 2), the best solution with respect to the total annual cost needs -1830 € for designing of the system and emits 31 730 kg CO_2 per year. This point on the Pareto front shows 40% improvement in the emission rate while 150% improvement is achieved in the total annual cost compared to conventional district. The negative sign implies that operation of equipment in the district generates high income i.e. the designed district is an “energy-plus” district energy system. The design is capable of compensating all its investment and operational costs by selling electricity to the utility grid to provide income for the buildings. The best solution associated with the emission requires 1325 € per year and emits 20 700 kg CO_2. This solution leads to 89% saving in cost together with 61% reduction in CO_2 release. Both best solutions with regard to each objective function are located at the ends of the Pareto front and marked with red color. The dashed line in Figure 4.9 forms a border between the districts receiving an income and the required budget for the design and operation. This threshold defines the “net-zero energy” district energy system, which produces 22 500 kg CO_2 per year. The solutions on the left hand side of the Pareto front are compact and close to each other. For instance, by earning less than only 20 € per year, the CO_2 emission increases rapidly by 1000 kg (from 31 000 kg to 32 000 kg). However, the situation is completely different on the right hand side of the dashed line where the solutions are more distant and there is a gap among them.

For the grid connected district with storage systems installed (scenario 3), the best solution with respect to total annual generates 1920 € income and emits 29000 kg CO_2 per year. It shows an improvement of 5% in cost and 9% in emission in comparison with the district without any thermal storage. The best solution associated with the emission requires 1418 € per year and emits 18 500 kg CO_2. In this case, the cost of the system is a little higher but there is 18% less emission compared to the case without storage systems. The net-zero energy district in scenario 3, produces 20 800 kg CO_2 per year, which is 15% lower than that of scenario 2. Table 4.7 shows that only one big CHP unit (10 kW) is implemented in the district and located in building B1 and

its capacity is not enough to electrify all the buildings therefore PV units serve as a secondary power generator. Further analysis of the optimal lay-out in Figure 4.7, illuminates how the energy produced by the sole generator is distributed among the buildings through the network. In this scenario, all the buildings are connected to one united pipeline system. The direction of the flow in Figure 5.7 is counterclockwise because the distance between buildings B1 and B2 is less than that between buildings B1 and B7. In other words, the shorter path is followed by the optimization procedure to lower the pipeline costs associated with building a new distribution network.

For a net-zero energy district with storage systems, Table 4.8 lists all the technologies implemented in each building as well as their capacities. Electrical energy storage (battery bank) is selected by the optimization procedure in all buildings with the same size. Moreover all the buildings are equipped with PV units to their maximum available space. The results show that implementation of more low-capacity heat generation units (5 units) is more profitable than installation of less number of larger units (especially CHP plants) with higher capacity. Analysis of the optimal structure of pipelines in Figure 4.13 shows that the district consists of 4 sub-networks: (i) Buildings B2, B3, and B4 which are connected to each other, (ii) Building B6 and B7 are linked together, (iii) Building B1 alone, (iv) Building B5 alone. Other buildings are isolated from the distribution network and have their own individual technologies. For the buildings, which receive thermal energy through the distribution network (i.e. buildings B3, B4, and B6), no heat generation unit is implemented inside them, which shows the effectiveness of heat exchange among the consumers. For the isolated buildings, thermal energy storage with higher capacity is installed to store excess heat in a case that CHP units is generating and selling electricity to the utility grid. Three small thermal storages with 1.77 kWh capacity balance the mismatch between demand and received energy in the isolated buildings at some periods of time. On the other hand, isolated buildings have the same capacity for battery as other buildings because they are connected through wires to other producers and can receive extra energy to store. Considering any two points with the same emission on Figure 4.9 and Figure 4.10, this conclusion is drawn that implementation of energy storage lessens the cost by almost 1 000 € per year. For example, for the annual CO_2 emission equal to 22 000 kg, storage system is able to decrease the annual cost from 320 € to -700 € implying 318% saving. The same conclusion can be drawn by comparison between the points with same total annual cost. For instance, for 1000 € income per year, adding storage causes a reduction of more than 1500 kg in CO_2 emission. Therefore, utilization of energy storage is profitable in both economic and environmental aspects.

For a stand-alone district no utility grid exists and all the electricity is consumed internally. Since there is no opportunity to sell electricity, no income is provided and energy storage can play a significant role in smoothing the load. As Figure 4.11 depicts, the lowest cost to design such a district is 8600 € per year where the CO_2 emission is around 24500 kg. The highest cost corresponds to a point with more than 19 000 kg annual CO_2 emission and 10 500 € for overall design and operation costs. By selecting two points with the same emissions as two net-zero energy systems discussed earlier i.e. 20 800 kg and 22 500 kg for systems with and without storage, respectively, a comparison can be made for the costs. To reach the same emission as the second scenario an extra 9 300 € should be paid per year while for the third scenario and annual payment of 10 000 € should be met. For the configuration with lower cost (9 300 €), the list of implemented technologies in the district is summarized in Table 4.9. It can be seen that no heat distribution network exists among the buildings because there is no revenue to cover the costs of pipelines. The same explanation can be given for the area of the PV units where none of the buildings are equipped with them. All the buildings are isolated and host both boiler and CHP plants together with thermal and electrical storage systems to balance the mismatch between supply and demand profiles. It is important to mention that electrical connections among the buildings (electrical distribution network) still remain because unlike the pipeline, no cost is incurred for building such an electrical network. In fact, none of the optimal solutions for a stand-alone system requires heating connections among the buildings.

A comparison for purchased and sold electricity is given in Figures 4.14 and 4.15 for two net-zero energy districts. For the system without storage, PV units take the role of supplying the major part of the electricity demand as well as providing income. However, when the storage system is implemented, the share of electricity produced by CHP plants is raised considerably because the excess energy can be stored in the battery bank in each building or exported to other buildings to be used or to improve the charge status of batteries implemented in those buildings. This share includes both the energy injected to the grid and the energy used internally inside the buildings.

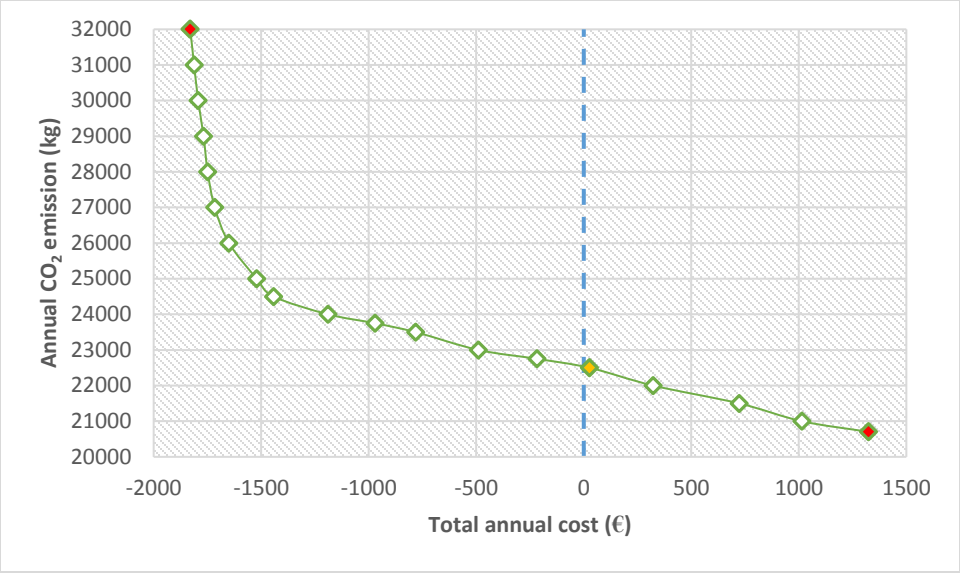

Figure 4.9 Pareto efficient solutions for design of the district energy system (grid connected without storage)

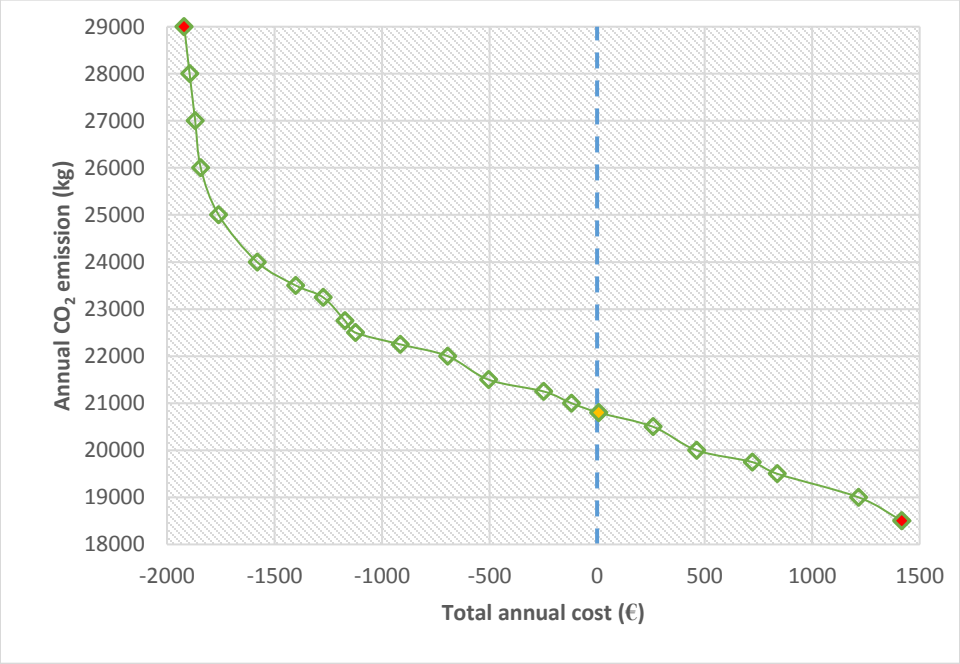

Figure 4.10 Pareto efficient solutions for design of the district energy system (grid-connected with storage)

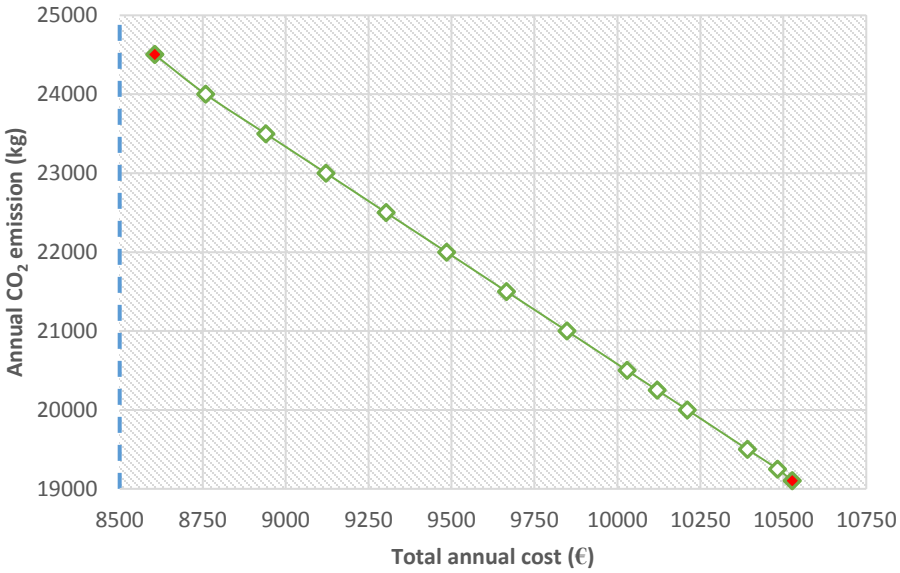

Figure 4.11 Pareto efficient solutions for design of the district energy system (stand-alone)

Table 4.7 Technologies implemented and their sizes for the optimized net-zero energy district without storage

	B1	B2	B3	B4	B5	B6	B7
CHP unit	10 kW	-	-	-	-	-	-
Boiler	-	-	-	-	-	-	-
PV	50 m^2	150 m^2	200 m^2	75 m^2	100 m^2	75 m^2	200 m^2

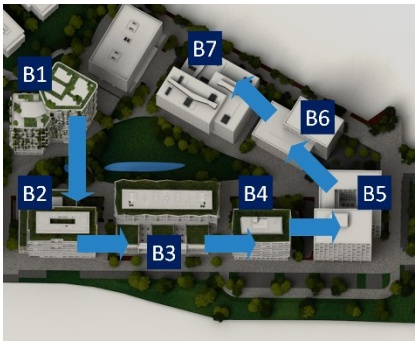

Figure 4.12 Optimal lay-out of the net-zero energy district without storage

Table 4.8 Technologies implemented and their sizes for the optimized net-zero energy district with storage

	B1	B2	B3	B4	B5	B6	B7
CHP unit	1 kW	5 kW	-	-	1 kW	-	5 kW
Boiler	1.18 kW	-	-	-	0.77 kW	-	-
TES	6.51 kW	1.77 kW	1.77 kW	1.77 kW	2.53 kW	1.77 kW	1.77 kW
Battery	5.47 kW	5.47 kW	5.47 kW	5.47 kW	5.47 kW	5.47 kW	5.47 kW
PV	50 m^2	150 m^2	200 m^2	75 m^2	100 m^2	75 m^2	200 m^2

Table 4.9 Technologies implemented and their sizes for the optimized stand-alone district with similar emission as net zero-energy district with storage

	B1	B2	B3	B4	B5	B6	B7
CHP unit	1 kW	1 kW	1 kW	1 kW	1 kW	1 kW	1 kW
Boiler	1.18 kW	1.18 kW	1.65 kW	1.65 kW	1.09 kW	1.52 kW	1.18 kW
TES	5.46 kW	4.45 kW	5.94 kW	5.94 kW	1.48 kW	5.45 kW	4.45 kW
Battery	5.05 kW	5.05 kW	5.05 kW	5.05 kW	5.05 kW	5.05 kW	5.05 kW
PV	-	-	-	-	-	-	-

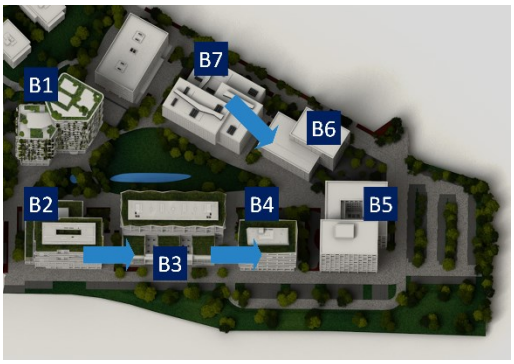

Figure 4.13 Optimal lay-out of the net-zero energy district with storage

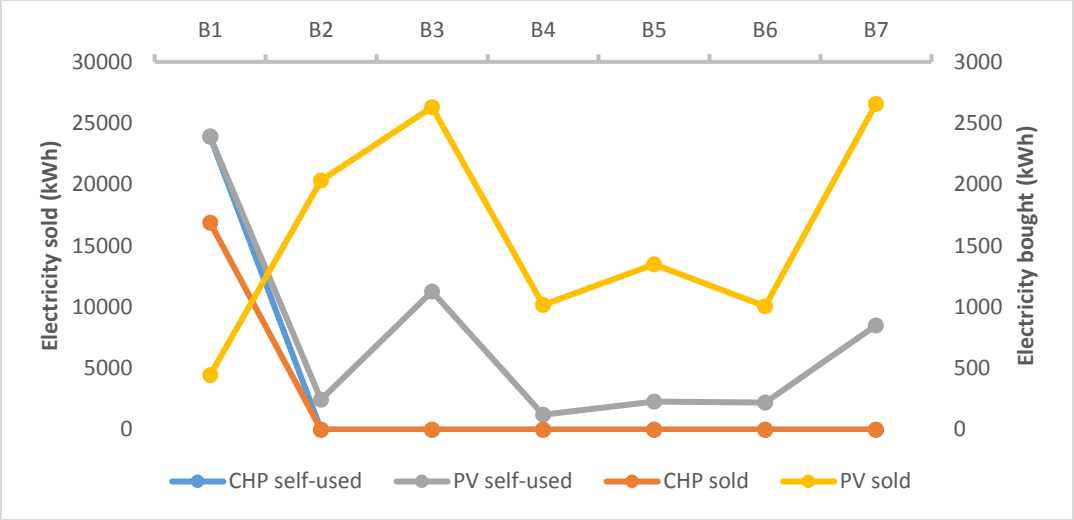

Figure 4.14 Power energy balance throughout the year for net-zero energy district without storage

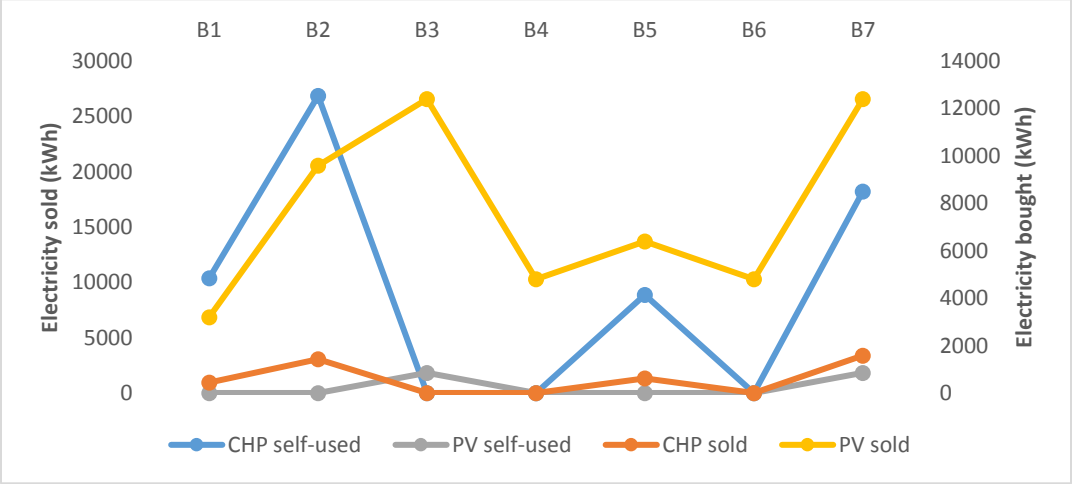

Figure 4.15 Power energy balance throughout the year for net-zero energy district with storage

The state of the charge for thermal storage for all the buildings in the district is illustrated in Figure 4.16. Building B1 has the higher level of charge because both boiler and CHP unit supply it and it is not connected to the thermal distribution network. Therefore the excess energy cannot be exported to other buildings through the pipelines and should be stored. Unlike building B1, buildings B2, B3, and B4 create a sub-network and provide the opportunity to export and receive heat. Hence, their state of the charge has the least levels among other storage systems.

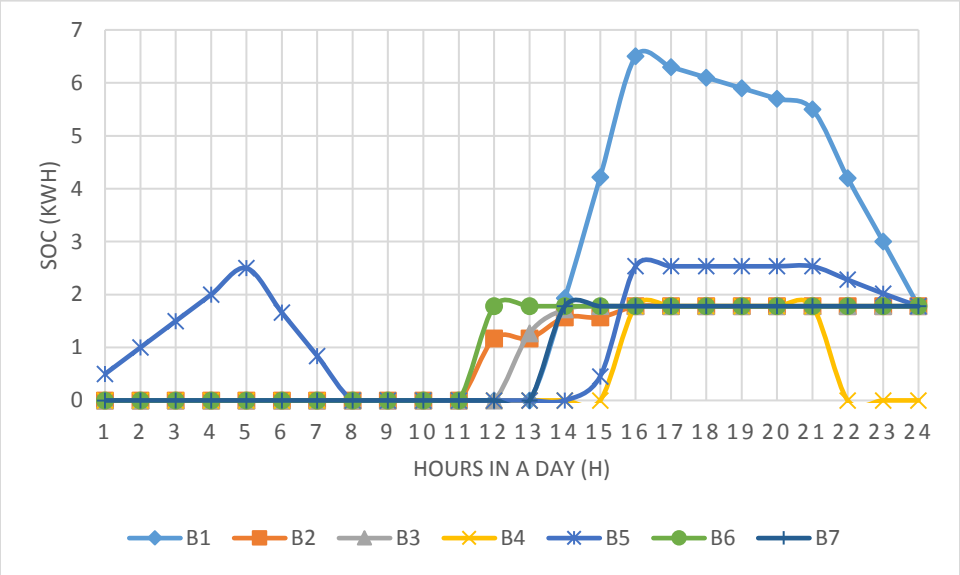

Figure 4.16 Optimal state of charge for thermal storage inside all buildings in winter

Unlike the heat storage, the trend for battery bank storage level in Figure 4.17 is virtually the same for all the buildings because there is an opportunity for the district to deliver the electricity back to the grid and generate income. Because a CHP unit with 5 kW capacity is installed in building B7, the excess electricity is exported to other consumers and therefore its level of charge is lowest in comparison with other battery banks implemented in the neighborhood.

In order to check the hourly energy balance, buildings B1 and B7 are selected and their hourly production and consumption are illustrated in Figures 4.18 and 4.19. The electricity demand curve sometimes drops below the CHP generation curve because some of the energy is transferred to other buildings and/or the battery bank is being charged.

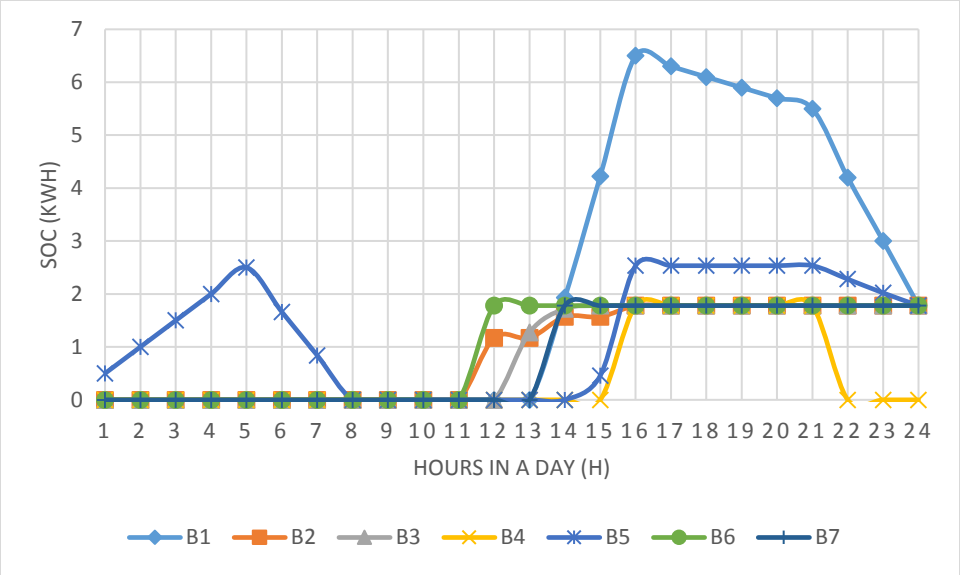

Figure 4.17 Optimal state of charge for battery bank inside all buildings in mid-season

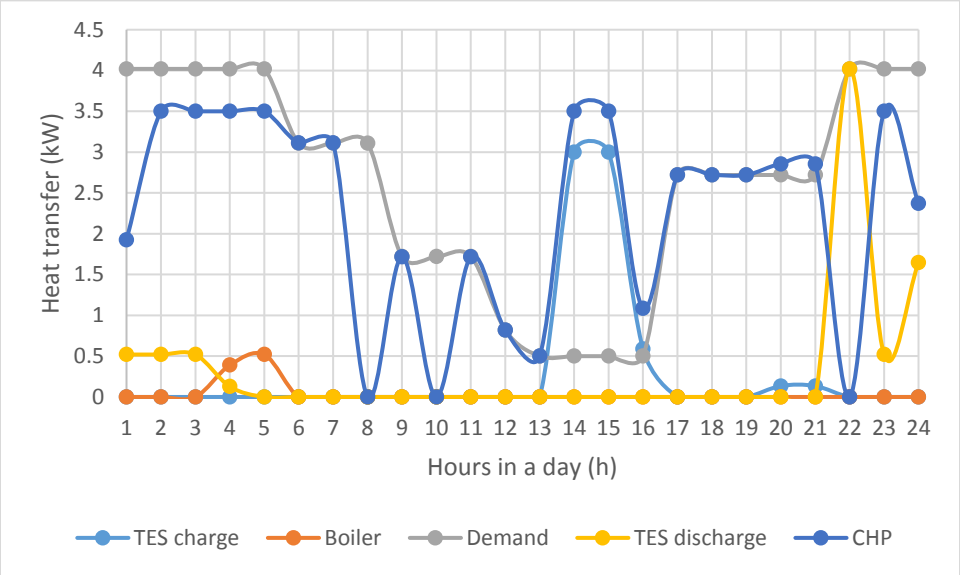

Figure 4.18 Thermal energy balance of building B1 during a typical day in mid-season

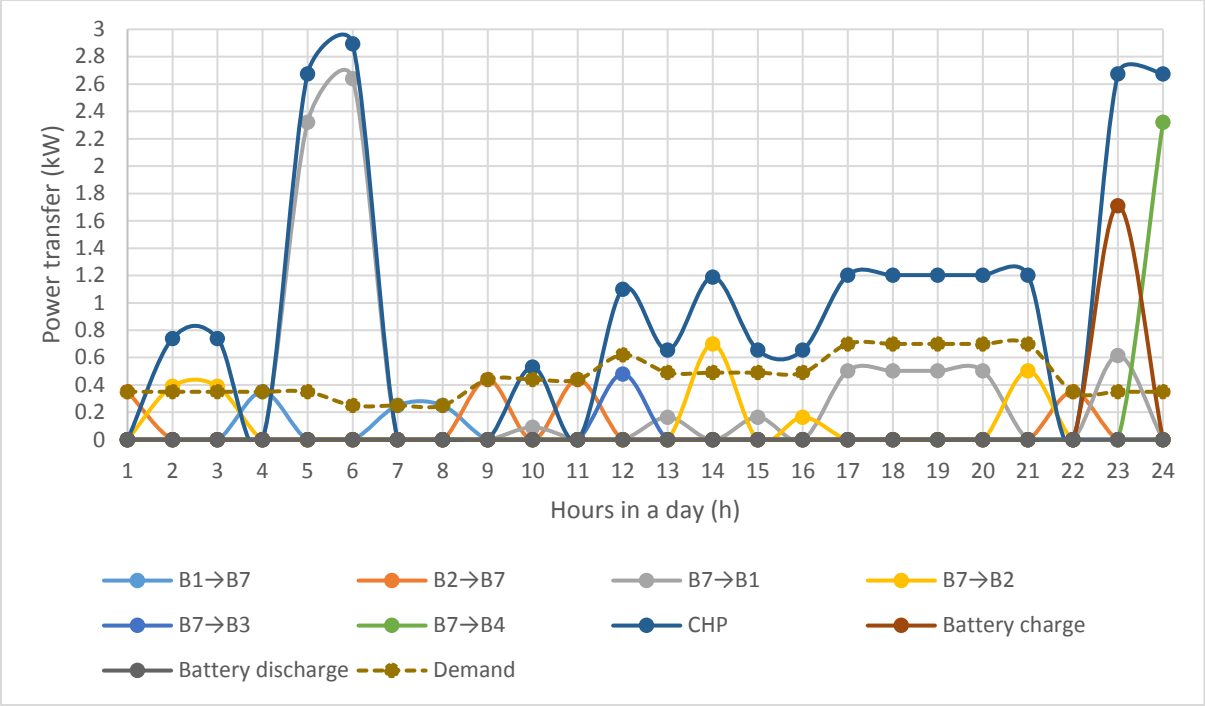

Figure 4.19 Electricity balance of building B7 during a typical day in winter

4.5 Conclusions

A comprehensive MILP optimization model is developed to optimize the design and operation of a new district system and implemented under four scenarios.

- A conventional grid-connected district with only boilers inside the buildings: This scenario has the highest cost and CO_2 emission which costs 12 000 € and emit 52 300 kg CO_2 per year.

- A grid-connected district with heat and electricity exchange and without any storage system: a net-zero energy districts is recognized in the Pareto front which offer 56% decrease in emission compared to conventional district. The optimal topology of the case without storage has only one network where all the buildings are connected to each other through the shortest path.

- A grid-connected district with heat and electricity exchange and storage system: a net-zero energy districts is recognized in the Pareto front which offer 60% decrease in CO_2

release. Structure of the system with storage has three sub-networks because releasing and storing of energy makes the buildings less independent of receiving and exporting to other buildings. With the same total annual emission, a district with storage provides more income (or costs less) compared to the district without storage. Likewise, for the same total annual cost, a district with storage release more CO_2 in comparison with the district without storage.

- For a stand-alone district, all the buildings are thermally isolated for all the optimal solutions in the Pareto front but there are still electrical connections among the buildings. The lowest cost of a stand-alone system costs 28% less per year compared to the conventional district where the CO_2 emission is reduced by 53%. The highest cost corresponds to a point with more than 63% decrease in annual CO_2 emission and 13% saving in overall design and operation costs.

Therefore, the district energy system with storage provides the best solution regarding both environmental and economic issues. Implementation of storage not only smooths the load allocation but also generates more income by selling electricity through suitable response to the heat and power demand. It is recommended for the future work to study the optimal location of power generation units in a centralized district and compare the results with a similar decentralized district.

Chapter 5

Hybrid solar and heat-driven district cooling system: a method for optimal integration and control strategy

5.1 Introduction

An optimal design and well-scheduled district cooling system is crucial for the success of the implementation of such systems especially when the cooling plant(s) are intended to connect to a group of newly-built consumers. In order to supply such customers demanding cold, a huge capital and operation investment in district cooling network is a necessity if the cooling grid is separated from the heating production units. One solution scheme is to take advantage of the heating generation units, which are off during summer to drive the cooling equipment. However, among various design parameters, the most important one is the desirable selection and combination of the heating and cooling generation equipment within the district of interest. A least-annualized-cost mathematical approach based on the mixed integer linear programming (MILP) is described in this chapter to determine the optimal integration as well as the optimal control of the flow and the storage. The test case study showed that the methodology was effective to give a huge savings in both total annual cost and emission in a wide range. Considering several heating and power sources to supply the chiller units, their integration must take into account their characteristics, operating costs and technical constraints. As a consequence, even with a limited number of plants, the best solution to the location, type and size of the hybrid technologies as well as the optimal control strategy in which the district plants operate to incur the lowest cost or exploit the highest available share of renewable sources, or other desirable goals. The current

work concentrate on finding a solution to the following issues by proposing a mathematical approach: (1) **optimal integration** of heating technologies into district cooling, (2) **optimal layout** of the cooling grid, and (3) **optimal control** of the chilled water flow and storage media.

5.2 Model description

In this chapter, the district cooling system is composed of the production and consumption of cooling energy, storage of the chilled water and its distribution to individual buildings on the site through the pipeline grid, storage of hot water to be supplied to the absorption chiller, and the power network among the buildings and their interaction with the utility grid. As it can be seen in Figure 1, each building can host the potential heating and cooling technologies as well as the photovoltaic panels and storage tanks. The heat generated in the boiler, combined heat and power (CHP), and solar thermal panels are utilized as the input to the absorption chiller and may be stored to be consumed during the on-peak hours or when solar energy does not provide sufficient heat. The electric compression chiller may be driven by the electricity generated in the CHP units, PV electricity, and the electricity purchased from the utility grid. The cooling units (absorption and compression chillers) shall lower the return water temperature that circulates in the cooling distribution grid to the desired water temperature. The aim of the cold storage is to store the chilled water produced in cooling plants during low consumption periods and inject the water into the host building and/or the cooling grid during hours with high demands. It is also assumed that no equipment are considered as preinstalled in the district as well as the distribution network that connects the buildings together. It is assumed that all the buildings and the technologies in the district runs under one management (owner) so that none of the buildings get benefits because of sending electricity or cold to other buildings or due to installation of generation plants. Sharing of cooling and power among the buildings are allowed similar to the heat exchange featuring in 4^{th} generation district heating [106], however, cold circulation is avoided to prevent erroneous results.

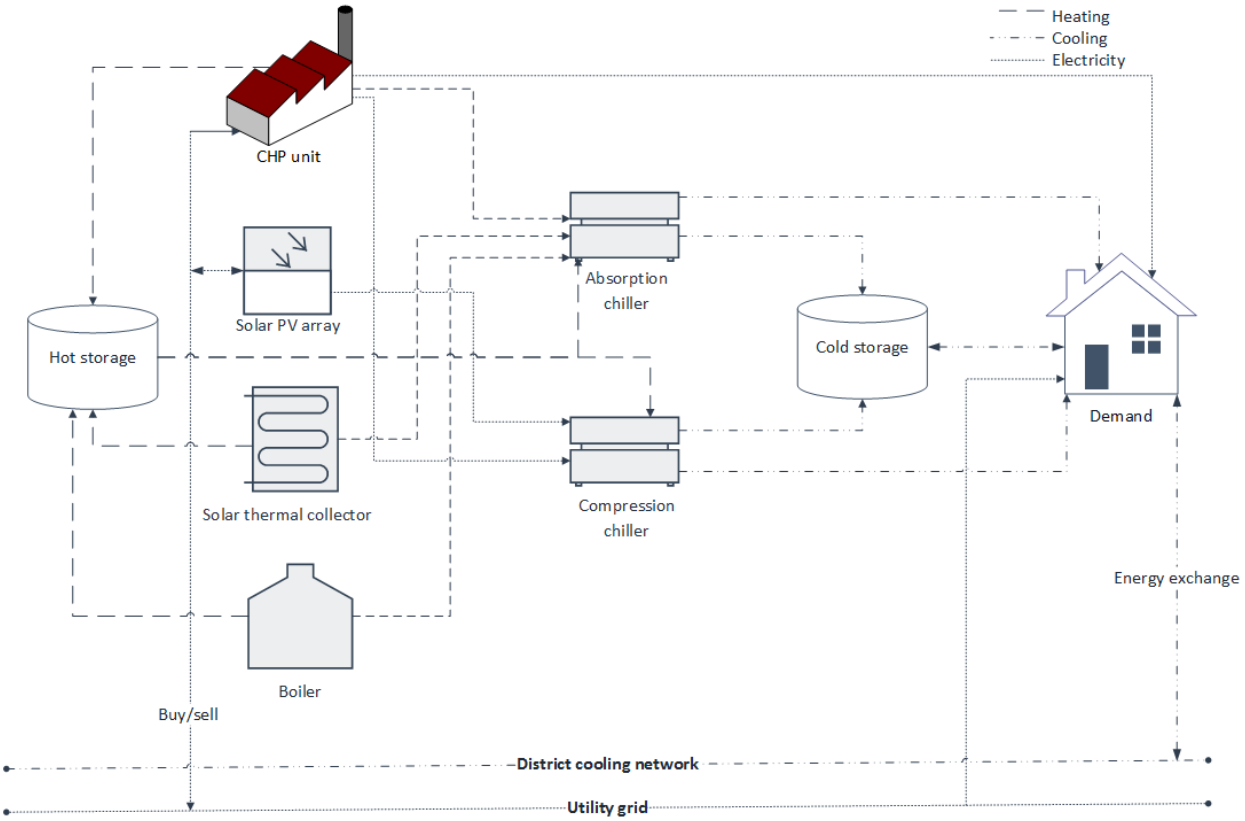

Figure 5.1 Schematic view of the proposed district cooling integrated with heating and power network

5.2.1 Objectives definition

The problem is defined as the minimization of the total annualized cost including both the capital and operating costs for any energy equipment implemented in the district as well as the cost arises from purchasing/selling electricity from/to the utility grid and the capital cost required to establish the cooling pipelines. Moreover, the CO_2 emission resulted from combustion of fossil fuels in the boiler and the CHP units together with the equal CO_2 emission comes from purchasing electricity from the utility grid are both included in the objective functions. The annuity factor is utilized in calculation of the capital cost for various technologies and cooling pipelines. The annualized operational costs are calculated as sum of the operational costs for all the equipment over several defined periods. Thus the objective function can be expressed as:

$$objective\ one = C_{inv} + C_{op} + C_{elec,net} \tag{1a}$$

$$objective\ two = \frac{C_{car}}{C_{ct}} \tag{1b}$$

Investment cost: The overall investment cost is comprised of the costs for the solar photovoltaic array (PV), solar thermal collector panels (sol), boilers, the CHP technologies, electric compression chiller (cc), absorption chiller (ac), hot water tank (hs), cold water tank (cs), and the investment cost of the network, which all are annualized utilizing the annuity method through multiplying the price of each equipment by the annuity factor (AF) as:

$$\begin{aligned} C_{inv} = & \sum_q \sum_i AF_q^{PV} C_q^{PV} G_q^{PV} A_{i,q}^{PV} + AF^B C^B \sum_i G_i^B + \sum_k \sum_i AF_k^{CHP} C_k^{CHP} X_{i,k} \\ & + AF^{pipe} \sum_i \sum_j C^{pipe} d_{i,j}\, Y_{i,j} + \sum_r \sum_i AF_r^{sol} C_r^{sol} G_r^{sol} A_{i,r}^{sol} \\ & + \sum_l \sum_i AF_l^{cc} C_l^{cc} Z_{i,l} + \sum_m \sum_i AF_m^{ac} C_m^{ac} T_{i,m} + \sum_i AF_i^{hs} C_i^{hs} G_i^{hs} \\ & + \sum_i AF_i^{cs} C_i^{cs} G_i^{cs} \end{aligned} \tag{2}$$

Different types of each technology is identified by the second index in the summation in equation (2), for example for PV array, index q shows various types of candidate PVs. The nominal capacity of each equipment is denoted by G and indices i and j show the buildings labels.

In Eq. (2), the CHP technologies, solar arrays, and the cooling units for both compressor- and heat-driven cooling machines may be selected among several possible candidates. However, there is only one type for each of boiler, hot and cold storage media, and pipeline (basically pipe type and diameter) is considered in this study. Similar to the investment cost, the running costs are expressed linearly proportional to the generated electricity by the CHP units, consumed heat from the boiler or distributed cooling energy by the compression or absorption chillers. Moreover, different annuity factors may be envisaged for different components as considered in Eq. (2).

Operation cost: Running cost coefficients are defined for the different parts of the system. The overall operating cost is the sum of all costs for all kinds of technologies implemented in the district over the period the equipment are on to feed chillers with heat and/or electricity:

$$C_{op} = \sum_{t}\sum_{s}\sum_{i} \Delta_{s,t} \frac{Q^{B}_{i,s,t} p^{gas}_{s,t}}{\eta^{B}} + \sum_{k}\sum_{t}\sum_{s}\sum_{i} \Delta_{s,t} \frac{p^{gas}_{s,t} E^{CHP}_{i,s,t,k}}{\eta^{CHP}_{k}} \tag{3}$$

As it is indicated in Equation (3), the operation cost is proportional to the generated heat (Q) by the boiler (B), the produced electricity by the CHP units (E), the total duration of each period (t) for all representative seasons (s), and the price (p) of the gas. Different types of CHP units denoted by k may have different efficiencies (η).

Carbon emission cost: The heat production plant that consumes fossil fuels (i.e. boilers and CHP units) emit carbon dioxide. Likewise, part of the carbon emissions comes out of the electricity generated in conventional power plants for electricity production that is utilized by the electric cooling machine to distribute thermal energy as well as the electricity to satisfy the requirement of the district:

$$\begin{aligned} C_{car} = C_{ct} \Bigg[& \sum_{l}\sum_{t}\sum_{s}\sum_{i} \Delta_{s,t} E^{pur,cc}_{i,s,t,l} I^{grid} + \sum_{t}\sum_{s}\sum_{i} \Delta_{s,t} E^{pur,dem}_{i,s,t} I^{grid} \\ & + \sum_{t}\sum_{s}\sum_{i} \Delta_{s,t} \frac{Q^{B}_{i,s,p}}{\eta^{B}} I^{gas} + \sum_{k}\sum_{t}\sum_{s}\sum_{i} \Delta_{s,t} \frac{E^{CHP}_{i,s,t,k}}{\eta^{CHP}_{k}} I^{gas} \Bigg] \end{aligned} \tag{4}$$

The carbon emission cost is proportional to the carbon intensity (I) generated as a result of the boiler combustion fuels (B) or CHP units or because of the electricity (E) purchased from the national grid (i), during all seasons (s), for all periods (t), and for all types, i.e. k for CHP units and l for compression chillers (cc). A portion of the electricity purchased from the grid satisfies

the buildings electricity demand (dem) and the rest goes into the compression chiller to generate cooling (pur).

Electricity costs: The electricity ($elec$) purchased from the grid comprises of the electricity purchased for the electric cooling machines operation (cc) as well as the electricity required to cover the demand of the buildings (dem). Likewise, the income to the district is generated by injection of the surplus power produced by the PV panels as well as the CHP plants to the grid denoted by sel. The net electricity cost is then expressed by:

$$C_{elec,net} = C_{elec,pur} - C_{elec,sel} = C_{elec}^{cc} + C_{elec}^{dem} - C_{sel}^{CHP} - C_{sel}^{PV} \quad (5)$$

Equation (5) can be rewritten in terms of energy generation and consumption for each equipment as:

$$C_{elec,net} = \sum_{t}\sum_{s}\sum_{i}\left[\left(E_{i,s,t}^{pur,dem} + \sum_{l} E_{i,s,t,l}^{pur,cc}\right)p^{grid} - \sum_{q} E_{i,s,t,q}^{PV,sel} p^{PV} - \sum_{k} E_{i,s,t,k}^{CHP,sel} p^{CHP}\right]\Delta_{s,t} \quad (6)$$

Equation (6) gives freedom to the designer to set various purchase or buyback prices for different hours or periods.

5.2.2 System and component modeling

Building cooling balance: The cooling requirement (denoted by dem) at each building can be covered either by production of chilled water through the compression chiller (cc), absorption chiller (ac), cold storage medium (cs), or from other on-site producers via cooling distribution network. Other buildings (j) contribute to satisfy a consumer by exporting their surplus cooling energy through the network connecting them. It is noteworthy to mention that the building of interest (i) is able to send cooling energy received from other buildings or generated by its own machines to other buildings at the same time. Hence, the cooling energy balance around each building may be expressed by:

$$Q_{i,s,t}^{cold} = \sum_{l} Q_{i,s,t,l}^{cc,dem} + \sum_{m} Q_{i,s,t,m}^{ac,dem} + Q_{i,s,t}^{cs,out} + (1 - \sigma_{cold}) \sum_{j} Q_{j \to i,s,t} - \sum_{j} Q_{i \to j,s,t} \qquad (7)$$

Transportation heat loss through cooling network among the buildings is also considered in Eq. (7) by introduction of the loss coefficient σ_{cold}. In a case that buildings are connected closely to each other the coefficient approaches to 1. Electrical load of each consumer (denoted by $power$) is covered by the utility grid (pur) along with the energy generated by the PV arrays and the CHP plants as well as the power exchange among the buildings i and j:

$$E_{i,s,t}^{power} = E_{i,s,t}^{pur,dem} + \sum_{k} E_{i,s,t,k}^{CHP,dem} + \sum_{q} E_{i,s,t,q}^{PV,dem} + \sum_{j} \left(E_{j \to i,s,t} - E_{i \to j,s,t}\right) \qquad (8)$$

No transmission loss is deemed for sharing of power, as their relative distance is short. Equations (7) and (8) are for all technologies (k for CHP and m for absorption chillers) installed at a given site i.

Cooling supply equipment: The linear relationship between the cooling energy and the required electricity in the compression chiller (cc) can be indicated by the definition of the energy efficiency ratio (EER) which is considered as a constant for the whole range of cooling production:

$$E_{i,s,t,l}^{cc} = \frac{Q_{i,s,t,l}^{cc}}{EER_{l}^{ac}} \qquad (9)$$

The same formula can be envisaged for the absorption chiller (ac) except for the type of input energy, which is the heat. The heat is supplied to the absorption chiller through the CHP units, solar thermal array (sol), hot thermal storage (hs) and the boiler (B) as:

$$Q_{i,s,t}^{B,ac} + \sum_{k} Q_{i,s,t,k}^{CHP,ac} + \sum_{r} Q_{i,s,t,r}^{sol,ac} + Q_{i,s,t}^{hs,out} = \sum_{m} \frac{Q_{i,s,t,m}^{ac}}{EER_{m}^{ac}} \qquad (10)$$

The output energy flux for the heat storage in Equation (10) should always take positive values. Likewise, the electricity injected to the electrical chiller comes from PV panels and CHP units:

$$\sum_{q} E_{i,s,t,q}^{PV,cc} + \sum_{k} E_{i,s,t,k}^{CHP,cc} + \sum_{l} E_{i,s,t,l}^{pur,cc} = \sum_{l} \frac{Q_{i,s,t,l}^{cc}}{EER_{l}^{cc}} \qquad (11)$$

A portion of the cooling power generated by the cooling machines and the rest is used by the consumer on-site or directed towards the other buildings through the distribution network:

$$\sum_{m} Q_{i,s,t,m}^{ac} = \sum_{m} Q_{i,s,t,m}^{ac,sto} + \sum_{m} Q_{i,s,t,m}^{ac,dem} \tag{12}$$

$$\sum_{l} Q_{i,s,t,l}^{cc} = \sum_{l} Q_{i,s,t,l}^{cc,sto} + \sum_{l} Q_{i,s,t,l}^{cc,dem} \tag{13}$$

To represent the capacity of the cooling machines, another inequality constraint is introduced to limit their operation as:

$$Q_{i,s,t,l}^{cc} \leq G_{l}^{cc} Z_{i,l} \tag{14}$$

$$Q_{i,s,t,m}^{ac} \leq G_{m}^{ac} T_{i,m} \tag{15}$$

The binary variables (Z and T) are introduced to determine the existence of the absorption chiller (ac) of type m or compression chiller (cc) of type l by getting the value 1 or its non-existence by getting the value 0.

Hot and cold-water storage media: The storage systems (cs for cold tank and hs for hot tank) are usually constructed from stainless steel and may be placed under or above the ground. The equation for the continuity of the storage (sto) capacity (SOC) incorporates the input and output flows with its state of the charge at each point of the time as:

$$SOC_{i,s,t}^{cs} = \eta^{cs} SOC_{i,s,t-1}^{cs} + \left(\sum_{m} Q_{i,s,t,m}^{ac,sto} + \sum_{l} Q_{i,s,t,l}^{cc,sto} - \eta^{out} Q_{i,s,t}^{cs,out} \right) \delta_{p} \tag{16}$$

The duration of each period in which the charging and discharging occurs is given by (δ_p). The same equation can be written for the hot water tank considering that it is connected with solar thermal collector and CHP units as:

$$SOC_{i,s,t}^{hs} = \eta^{hs} SOC_{i,s,t-1}^{hs} + \left(Q_{i,s,t}^{B,sto} + \sum_{k} Q_{i,s,t,k}^{CHP,sto} + \sum_{r} Q_{i,s,t,r}^{sol,sto} - \eta^{out} Q_{i,s,t}^{hs,out} \right) \delta_{p} \tag{17}$$

Storing (sto) and discharging (out) efficiencies (η) are included in equations (16) and (17) for both storage hot (hs) and cold (cs) tanks. The capacity of thermal storage tanks is determined only by

using the parameters G_i^{hs} and G_i^{cs}. They indicate the highest storable energy for hot and cold storage tanks, respectively. Hence, another constraint is introduced for the state of the charge to be bound:

$$Q_{i,s,t}^{hs,out} \leq SOC_{i,s,t}^{hs} \leq G_i^{hs} \tag{18}$$

$$Q_{i,s,t}^{cs,out} \leq SOC_{i,s,t}^{cs} \leq G_i^{cs} \tag{19}$$

The upper bounds in the above equations represent the implemented storage tank in each building. The heat flux from the storage system should not exceed the available stored energy within the tank.

PV array: The total electricity produced by different types (q) of the PV array can be split into three portions: part of it is consumed internally (dem) or to feed electric compression chiller (cc) while the surplus power is injected back to the utility grid (sel) to generate income:

$$\sum_q E_{i,s,t,q}^{PV} = \sum_q E_{i,s,t,q}^{PV,dem} + \sum_q E_{i,s,t,q}^{PV,cc} + \sum_q E_{i,s,t,q}^{PV,sel} \tag{20}$$

It is noteworthy to mention that the total PV generated electricity (E) for each type (q) is bounded by its nominal capacity (G) and the available level of solar irradiation (S) at the site for each period (t) and season (s) [62, 24, 92]:

$$E_{i,s,t,q}^{PV} = A_{i,q}^{PV} \times \min\{\eta_q^{PV} S_{s,t}, G_q^{PV}\} \tag{21}$$

Solar thermal collector: A portion of the heat produced (Q) in the solar thermal collectors (sol) are stored in hot water tank (sto) while the rest is being consumed in the absorption chiller (ac) to create cooling energy:

$$\sum_r Q_{i,s,t,r}^{sol} = \sum_r Q_{i,s,t,r}^{sol,ac} + \sum_r Q_{i,s,t,r}^{sol,sto} \tag{22}$$

Similar to the PV array, the total heat generated by the solar thermal collector of type r is bounded by its nominal capacity and the level of solar irradiated on its surface:

$$Q_{i,s,t,r}^{sol} = A_{i,r}^{sol} \times \min\{\eta_r^{sol} S_{s,t}, G_r^{sol}\} \tag{23}$$

The total area (A) covered by the PV arrays and solar thermal collector is bounded due to the available space (max) at each building i:

$$\sum_{q} A_{i,q}^{PV} + \sum_{r} A_{i,r}^{sol} \leq A_{i}^{max} \tag{24}$$

CHP units: Similar to the cooling machines, the significant aspect with respect to the formulation of the CHP units is to keep a linear relationship between the output heat (Q) and output power (E) in the model. The hypothesis of heat to electric ratio (HER) is employed as:

$$Q_{i,s,t,k}^{CHP,ac} + Q_{i,s,t,k}^{CHP,sto} = HER_{k} \times E_{i,s,t,k}^{CHP} \tag{25}$$

A portion of the heat is stored in the hot water tank (sto) while the rest is fed to the absorption chiller (ac).

This linear relationship is accompanied with an additional constraint to represent the highest generated electricity (capacity of CHP or G) if the type k of the CHP unit is installed (binary variable X) in building i:

$$E_{i,s,t,k}^{CHP} \leq G_{k}^{CHP} X_{i,k} \tag{26}$$

The total electricity generated by the type k CHP unit in season s and period p can be expressed into three terms: part of it is consumed internally (dem) to cover power demand, part of it feeds the electric compression chiller (cc), while the surplus power is injected back to the utility grid (sel) to increase the income for the district:

$$E_{i,s,t,k}^{CHP} = E_{i,s,t,k}^{CHP,dem} + E_{i,s,t,k}^{CHP,cc} + E_{i,s,t,k}^{CHP,sel} \tag{27}$$

Utility grid: The total electricity sold to the grid (sel) at any point of the time (season s and period p) is equal to the surplus electricity generated by the PV panels of type q plus the excess power produced in the CHP units of type k:

$$E_{i,s,t}^{sel} = \sum_{q} E_{i,s,t,q}^{PV,sel} + \sum_{k} E_{i,s,t,k}^{CHP,sel} \tag{28}$$

At any point of the time, building (i) may only sell the surplus electricity to the grid or purchase it but not both. A binary variable is employed to control simultaneous purchase and sell electricity.

However, at that instant, the whole district interacts with the utility grid to sell and buy electricity at the same time provided that the amount of the electricity injected back to the utility grid does not exceed the maximum (max) allowable power injection [62, 24, 92, 106]:

$$E_{i,s,t}^{sel} \leq E_{i,s,t}^{sel,max} W_{i,s,t} \tag{29}$$

$$E_{i,s,t}^{pur,dem} + \sum_{l} E_{i,s,t,l}^{pur,cc} \leq \kappa E_{i,s,t}^{power} (1 - W_{i,s,t}) \tag{30}$$

Binary variable W is equal to 1 when building i is in the process of selling power and it is equal to 0 when it is purchasing energy or there is no interaction with the grid. In Equation (30), κ is the selling coefficient and no restriction is applied for the district to purchase electricity from the electrical utility grid by introducing a big number κ in Equation (30). If $\kappa = 1$, then each building can probably only purchase electricity to fully cover its power requirement and no cooling energy may produce as a result of grid electricity.

Cooling distribution: The amount of the thermal energy exchanged between the buildings (from building i to building j) is bound by the capacity of the pipeline (denoted by max) constituting the distribution network as:

$$Q_{i \to j,s,t} \leq Q^{pipe,max} Y_{i,j} \tag{31}$$

In equation (31), a binary variable Y in introduced to represent the existence of the built connection between buildings i and j. Moreover, in a case that a pipeline is established, it is assumed that there exist only one direction of cold flow between the consumers [62, 24, 92, 106]:

$$Y_{i,j} + Y_{j,i} \leq 1 \tag{32}$$

Creation of cold fluid flow circulation can be avoided by introducing another constraint stem from the Travelling Salesman problem as follows [62, 24, 92]:

$$difference\ in\ visiting\ orders \leq 1 - (1 - Y_{i,j})|i| \tag{33}$$

Boiler: The total heat (Q) produced by the boiler (B) at season s and period t is either supplied to the absorption chiller (ac) or is stored in the hot water tank (sto) to be consumed later:

$$Q_{i,s,t}^{B} = Q_{i,s,t}^{B,sto} + Q_{i,s,t}^{B,ac} \quad (34)$$

The capacity of the boiler (G) is represented by the highest amount of storable energy (Q) it can receive during its operation considering that the volume (capacity) of the boilers are limited according to market availability:

$$Q_{i,s,t}^{B} \leq G_{i}^{B} \quad (35)$$

$$G_{i}^{B,min} \leq G_{i}^{B} \leq G_{i}^{B,max} \quad (36)$$

Market availability determines the lower (min) and upper bounds (max) for boiler in equation (36).

Power distribution: Another network similar to the thermal distribution called power network is considered among the buildings (see Equation 8) to share electricity. No especial constraints are imposed on the direction or highest capacity of electricity exchange among the consumers.

5.3 Definition of scenarios

To implement a comparative analysis, four different scenarios are considered for the optimization model developed above to investigate the impact of the importance of solar energy utilization on the total cost and emission of the district cooling energy system. The first scenario represents the ***conventional district cooling*** where the compression electric chillers are implemented inside each building separately and there is no interaction among the consumers regarding the heat or electricity sharing through the established pipelines or electrical grids. The second scenario describes a ***solar-driven district cooling*** system including both PV and solar thermal collectors to feed the compression and absorption chillers and to provide the consumers with their power requirements. Interaction between the utility grid and the neighborhood may also be deemed while heat and cold storage media are incorporated in the buildings. The third scenario depicts an integration of district heating driven by non-solar equipment with a district thermal network. Therefore, such a ***non-solar-driven district cooling*** obtain the required heat or power from the CHP plants or the boilers and an interaction between the utility grid and the buildings may be studied to potential of ***stand-alone district cooling*** in regions with no access to the national power grid. Similar to the scenario three, storage tanks (both hot and cold) are included in the configuration of the system. Finally, the forth scenario put forward the hypothesis of a ***hybrid district cooling*** in which all solar and non-solar equipment cooperate together to constitute a

much more efficient poly-generation system and more degree of freedom to generate and distribute. The summary of the main scenarios and the sub-scenarios under examination can be found in **Table 5.1** in details where inclusion of various components as well as the interaction with the grid are given for more clarification.

5.4 Case description and data

An urban area is selected as an exemplary case with seven residential and office buildings. In fact, the region has not completely built and therefore a district cooling system has neither been installed nor in operation, therefore, the consumer demand data is evaluated according to existing district cooling systems. All the buildings are given as optional plant sites together with all the mainline routes among the consumers to compose the thermal distribution network. In the current research, only the location of buildings, their power demands, and thermal (cooling) requirements in various hours (periods) and representative seasons are fixed. The access to the national electricity grid is presumed in some cases and buildings may sell their excess power to the grid. It is assumed that no existing heating or cooling units, power generation plants, hot or cold storage tanks, or pipelines beforehand in the neighborhood.

Table 5.1 Setting the scenarios by inclusion (■) and exclusion (□) of components

Equipment	Scenarios			
	Conventional	*Solar-driven*	*Non-solar-driven*	*Hybrid*
Solar heat	□	■	□	■
PV	□	■	□	■
CHP	□	□	■	■
Boiler	□	□	■	■
Hot tank	□	■	■	■
Grid interaction	■	□*/■	□*/■	□*/■
Compression chiller	■	■	■	■
Absorption chiller	□	■	■	■
Cold tank	□	■	■	■
Cooling network	□	□/■	□/■	□/■
Power network	□	□/■	□/■	□/■

*stand-alone district cooling

The urban region called Suurstoffi district is situated in Risch Rotkreuz, Switzerland with several blocks. Schematic map of the district area as well as the consumers under study are illustrated in **Figure 5.2** in which the labeled buildings are still under construction [107]. The available area for each building for PV and solar thermal collector arrays installation are also given in **Figure 5.2**. The locations of the buildings (horizontal and vertical coordinates) are shown in **Figure 5.3** in which the distances among the buildings can be easily derived. These coordinates provide input information to determine the mainline routes among the consumers to establish the cooling distribution network and find the optimal connections. It is noteworthy to mention that the district area of investigation in **Figure 5.3** is around 8500 m^2.

Figure 5.2 Schematics map of the district and the area under study with available solar space (from *[107]* with several modifications)

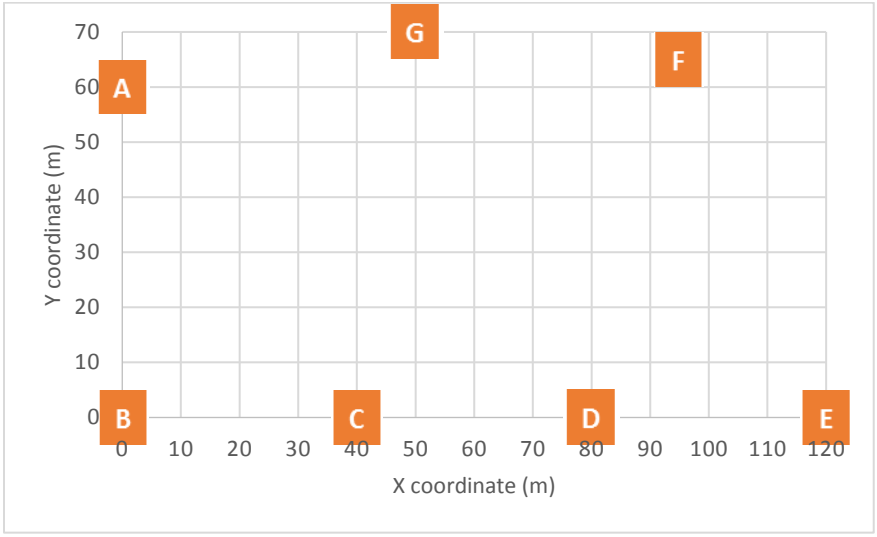

Figure 5.3 Coordinates of the consumers to be used in determination of main routes

The list of optional components considered in this case study and their corresponding production efficiencies, investment costs, and technical characteristics are given in **Table 5.2**. The lifetimes for all the equipment are assumed to be 20 years. As it is listed in the table, five CHP technologies with different capacities, gas-fired boiler with limited capacity, and solar thermal collectors are envisaged as the heat prime movers. Furthermore, four different choices for absorption cooling

machines and two choices for compression chillers are nominated as the cooling energy generators. Beside the CHP units, PV arrays are also available to generate solar electricity considering that the price of inverters is already included in PV capital cost.

The full calendar year is broken up into three representative seasons, namely, winter, mid-season, and summer as listed in **Table 5.3** with a typical day in each season considering the climatic conditions along with the variations in energy consumptions on an hourly or seasonal basis. Each typical day is divided into six periods as shown in **Table 5.4** with different number of hour in each period. **Figures 5.4** and **5.5** depict the instantaneous thermal (cooling) and electricity demand profiles throughout the year for each of the seven buildings presented in the illustrative case considering the seasons and the periods defined earlier. The exemplary cooling demands are not the actual requirements of the districts as it has not constructed yet, however, it is assumed they have the same trend as heating load [92] and presumed they are several times bigger than the heating loads. The cooling requirements are undoubtedly are equal to zero during the winter and no graph represents the demand for those months, however, operation of buildings during summer and mid-season calls for covering cooling demands.

Table 5.3 Division of the year into three equalized seasons

Season	Months	Duration (hours)
Winter	Jan, Feb, Mar, and Dec	2 904
Mid-season	Apr, May, Oct, and Nov	2 928
Summer	Jun, Jul, Aug, and Sep	2 928

Table 5.4 Definition of several periods in a typical day

Periods	Time	Duration (hours)
P1	6:00 AM to 9:00 AM	3
P2	9:00 AM to 12:00 PM	3
P3	12:00 PM to 1:00 PM	1
P4	1:00 PM to 5:00 PM	4
P5	5:00 PM to 10:00 PM	5
P6	10:00 PM to 6:00 AM	8

Table 5.2. System components and technical specifications ([62, 24, 92, 108, 105, 104])

Component	Minimum capacity	Maximum capacity	Efficiency/COP/EER	Investment cost	Comment
Heating equipment					
Solar thermal collector	0	0.7 kWth/m^2	65%	200 €/m^2	Flat plate collector (FPC)
Boiler	1 kWth	20 kWth	80%	150 €/kW	Gas-fired
Hot tank storage	0	50 kWh	Storing: 95% Discharge: 95%	100 €/kWh	Diurnal application
Combined heating and power equipment					
CHP (type I)	0	1 kWe	12%	9 000 €	Stirling engine (HER=6.7) 0.781 kg/kWh CO_2
CHP (type II)	0	9.5 kWe	24%	25 000 €	Stirling engine (HER=3.0) 0.781 kg/kWh CO_2
CHP (type III)	0	4.7 kWe	25%	11 750 €	Gas engine (HER=2.6) 0.781 kg/kWh CO_2
CHP (type IV)	0	5.5 kWe	27%	13 750 €	Gas engine (HER=2.3) 0.781 kg/kWh CO_2
CHP (type V)	0	4 kWe	25%	140 000 €	Fuel cell (HER=2.2) 0.781 kg/kWh CO_2
Cooling equipment					
Sorption chiller (type I)	0	15 kWth	0.45	600 €/kW	
Sorption chiller (type II)	0	17.6 kWth	0.70	400 €/kW	Absorption H2O-LiBr

					Single Effect
Sorption chiller (type III)	0	23.0 kWth	1.2	700 €/kW	Absorption H2O-LiBr Double Effect
Sorption chiller (type IV)	0	17.7 kWth	0.6	700 €/kW	H2O-NH3 GAX
Electric compression chiller (type I)	0	17.0 kWth	4.2	300 €/kW	VC_w
Electric compression chiller (type II)	0	16.5 kWth	2.9	300 €/kW	VC_a
Cold tank storage	0	50 kWh	Storing: 95% Discharge: 95%	100 €/kWh	Diurnal application
Electricity					
PV	0	0.15 kWe/m^2	12%	4 300 €/kWe	PV mSi
Distribution Network					
Pipeline	0	10 kWth	Transmission: 90%	40 €/m	
Utility grid					
Electricity withdrawal	0	See eq. (30) $\kappa = 3$	100% (no loss)	0.11 €/kWh	0.781 kg/kWh CO_2
Electricity injection	0	10 kW	100% (no loss)	PV: 0.55 €/kWh CHP: 0.13 €/kWh	No CO_2 credit

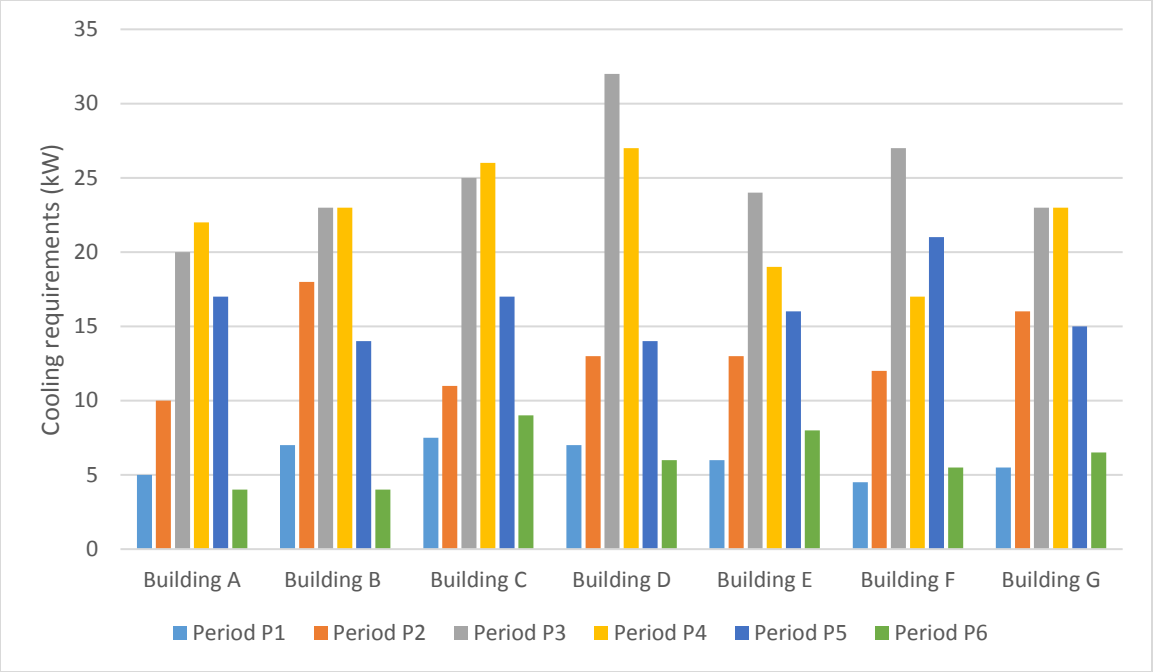

(a)

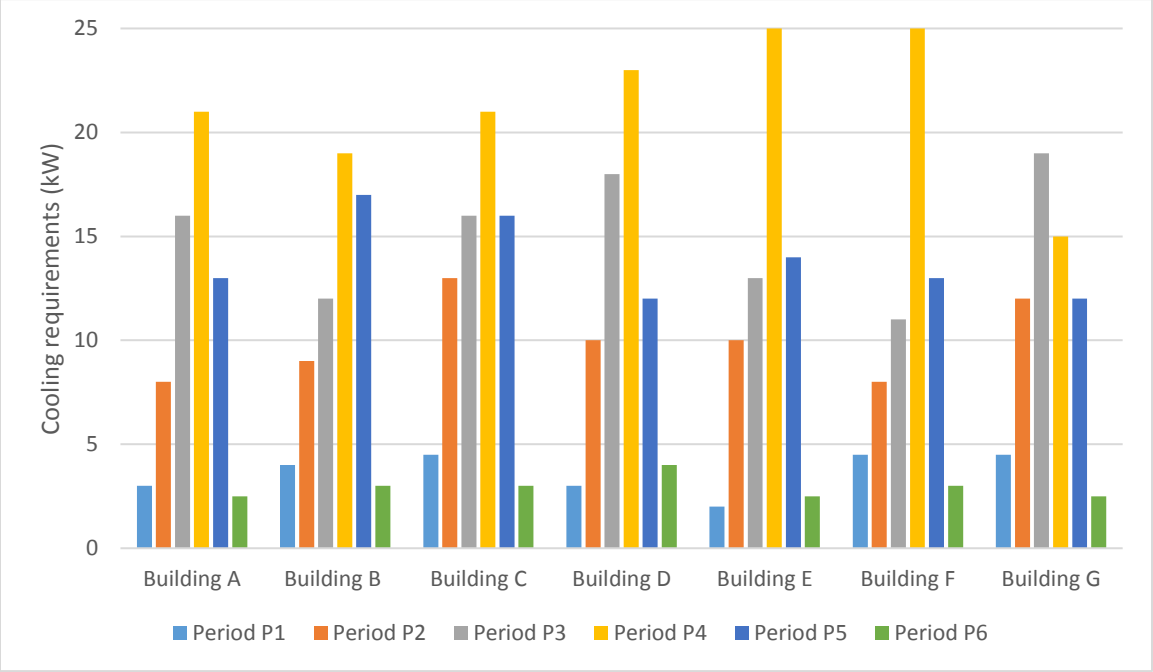

(b)

Figure 5.4 Cooling demands during (a) summer and (b) mid-season in different periods

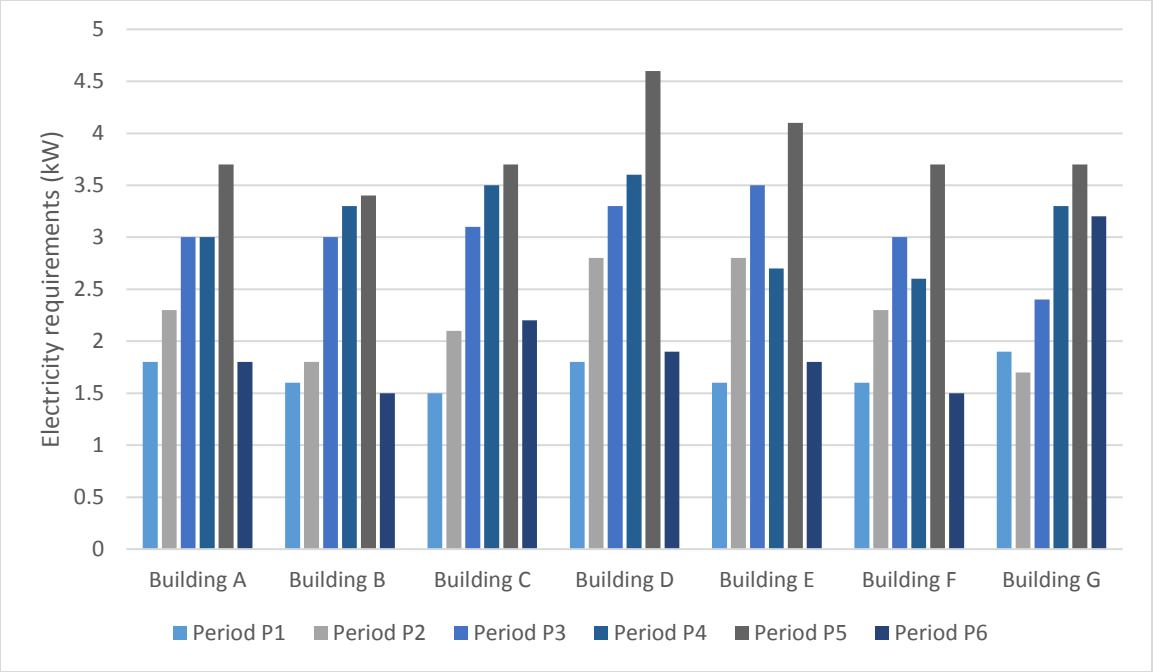
Electricity requirements (kW)
5
4.5
4
3.5
3
2.5
2
1.5
1
0.5
0
Building A
Building B
Building C
Building D
Building E
Building F
Building G
Period P1
Period P2
Period P3
Period P4
Period P5
Period P6

(a)

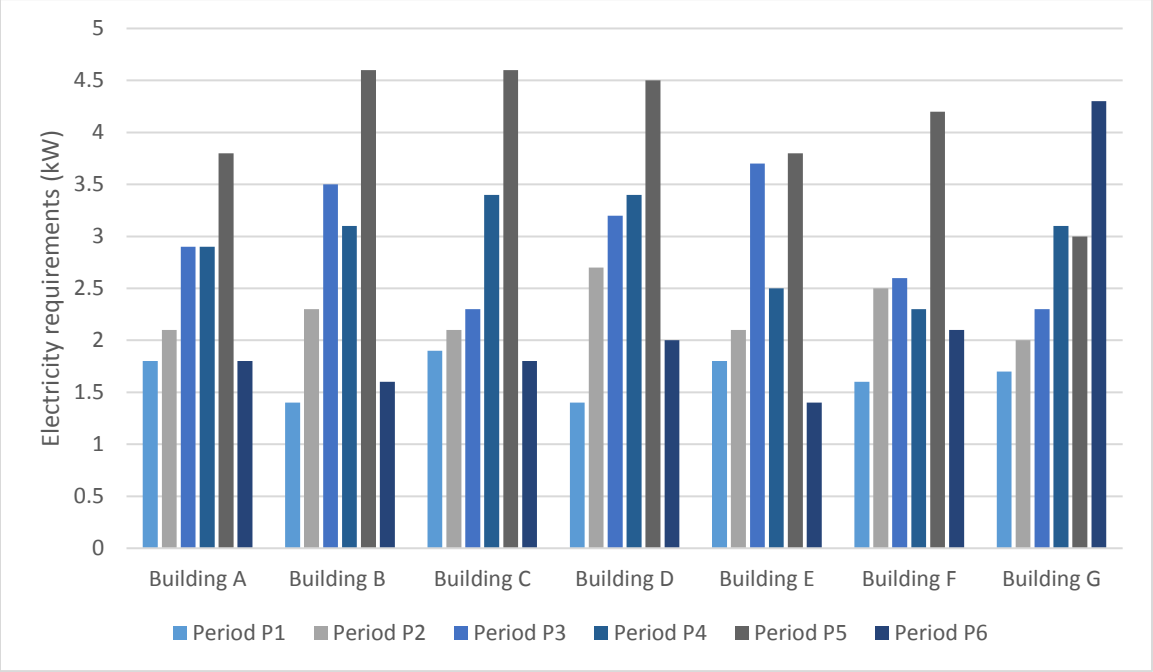
Electricity requirements (kW)
5
4.5
4
3.5
3
2.5
2
1.5
1
0.5
0
Building A
Building B
Building C
Building D
Building E
Building F
Building G
Period P1
Period P2
Period P3
Period P4
Period P5
Period P6

(b)

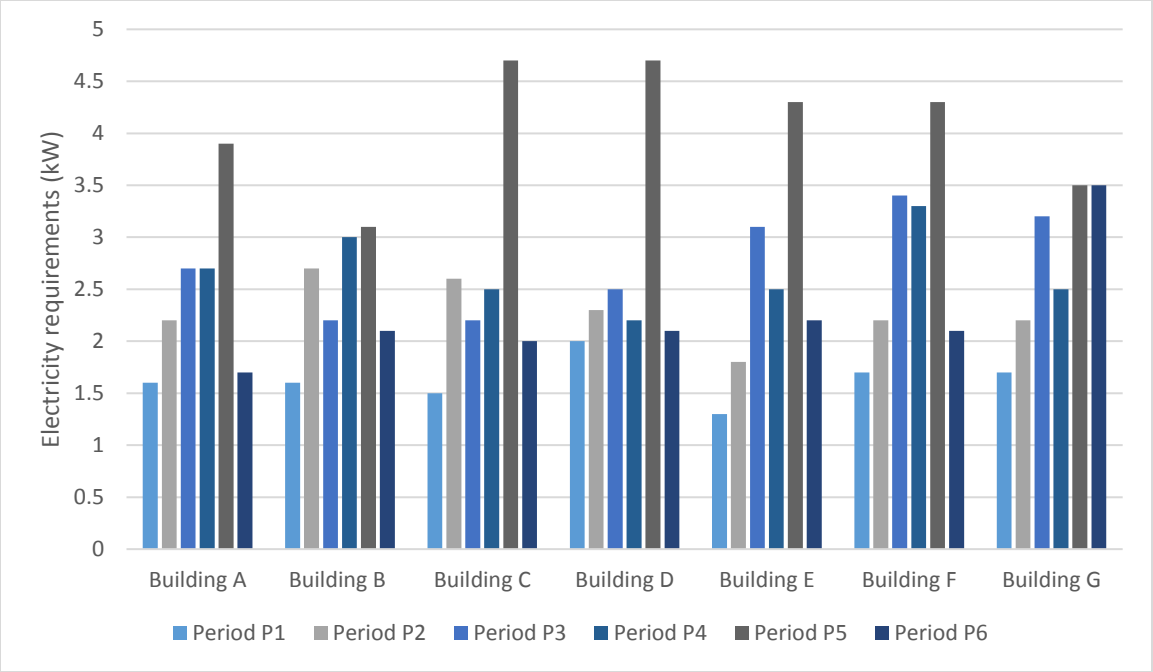

(c)

Figure 5.5 Electricity demands during (a) summer, (b) midseason, and (c) winter in different periods

In addition, building ***D*** is characterized by its highest electricity demand during summer and mid-season while building ***F*** represents the maximum electricity requirement during winter. Periods ***P3*** and ***P4*** (from 12:00 PM to 5:00 PM) represents the highest cooling demand for all seasons where period ***P5*** requires more electricity that other periods all along except for building ***G*** during the mid-season.

5.5 Solution procedures

Branch and bound (B&B) technique is employed to solve the MILP problem for design and control of the district cooling system. Not the entire feasible set of integers is explored by adopting this approach; instead, bounds are created to limit the search feasible sets. The approach is composed of two main steps as its name represents: branching and bounding. In the first step, the optimization problem is partitioned into several sub-problems by splitting the integer search space as shown in **Figure 5.6**. Solution to each sub-problem leads to generate a lower or upper bound for a minimization or maximization problems, respectively. Linear programming relaxation may be employed to create the lower bounds. The optimal solution to other sub-problems (if

exists) is evaluated accompanying the created bound available in the memory of the algorithm. In cases that the latest obtained values for decision variables provide a better solution, the new achieved bound replaces the old one and the process continues [109, 34].

In order to get the variety of solutions with respect to the both cost and emission objectives, each simulation is carried out by imposing an additional constraint on the upper bound of the total emission. Adjustment of this constraint results in a cloud of optimal solution for each of the scenarios which gives an ability to the designer to make the best decision considering their limitations on energy sources, project budget, local or national emission regulations, or available components and technologies.

The optimal configuration (selection of equipment and distribution network) and control strategy of the district cooling is then achieved as the solution to the MILP optimization approach developed through equations (1) to (36) with the given energy requirement, optional components, price, emission factors and location data as the input. The size and operation optimization problem was tested under several scenarios described in section 3. Different problems were solved using GAMS [90] software.

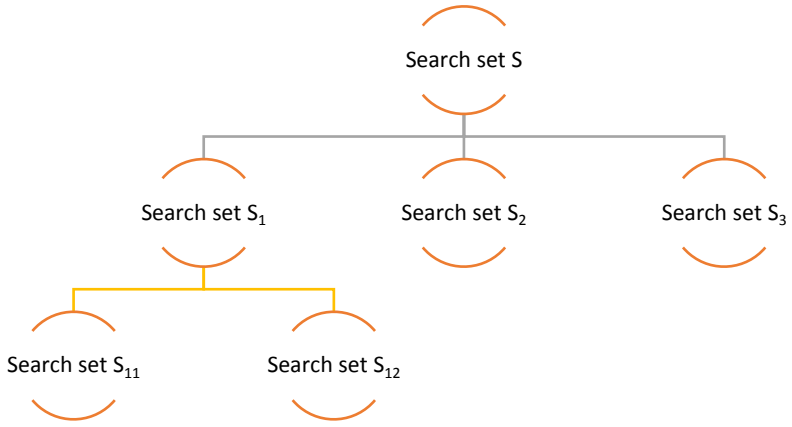

Figure 5.6 A tree representing the branching step

5.6 Results and discussions

In this section, the general results for the trade-off between cost and CO_2 emissions are presented with the optimal choice and control strategy as well as the effects of the important parameters, price, and some technical and spatial restrictions on the components and consumers.

5.6.1 Enviro-economic analysis

The results of the optimal enviro-economic cloud are represented in **Figure 5.7** for various scenarios. For the default value for coefficient of power purchase, $\kappa = 3.0$, the simulation results in an infeasible solutions since for the aforementioned scenario generates cooling energy only through the electric compression chiller which utilizes only electricity as the input. By restricting the amount of power withdrawn from the utility grid to less than 3 times the electricity load, not enough energy is provided for the cooling machines. Repeating the simulation for higher coefficient of power purchase eventually arrives to the lowest value $\kappa_{min} = 4.0$ in which the annual cost for design and operation of the system is 37 000 €. It is noteworthy to mention that the rest of simulations in this section will be performed by this coefficient of power purchase unless other value is mentioned. Sharing energy (both electricity and cooling) among the buildings still does not change the optimal solution, as the district prefers to implement technologies for each building separately without any interaction or grid among them. The conventional district also emits almost 210 000 kgCO_2 per year where all of it is generated from withdrawal of electricity from the grid and such emission is produced in the conventional thermal power plants outside of the district.

As **Figure 5.7** illustrates, for a stand-alone solar-driven district cooing without *any* internal network, the heat generated by the thermal supply chain is not capable to satisfy all the demands of the district and therefore no solution exists. The reason is mainly because of the demand at night where the PV or solar thermal collectors cannot produce any heat even if the storage tanks are placed inside the buildings. In addition, implementation of internal thermal and power grid do not lead to any feasibility of the optimal solution. As a result, the district cooling should be a grid-connected system to eliminate the energy deficits especially when the sun is not shining. The point corresponds to the highest total annual cost shows 36 000 € along with 202 750 kg CO_2 emission which are both economically and environmentally more beneficial than the conventional district cooling, i.e. 3.5% and 2.7 % reductions in cost and emission, respectively.

Figure 5.7 also shows that a non-solar driven district cooling has always higher cost for the same emission as solar-driven district cooling and also more emission at the same cost. A conclusion can be drawn that adding solar components lowers costs by either selling electricity or by its internal utilization which in turn results in avoiding buying electricity from the grid and cuts emission in conventional power plants. Solar heat elements also provide carbon-free supply to the absorption chillers and reduce the operation of electric compression chillers. Moreover, the non-solar district cooling is not able to cut CO_2 emission less than 120 000 kg per year, which is 33% higher than the lowest emission achieved by the solar driven district cooling. Even the

inclusion of cooling and power sharing among the consumers cannot reduce the emission compared to the configuration without the cooling distribution network, although the total cost is lowered by 9% i.e. from 67 500 € to 61 000 € per annum. Both network-integrated and network-free eventually intersects at the same point as the conventional system indicating this fact that conventional system still represents the lower cost. At lower costs, the effects of the network becomes less noticeable where between 40 000 € and 45 000 €, two graphs intersect each other. The reason for this is that higher emissions, buildings tend to implement their own electric compression chillers, consume its cooling energy on-site and buy electricity from the grid at lower cost instead of distributing the cooling thermal energy among the neighbors. The only way of generating income in this scenario is selling of excess electricity to the grid generated by CHP units, however, the heat outcome should be injected to an absorption chiller which has higher cost than the electric compression chillers, and hence ineffectiveness of power distribution network among the consumers is evident at lowest cost where electric machines operate.

Finally, a hybrid district cooling in **Figure 5.7** offers more decrease in CO_2 emission (more than 22%) in comparison with lowest emission in other scenarios with the penalty of higher annual cost of around 79 000 €. The reason for this is that the presence of CHP units and individual boilers can replace the required electricity purchase from the utility grid to offset the carbon emission through the national utility grid, on the other hand, the solar driven district cooling can only cut the emission by installing more arrays but it is still restricted by the roof area and the level of available irradiation. For less than 40 000 €, the optimal cluster almost coincide with the outcome of solar-driven cooling system.

5.6.2 Equipment selection and distribution configuration

Each point in the optimal cloud presents a specific combination of technologies and distribution network. For simplicity, some representative solutions are shown and compared in this section. It includes the terminal points and a point in the middle of each cluster. These middle points are selected as the first solutions appeared right after 50 000 € on the horizontal axis in **Figure 5.7**. This value is the mid-point between the extreme points of the conventional and solar-driven set of solutions. **Table 5.3** lists the characteristic points in which the right point indicates the solution with lowest CO_2 emission. For a conventional district cooling system, all the buildings are equipped similarly with two types of cooling machines with the capacities of 17 kW and 16.5 kW (see **Table 5.2**). Adoption of non-solar approach reduces the number and size of electric chillers

for both the mid-point and the farthest point on the right side. Comparing the aforementioned, two points show that one electric chiller with sizes 17 kW are replaced with absorption machines with the capacity of 23 kW for further reduction in emission. The heat storage is implemented to their highest capacity (50 kWh) to store the excess heat generated from installed CHP plants. However, for the mid-point most of the buildings does not host any hot thermal storage. Even for the cold storage system and except for the building ***B***, the largest possible cold storage tank is put in for each consumer. Although, the size of the cold storage (44 kWh) is still high in building ***B*** showing its high effect in shifting loads and creating income. In addition, the number and capacity of CHP units in the midpoint is higher than the solution on the right side. It may seem to be contradictory since these gas-fired plants contribute to more release of CO_2, however, replacing electric cooling machines with CHP units provide less emission through lowering the volume of electricity purchased from the utility grid and also through storing both heat, which is eventually converted to thermal cooling. The overall effect, plays a big part in emission reduction of around 35 000 kg accounted for 23% decrease as it can be seen from **Figure 5.7**. The selected points on the optimal solar-driven district cooling system have virtually the same design configuration, however, the right point has 27 000 kg CO_2 less than the mid-point. Beside the removal of one compression chiller of type I (17.0 kW), the explanation for such a decrease lies in the control of selling and purchasing electricity to avoid the withdrawal of electricity from the utility grid which causes more emission. All the available solar spaces on top of buildings are occupied by heat or electricity panels, and their share for both representative points are practically the same. Moreover, buildings ***A*** and ***D*** tend not to install any PV units for both the optimal solutions. Finally, the representative points on hybrid district cooling system is effectively a **heat-only driven** layout as no electric chillers operates in the buildings and all the cooling energy stem from the heating components. This conclusion demonstrates that any point between these two points also does not implement any electrical cooling machine and the district is a **heat-only driven district cooling system**. In comparison with the solar-driven configuration, the hybrid design has smaller solar thermal array since no electricity-consuming machine exist.

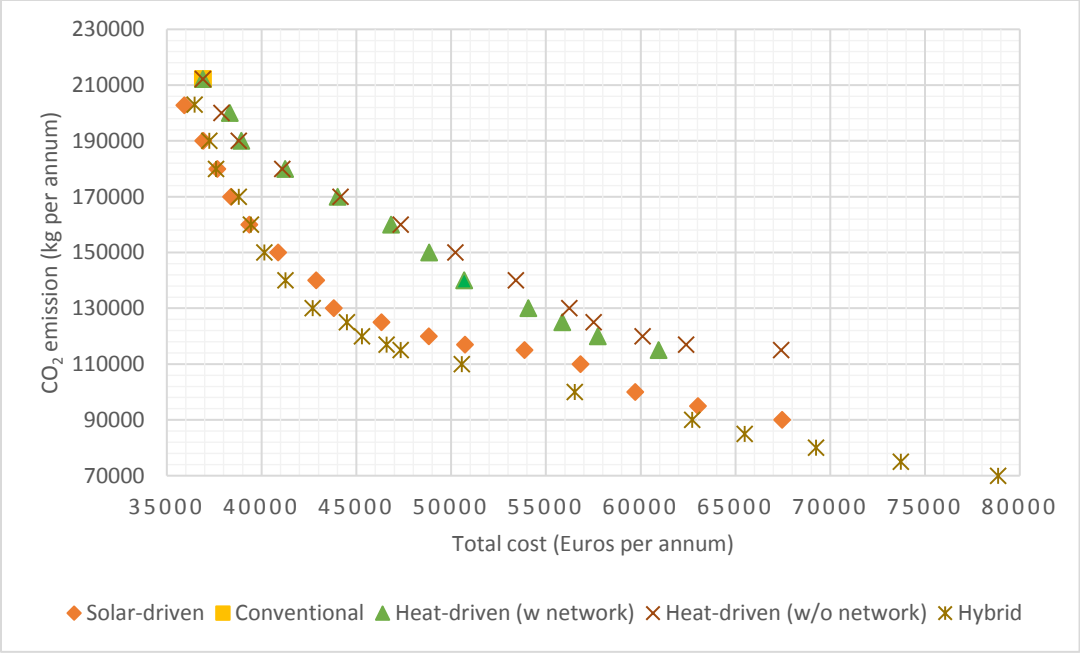

Figure 5.7 Trade-off between the annual cost and CO2 emissions for grid-connected district cooling system

Table 5.3 Optimal configuration of the equipment for representative solutions

Components	Building	Characteristic points						
		Conv	NSD-mid	NSD-right	SD-mid	SD-right	Hyb-mid	Hyb-right
Boiler size (kW)	A	-	0	0	-	-	1.0	0
	B	-	0	0	-	-	0	0
	C	-	1.6	0	-	-	0	0
	D	-	0	0	-	-	0	0
	E	-	0	0	-	-	0	0
	F	-	0	0	-	-	0	0
	G	-	1.0	0	-	-	1.0	0
CHP type	A	-	0	IV	-	-	III	IV
	B	-	III	IV	-	-	IV	IV
	C	-	IV	IV	-	-	IV	IV
	D	-	IV	IV	-	-	IV	IV
	E	-	IV	IV	-	-	IV	IV
	F	-	IV	IV	-	-	IV	IV

	G	-	0	IV	-	-	IV	IV
PV array size (m^2)	A	-	-	-	0	0	0	7.8
	B	-	-	-	76.5	78.8	142.8	103.5
	C	-	-	-	123.1	122.6	175.0	152.3
	D	-	-	-	0	0	62.5	21.4
	E	-	-	-	25.7	25.0	75.1	57.1
	F	-	-	-	3.1	5.4	53.8	36.7
	G	-	-	-	128.9	133.2	166.7	155.2
Solar thermal collector size (m^2)	A	-	-	-	50.0	50.0	49.2	42.2
	B	-	-	-	73.5	71.2	7.2	46.5
	C	-	-	-	76.9`	77.4	24.9	47.6
	D	-	-	-	75.0	75.0	12.5	53.6
	E	-	-	-	74.3	74.9	24.9	42.9
	F	-	-	-	71.9	69.6	21.3	38.3
	G	-	-	-	71.1	66.8	33.3	44.8
Hot storage size (kWh)	A	-	0	50.0	50.0	50.0	35.8	49.0
	B	-	18.6	50.0	50.0	50.0	23.5	38.0
	C	-	14.2	50.0	45.6	50.0	24.7	39.0
	D	-	0	50.0	41.8	50.0	23.5	36.0
	E	-	0	50.0	50.0	50.0	24.7	50.0
	F	-	0	50.0	50.0	50.0	46.7	50.0
	G	-	0	50.0	38.6	45.8	25.4	36.8
Cold storage size (kWh)	A	-	44.2	50.0	23.3	24.8	21.0	10.0
	B	-	36.4	43.9	30.6	43.5	7.0	18.0
	C	-	36.4	50.0	37.1	40.8	17.3	17.3
	D	-	36.4	50.0	49.5	49.5	29.7	29.7
	E	-	36.4	50.0	39.2	48.9	10.1	13.0
	F	-	49.6	50.0	43.8	49.0	10.1	12.0
	G	-	50.0	50.0	23.0	23.0	5.5	16.0
Electric chiller type	A	I, II	I	I	I	I	0	0
	B	I, II	0	0	0	0	0	0
	C	I, II	0	0	I	I	0	0
	D	I, II	I	I	I	I	0	0
	E	I, II	I	I	I	I	0	0
	F	I, II	0	0	0	I	0	0
	G	I, II	I	0	I	I	0	0

Sorption chiller type	A	-	0	III	III	III	III	III
	B	-	III	III	III	III	III	III
	C	-	III	III	III	III	III	II, III
	D	-	II	III	III	III	III	II, III
	E	-	III	III	III	III	III	III
	F	-	III	III	III	III	III	III
	G	-	0	III	III	III	III	III

conv: conventional, mid: mid-point, SD: solar-driven, NSD: non-solar driven, hyb: hybrid, right: right-hand point

The optimal layout of the distribution network for the characteristic points are illustrated in **Figure 5.8** where the buildings in the rest of the solutions (four of the seven mentioned points) do not share cooling energy with each other and remain isolated. It is also clear how a cooling network contributes to lower emissions since the mid-point of the solar-driven solutions has only one pipeline from building ***B*** to building ***A*** while the solution with lowest emission has three pipelines. However, comparison of the results in this work with another studies on district heating [106, 92] reveals that cooling exchange is not as effective as heating exchange to bring economic and environmental benefits.

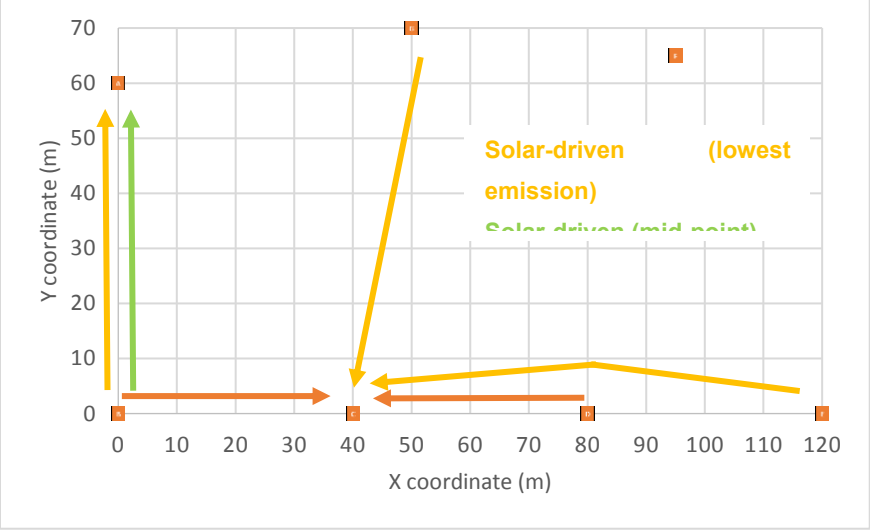

Figure 5.8 Optimal thermal connections among the buildings

5.6.3 Cost analysis

As **Figure 5.9** depicts, the highest investment cost is imposed on the hybrid district cooling since it has more optional components for installment. To compensate this high cost, the system takes advantage of the buy-back price by injection of electricity into the grid and as well as lowering the purchased electricity from the utility grid. Solar-driven and conventional designs do not have any operational cost since no boiler or CHP unit are included in the configuration. On the other hand, the non-solar design has the highest operation cost which is equal to its investment cost since the boiler or CHP units are not too expensive but great demand for heat requires large volume of gas, which is expensive. The hybrid arrangement with lowest emission tries to cut CO_2 release in comparison with the mid-point through two approaches: (i) minimization of energy purchased from the utility grid by more utilization of PV output not the CHP units as these units produce emissions as well, and (ii) maximization of the solar heat to keep the running time of CHP units as low as possible. The results of the optimization confirms that the total electrical energy produced by all CHP units is equal to 65 862 kWh in the lowest-emission scenario while it accounts to be 101 900 kWh for the mid-point solution. For the solar thermal utilization, the total annual production shows a rapid escalation from 120 740 kWh to 209 660 kWh meaning virtually doubled. On the other hand, the solar-driven arrangement adopt only approaches to reduce the emission: injection more solar electricity into the buildings to cover their power requirements and hence become more independent from the grid. In other words, the electricity that was supposed to create income through injection back into the utility grid is utilized more internally. Improvement of solar heat for absorption chillers and increasing their generation as well as lowering the operation time of electric cooling machines are not acceptable strategies. Examining the optimization results supports such hypothesis: The total solar heat generation and the overall solar electricity injected to compression chillers in the mid-point solution equals to 329 500 kWh and zero, respectively. In addition, 4 480 kWh electricity is supplied to compression chillers through the utility grid at this point. For the right point in the solar-driven cluster, solar heat, solar electricity for cooling, and grid electricity for cooling are equal to 331 930 kWh, 4 058 kWh and 248 kWh, respectively, which are practically the same as the mid-point layout. However, solar electricity supplied to the demand equals to 48 445 kWh which is much higher than the corresponding value 14 296 kWh for the midpoint solution.

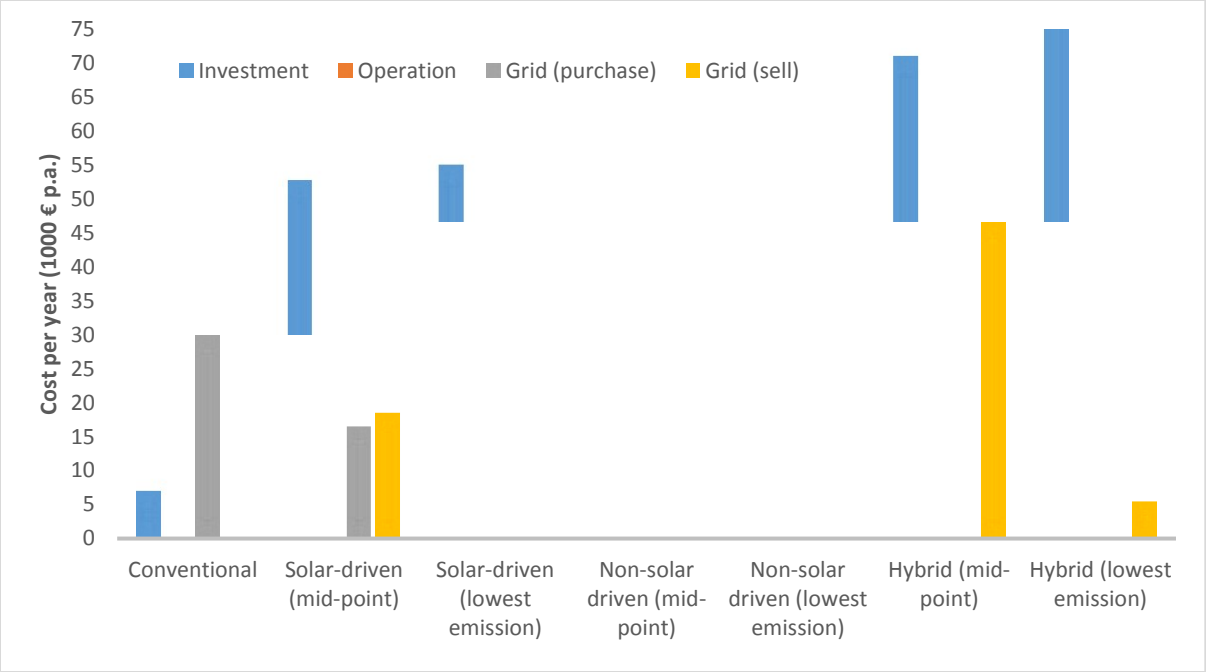

Figure 5.9 Various terms of cost objective function

5.6.4 Energy supply and demand

The mismatch between the cooling load and the heat production components (solar heat, boiler, and CHP units) or the electric cooling machines (through solar PV and utility grid) is balanced through both hot and cold storage tanks. As **Figure 5.10** illustrates for the hybrid design with lowest emission, the charging process is mostly involved during winter and also between mid-season and summer while the process is reversed over mid-season and summer. It is noteworthy to mention that the volume of the energy generated by all heating equipment is not equal to the total cooling requirements throughout the year since the concept of EER diminishes portion of that. It should be noted that for the scenario considered in **Figure 5.10**, the arrangement is only heat-driven otherwise the thermal cooling energy produced by the electric chillers should also be taken into consideration.

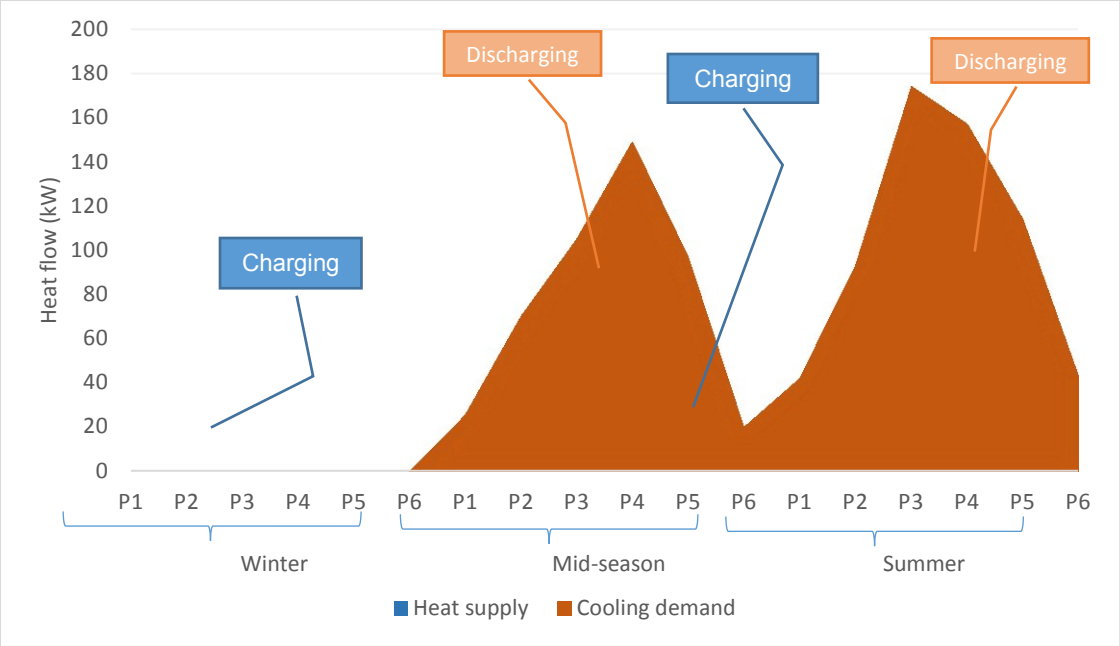

Figure 5.10 Overall operation and impact of thermal storage media in a hybrid design

As it was discussed earlier, despite the importance and effectiveness of the thermal network in district heating, buildings in district cooling opt not to share their cooling energy, however, the electrical network still play a key role to bring economic benefits. On the other hand, denying access to the utility grid accentuates the effect of thermal network. To demonstrate the hypothesis, the results for the amount of thermal exchanged energy (both cooling and electricity) considering the solar-driven, non-solar driven, and hybrid configurations are compared in **Figure 5.11**. When the buildings are disconnected from the utility grid, they no longer are able to purchase electricity and run their own cooling machines or cover their electricity demands. All the electrical requirements should be satisfied by the PV power production. Instead, to keep the emission low, buildings start to utilize as much as possible from solar heat and also distribute their excess thermal cooling energy to reduce the operation time of the electric cooling machines. However, it is not perfectly valid for the solar-driven arrangement it is already virtually independent from the utility grid.

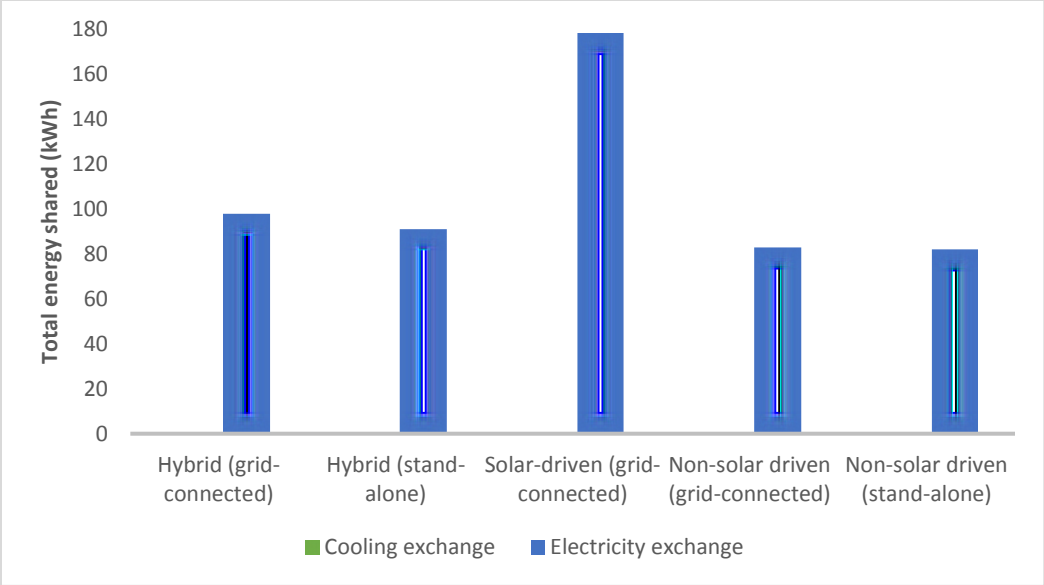

Figure 5.11 Overall annual heat and electricity flow shared among the consumers for lowest emission scenario

5.7 Conclusions and future remarks

A mathematical programming approach is proposed for optimal combination of heating side and cooling side in district energy to achieve the best performance of the overall system and to produce thermal cooling energy and electricity in terms of cost and emission:

- Despite the importance and effectiveness of the thermal network in district heating, buildings in district cooling opt not to share their thermal cooling energy, however, the electrical network still play a key role to bring economic benefits.
- Losing the access to the utility grid accentuates the effect of thermal network with no or less impact on power internal grid.
- Interaction with the grid with a goal of generating income is lower than that observed in the optimization of district thermal heating performance. One reason can be explained as the competitiveness of solar thermal collector in the available space.
- A hybrid district thermal cooling offers more decrease in CO_2 emission (more than 22%) in comparison with lowest emission in other scenarios.

- Adoption of non-solar approach reduces the number and size of electric chillers for both the mid-point and the farthest point on the right side.
- A non-solar driven district cooling has always, higher cost in the same emission as solar-driven district cooling and also more emission at the same cost.
- There are two pints on the curve of the hybrid design where any point between these two does not implement any electrical cooling machine and the district is called a heat-only driven district cooling system.
- Implementation of both thermal heat and cold storage tanks is recognized to have a great effect on matching load and demand in mid-season and summer practically at the same degree. Thermal hot water tank storage was more utilized than the thermal cold tank medium.

The proposed methodology has this drawback that the demand profiles are assumed to stay unchanged for the lifetime of the system and district. Prediction of both cooling and electricity load as well as the intensity of solar radiation [21] and temperature is recommended prior to the optimization of the performance. Moreover, the number of buildings in a district may change throughout the coming years and this variation should be taken into account while providing a more accurate analysis.

Chapter 6

Conclusions and future remarks

6.1 Conclusions

The development of the future district energy systems is vital to reach the goal of smart energy systems which are able to fulfil the aims for the future low-carbon standards and strategies. With more flexible distribution of energy, the design can take advantage of the renewable energy sources especially on-site while meeting the requirements of low and zero-energy. Furthermore, the potential of future district cooling systems is closely related to the concept of district heating applications. Energy simulation tools typically fail to take into consideration all the parameters simultaneously. Therefore, to perform such a complicated task, mathematical programming approaches have been employed for a wide range of applications to make informed decisions about the optimal design and management of district energy systems. Current dissertation begins demonstrating the necessity of an agile methodology for planning, designing and optimizing of an energy supply system for a decentralized district energy system. The production side is composed of combination of energy conversion units together with the heating, cooling, and electricity distribution networks (configuration) :

1. What is the optimal size of each energy generation technology which perfectly matches the given district, the optimal coordinates of installation, and the optimal distribution network?
2. To what degree (percentage) the cost and emission can be reduced?
3. What is the effect of thermal (heating and cooling) and power distribution
4. What is the optimal operation of the implemented equipment?
5. What is the effect of the energy storage (both battery and hot water tank) on cost and emission?
6. How can one select an optimal design and operation for a net-zero energy district?

7. How can a district system with combined cooling and power network be designed at a preliminary stage?
8. What is the effect of the combination (integration) of the heating and cooling systems of a district energy system on cost and emission?

The developed optimization methodology allows for the operation of several efficient poly-generation energy conversion equipment together with the consideration of the equipment constraints and limitations at which the heating and cooling demand need to be satisfied. The main outcome of the methodology that addresses the abovementioned questions is the Pareto optimal frontier, presenting the trade-offs between the economic objective (total cost) and environmental objective (CO_2 emissions) for many different combinations. Several scenarios were applied to consider heat exchange, power exchange, thermal storage, battery bank, and renewable sources. Further analysis of each solution (configuration) demonstrate that the methodology is capable of handling several tasks, such as, for example:

1. Expanding the boundary of the distribution network to incorporate more consumers;
2. Pre-definition of the heating, cooling, or power distribution network or technologies;
3. Restrictions on the buildings to install generation plants;
4. Addition or removal of various constraints in the location, technology, emission, etc.;
5. Addition or removal of constraints for the scheduling of the generation and storage ;
6. Installment of the energy extraction units outside of the building as a central unit(s);
7. Restriction on the feeding technologies when it is integrated to other equipment;
8. Co-simulation and linkage to other energy simulation commercial tools.

Besides demonstrating the applicability of the proposed optimization model, the results further point out the importance of using energy storage and energy exchange and of having an optimally integrated energy system, both in terms of CO_2 emissions and costs. The thesis also includes the description and optimization of a new definition “net-zero district energy system” which reinforces utilization of the renewable-based energy resources such as PV units. The model can help to design the energy systems for a wide range of districts such as location of buildings and district, levels of demands, type of building, etc. considering a wide range of heating, cooling, and power conversion technologies.

6.2 Future remarks

The development and application of the propose methodology and tool brought to the fore the following limitations for which the tool did not address and that calls for further development:

- It is recommended that a parametric sensitivity is carried out to investigate the effect of each parameter on the objective functions and the performance of the technologies. It will be more important to consider the fluctuations in the price of the technologies such as increment of the cost of photovoltaic panels. Increasing the cost of the fuel and the buy-back price should also be taken into consideration in the optimization model.
- Regarding the cost objective function, the maintenance cost is ignored in the model which can be added to study the effect of failure of each component on the operation. Regarding the environmental objective function, emission of the CO_2 is considered to have negative impact at any level, however, by considering a target CO_2 level, a penalty or bonus can be defined which affects the final solution with regard to the selection of the technologies and their operation.
- Since all the technologies are considered separately, it would be interesting in terms of energy efficiency and maybe cost to consider the optimal combination of technologies as a hybrid system. However, this case was considered for the design of district cooling system, the district heating system can also be expanded to have such a combination. For example, geothermal and solar technologies may work as a hybrid system to satisfy low- and high-temperature demands.
- The model presented in this thesis does not take into consideration performance time delays of different energy conversion technologies including start-up and shut-down delay. In other words, it is assumed that they are completely functional while they are operating to meet the power or heat demands.
- One challenge is the prediction of the energy demand in the future to keep supply and demand balanced. Since the energy consumption results in new types of demands, the future energy usage increase rate should be considered when designing a system. The change in the number of occupants and their demand can create different scenarios where
- Innovative technologies are usually studied as single, very detailed systems, and the results of these approaches may not be useful when devising a model based on a “black-box” approach, when only the performance of the technology is taken into consideration. For example, the heat storage in the pipes can be added to the optimization model.

Bibliography

[1] H. Lund, B. Möller, B. V. Mathiesen and A. Dyrelund, "The role of district heating in future renewable energy systems," *Energy,* vol. 35, no. 3, pp. 1381-1390, 2010.

[2] B. V. Mathiesen, H. Lund, D. Connolly, H. Wenzel, P. A. Østergaard, B. Möller, S. Nielsen, I. Ridjan, P. Karnøe, K. Sperling and F. K. Hvelplund, "Smart Energy Systems for coherent 100% renewable energy and transport solutions," *Applied Energy,* vol. 145, pp. 139-154, 2015.

[3] I. Dinçer and C. Zamfires, "District Energy Systems," in *Sustainable Energy Systems and Applications*, Springer, 2011, pp. 289-429.

[4] H.-H. Rogner, "Clean energy services without pain: district energy systems," *Energy studies review,* vol. 5, no. 2, pp. 114-120, 1993.

[5] I. Dincer and C. Zamfirescu, Sustainable Energy Systems and Applications, DOI 10.1007/978-0-387-95861-3_10 ed., Springer, 2011.

[6] S. Werner, "International review of district heating and cooling," *Energy,* vol. 137, pp. 617-631, 2017.

[7] R. Sena and S. C. Bhattacharyya, "Off-grid electricity generation with renewable energy technologies in India: An application of HOMER," *Renewable Energy,* vol. 62, pp. 388-398, 2014.

[8] D. Schnitzer, D. S. Lounsbury, J. P. Carvallo, R. Deshmukh, J. Apt and D. M. Kammen, Microgrids for Rural Electrification: A critical review of best practices based on seven case studies, 2014.

[9] A. Gasparrini, Y. Guo, M. Hashizume, E. Lavigne, A. Zanobetti and J. Schwartz, "Mortality risk attributable to high and low ambient temperature: a multicountry observational study.," *Lancet,* vol. 386, no. 9991, pp. 369-375, 2015.

[10] S. Werner, "Avoided carbon dioxide emissions from the use of DH and CHP," *Euroheat Power Engl,* vol. 1, pp. 20-24, 2003.

[11] S. Frederiksen and S. Werner, "District heating and cooling," *Lundstudentliterature,* 2013.

[12] IEA, "World energy balances until 2014," International Energy Agency, Paris, 2016.

[13] H. Gadd and S. Werner, "18-Thermal energy storage for district heating and cooling," in *Advances in thermal energy storage systems*, Woodhead publishing, 2015, pp. 467-478.

[14] N. Klinghoffer and M. Castaldi, "Waste to energy conversion technology," Oxford: Woodhead Publishing Series in Energy no. 29, 2013.

[15] W. R. Moomaw, "Industrial emissions of greenhouse gases," *Energy Policy ,* vol. 24, no. 10/11, pp. 951-968, 1996.

[16] IPCC, "2006 guidelines for national greenhouse gas inventories," *Energy, intergovernmental panel on climate change,* vol. 2, 2006.

[17] A. S. Makarova, T. G. Pankrushina, L. V. Urvantseva and A. A. Khorshv, "Combined heat and power in the draft of the new Russian energy strategy," *Thermal engineering,* vol. 62, no. 6, pp. 389-395, 2015.

[18] H. Yu, S. Y. Pan, B. J. Tang, Z. F. Mi, Y. Zhang and Y. M. Wei, "Urban energy consumption and CO2 emissions in Beijing: current and future," *Energy efficiency,* vol. 8, no. 3, pp. 527-543, 2015.

[19] Y. Yang, S. Zhang and Y. Xiao, "An MILP (mixed integer linear programming) model for optimal design of district-scale distributed energy resource systems," *Energy,* vol. 90, pp. 1901-1915, 2015.

[20] A. Alarcon-Rodriguez, G. Ault and G. S, "Multi-objective planning of distributed energy resources: a review of the state-of-the-art," *Renewable and Sustainable Energy Reviews,* vol. 14, no. 5, pp. 1353-1366, 2010.

[21] M. Sameti, M. A. Jokar and F. R. Astaraei, "Prediction of Solar Stirling Power Generation in Smart Grid by GA-ANN Model," *International Journal of Computer Applications in Technology,* vol. 55, no. 2, pp. 147-157, 2017.

[22] F. R. Astaraei, M. Sameti, M. A. Jokar and F. Pourfayaz, "Numerical simulation of solar-driven Kalina cycle performance for centralized residential buildings in Iran," *Intelligent Buildings International,* vol. Article in Press, pp. 1-25, 2016.

[23] D. Buoro, M. Casisi, A. D. Nardi, P. Pinamonti and M. Reini, "Multicriteria optimization of a distributed energy supply system for an industrial area," *Energy,* vol. 58, pp. 128-137, 2013.

[24] E. D. Mehleri, H. Sarimveis, N. C. Markatos and L. G. Papageorgiou, "Optimal design and operation of distributed energy systems: application to Greek residential sector," *Renewable and Sustainable Energy Reviews ,* vol. 51, pp. 333-342, 2013.

[25] C. Weber, F. Maréchal and D. Favrat, "Design and optimization of district energy systems," *Computer aided chemical engineering,* vol. 24, pp. 1127-1132, 2007.

[26] J. Allegrini, K. Orehounig, G. Mavromatidis, F. Ruesch, V. Dorer and R. Evins, "A review of modelling approaches and tools for the simulation of district-scale energy system," *Renewable and Sustainable Energy Reviews,* vol. 52, pp. 1391-1404, 2015.

[27] D. Olsthoorn, F. Haghighat and P. A. Mirzaei, "Integration of storage and renewable energy into district heating systems: A review of modelling and optimization," *Solar Energy,* vol. 136, pp. 49-64, 2016.

[28] A. Lake, B. Rezaie and S. Beyerlein, "Review of district heating and cooling systems for a sustainable future," *Renewable and Sustainable Energy Reviews,* vol. 67, pp. 417-425, 2017.

[29] H. Lund, S. Werner, R. Wiltshire, S. Svendsen, J. E. Thorsen, F. Hvelplund and B. V. Mathiesen, "4th Generation District Heating (4GDH): Integrating smart thermal grids into future sustainable energy systems," *Energy,* vol. 68, pp. 1-11, 2014.

[30] H. Lund, N. Duic, P. Alberg, Østergaard and B. V. Mathiesen, "Smart energy systems and 4th generation district heating," *Energy,* vol. 110, pp. 1-4, 2016.

[31] J. L. Bernal-Agustín, R. Dufo-López and D. M. Rivas-Ascaso, "Design of isolated hybrid systems minimizing costs and pollutant emissions," *Renewable Energy,* vol. 13, pp. 2227-2244, 2006.

[32] E. K. P. Chong and S. H. Zak, An introduction to optimization, New York: John Wiley & Sons, 2013.

[33] T. Falke, S. Krengel, A.-K. Meinerzhagen and A. Schnettler, "Multi-objective optimization and simulation model for the design of distributed energy systems," *Applied Energy,* p. Article in Press, 2016.

[34] S. S. Rao, Engineering optimization, New Jersy: John Wiley & Sons, 2009.

[35] S. C. Chapra and R. P. Canale, Numerical methods for engineers, New York: McGraw-Hill, 2012.

[36] R. Roy, S. Hinduja and R. Teti, "Recent advances in engineering design optimisation: challenges and future trends," *CIRP Annals—Manufacturing Technology,* vol. 57, 2008.

[37] G. T. Kolda, M. R. L. R and V. Torczon, "Optimization by direct search: new perspectiveson some classical and modern methods," *SIAM Review,* vol. 45, pp. 385-482, 2003.

[38] T. Fang and R. Lahdelma, "Genetic optimization of multi-plant heat production in district heating networks," *Applied Energy,* vol. 159, pp. 610-619, 2015.

[39] J. J. Wang, Z. L. Xu, H. G. Jin, G. h. Shi and C. Fu, "Optimal design of district heating and cooling pipe network of seawater-source heat pump," *Energy and Buildings,* vol. 42, pp. 100-104, 2010.

[40] S. Barberis, M. Rivarolol, A. Traverso and A. Massardo, "Thermo-economic analysis of the energy storage role in a real polygenerative district," *Journal of energy storage,* vol. 5, pp. 187-202, 2016.

[41] J. Zeng, J. Han and G. Zhang, "Diameter optimization of district heating and cooling piping network based on hourly load," *Applied Thermal Engineering,* vol. 107, pp. 750-757, 2016.

[42] R. Evins, "A review of computational optimisation methods applied to sustainable building design," *Renewable and Sustainable Energy Reviews,* vol. 22, pp. 230-245, 2013.

[43] W. M. Amutha and V. Rajini, "Cost benefit and technical analysis of rural electrification alternatives in southern India using HOMER," *Renewable and Sustainable Energy Reviews,* vol. 62, pp. 236-246, 2016.

[44] T. Maatallah, N. Ghodhbane and S. B. Nasrallah, "Assessment viability for hybrid energy system (PV/wind/diesel) with storage in the northernmost city in Africa, Bizerte, Tunisia," *Renewable and Sustainable Energy Reviews,* vol. 59, pp. 1639-1652, 2016.

[45] M. Sameti and M. A. Jokar, "Numerical modelling and optimization of the finite-length overhang for passive solar space heating," *Intelligent Buildings International,* vol. Article in Press, pp. 1-20, 2016.

[46] S. S. Bahari, M. Sameti, M. H. Ahmadi and M. S. Haghgooyan, "Optimisation of a combined Stirling cycle–organic Rankine cycle using a genetic algorithm," *International Journal of Ambient Energy,* vol. 37, no. 4, pp. 398-402, 2016.

[47] L. Li, H. Mu, N. Li and M. Li, "Economic and environmental optimization for distributed energy resource systems coupled with district energy networks," *Energy,* vol. 109, pp. 947-960, 2016.

[48] Q. Wu, R. Hongbo, J. Ren and W. Gao, "Multi-objective optimization of a distributed energy network integrated with heating interchange," *Energy,* vol. 109, pp. 353-364, 2016.

[49] I. Y. Kim and O. L. De Weck, "Adaptive weighted sum method for multiobjective optimization: a new method for Pareto front generation," *Structural and multidisciplinary optimization,* vol. 31, no. 2, pp. 105-116, 2006.

[50] V. Machairas, A. Tsangrassoulis and K. Axarli, "Algorithms for optimization of building design: A review," *Renewable and sustainable energy reviews,* vol. 31, pp. 101-112, 2014.

[51] G. Chicco and P. Mancarella, "Distributed multi-generation: A comprehensive view," *Renewable and sustainable energy reviews,* vol. 13, pp. 535-551, 2009.

[52] D. Buoro, P. Pinamonti and M. Reini, "Optimization of a Distributed Cogeneration System with solar district heating.," *Applied Energy,* vol. 124, pp. 298-308, 2014.

[53] B. Bach, J. Werling, T. Ommen, M. Münster, J. M. Morales and B. Elmegaard, "Integration of large-scale heat pumps in the district heating systems of Greater Copenhagen," *Energy,* vol. 107, pp. 321-334, 2016.

[54] H. Gopalakrishnan and D. Kosanovic, "Economic optimization of combined cycle district heating systems," *Sustainable Energy Technologies and Assessments ,* vol. 7, pp. 91-100, 2014.

[55] K. Sartor, S. Quoilin and P. Dewallef, "Simulation and optimization of a CHP biomass plant and district heating network," *Applied Energy,* p. Article in Press, 2014.

[56] H. Wang, W. Yin, E. Abdollahi, R. Lahdelma and W. Jiao, "Modelling and optimization of CHP based district heating system with renewable energy production and energy storage," *Applied Energy,* vol. 159, pp. 401-421, 2015.

[57] A. D. Ondeck, T. F. Edgar and M. Baldea, "Optimal operation of a residential district-level combined photovoltaic/natural gas power and cooling system," *Applied Energy,* vol. 156, pp. 593-606, 2015.

[58] C. Weber and N. Shah, "Optimisation based design of a district energy system for an eco-town in the United Kingdom," *Energy,* vol. 36, pp. 1292-1308, 2011.

[59] J. Pirkandi, M. A. Jokar, M. Sameti and A. Kasaeian, "Simulation and multi-objective optimization of a combined heat and power (CHP) system integrated with low-energy buildings," *Journal of Building Engineering,* vol. 5, pp. 13-23, 2016.

[60] M. Uris, J. I. Linares and E. Arenas, "Size optimization of a biomass-fired cogeneration plant CHP/CCHP (Combined heat and power/Combined heat, cooling and power) based on Organic Rankine Cycle for a district network in Spain," *Energy,* vol. Article in Press, pp. 1-11, 2015.

[61] M. Noussan, G. C. Abdin, A. Poggio and R. Roberto, "Biomass-fired CHP and heat storage system simulations in existing district heating systems," *Applied Thermal Engineering,* vol. 71, pp. 729-735, 2014.

[62] E. D. Mehleri, H. Sarimvais, N. C. Markatos and L. G. Papageorgiou, "A mathematical programming approach for optimal design of distributed energy systems at the neighbourhood level," *Energy,* vol. 44, pp. 96-104, 2012.

[63] C. Bordin, A. Gordini and D. Vigo, "An optimization approach for district heating strategic network design," *European Journal of Operational Research,* vol. 252, pp. 296-307, 2016.

[64] M. Ameri and Z. Besharati, "Optimal design and operation of district heating and cooling networks with CCHP systems in a residential complex," *Energy and Buildings,* vol. 110, pp. 135-148, 2016.

[65] M. Rivarolo, A. Cuneo, A. Traverso and A. F. Massardo, "Design optimization of smart poly-generation energy districts through a model based approach," *Applied Thermal Engineering,* vol. 99, pp. 291-301, 2016.

[66] I. Karschin and J. Geldermann, "Efficient cogeneration and district heating systems in bioenergy villages: an optimization approach," *Journal of Cleaner Production,* vol. 104, pp. 305-314, 2015.

[67] M. Vesterlund and J. Dahl, "A method for the simulation and optimization of district heating systems with meshed networks," *Energy conversion and management,* vol. 89, pp. 555-567, 2015.

[68] H. Wang, E. Abdollahi, R. Lahdelma, W. Jiao and Z. Zhou, "Modelling and optimization of the smart hybrid renewable energy for communities (SHREC)," *Renewable Energy,* vol. 84, pp. 114-123, 2015.

[69] E. Carpaneto, P. Lazzeroni and M. Repetto, "Optimal integration of solar energy in a district heating network," *Renewable Energy,* vol. 75, pp. 714-721, 2015.

[70] W. Wang, X. Cheng and X. Liang, "Optimization modeling of district heating networks and calculation by the Newton method," *Applied Thermal Engineering,* vol. 61, pp. 163-170, 2013.

[71] R. Khir and M. Haouari, "Optimization models for a single-plant District Cooling System," *European Journal of Operational Research,* vol. 247, pp. 648-658, 2015.

[72] Z. Zhou, P. Liu, Z. Li, E. N. Pistikopoulos and M. C. Georgiadis, "Impacts of equipment off-design characteristics on the optimal design and operation of combined cooling, heating and power systems," *Computers and Chemical Engineering,* vol. 48, pp. 40-47, 2013.

[73] J. S. K. Kody M Powell and K. K. J. L. M. J. D. H. a. T. F. E. Wesley J. Cole, "Thermal energy storage to minimize cost and improve efficiency of a polygeneration district energy system in a real-time electricity market," *Energy,* vol. 113, pp. 52-63, 2016.

[74] P. Jie, N. Zhu and D. Li, "Operation optimization of existing district heating systems," *Applied themal engineering,* vol. 78, pp. 278-288, 2015.

[75] X. Jiang, Z. Jing, Y. Li, Q. Wu and W. Tang, "Modelling and operation optimization of an integrated energy based direct district water-heating system," *Energy,* vol. 64, pp. 375-388, 2014.

[76] H. Ren, Q. Wu, W. Gao and W. Zhou, "Optimal operation of a grid-connected hybrid PV/fuel cell/battery energy system for residential applications," *Energy,* vol. 113, pp. 702-712, 2016.

[77] U. S. Kim, T. C. Park, L.-H. Kim and Y. K. Yeo, "Optimal operation of the integrated district heating system with multiple regional branches," *Korean Journal Chemical Engineering,* vol. 27, no. 1, pp. 6-18, 2010.

[78] P. Jie, X. Kong, X. Rong and S. Xie, "Selecting the optimum pressure drop per unit length of district heating piping network based on operating strategies," *Applied Energy,* vol. 177, pp. 341-353, 2016.

[79] J. Wang, Z. Zhou and J. Zhao, "A method for the steady-state thermal simulation of district heating systems and model parameters calibration," *Energy Conversion and Management,* vol. 120, pp. 294-305, 2016.

[80] N. A. Diangelakis, C. Panos and E. N. Pistikopoulos, "Design optimization of an internal combustion engine powered CHP system for residential scale application," *Computer Management Science,* vol. 11, pp. 237-266, 2014.

[81] K. Gaiser and S. Pieter, "The impact of scheduling appliances and rate structure on bill savings for net-zero energy communities: Application to West Village.," *Applied Energy,* vol. 113, pp. 1586-1595, 2014.

[82] K. Zhang, R. Thomas, M. Bohm and M. Miller, " An integrated Design approach for sustainable community development," in *Proceedings of the 42nd Hawaii International Conference on System Sciences, IEEE*, 2009.

[83] E. Provata, D. Kolokotsa, S. Papantoniou, M. Pietrini, A. Giovannelli and G. Romiti, "Development of optimization algorithms for the Leaf Community microgrid," *Renewable Energy ,* vol. 74 , pp. 782-795, 2015.

[84] F. A. Mohamed and H. N. Koivo., "Online management genetic algorithms of microgrid for residential application," *Energy Conversion and Management ,* vol. 64, pp. 562-568, 2012.

[85] G. Kyriakarakos, A. Dounis, K. Arvanitis and G. Papadakis, "A fuzzy logic energy management system for polygeneration microgrids," *Renewablw /energy,* vol. 41, pp. 315-327, 2012.

[86] J. Rawlings, P. Coker, J. Doak and B. Burfoot, "Do smart grids offer a new incentive for SME carbon reduction?," *Sustainable Cities and Society,* vol. 10, pp. 245-250, 2014.

[87] A. Fragaki, A. N. Andersen and D. Toke, "UK, Exploration of economical sizing of gas engine and thermal store for combined heat and power plants in the," *Energy,* vol. 33, no. 11, pp. 1659-1670, 2008 .

[88] N. Ouhajjou, W. L. S. Fenz and A. M. Tjoa, "Stakeholder-oriented Energy Planning Support in Cities," *Energy Procedia,* vol. 78, pp. 1841-1846, 2015.

[89] K. Vijeta and D. S. S. Sarma, "Protection of distributed generation connected distribution system.," in *In Advances in Power Conversion and Energy Technologies (APCET), International Conference on IEEE.*, 2012.

[90] M. Sameti, "Low-cost building integrated renewables through general algebraic modelling system," *International Journal of Renewable Energy Research,* vol. 4, no. 3, pp. 777-783, 2014.

[91] M. Sameti and A. Kasaeian, "Numerical simulation of combined solar passive heating and radiative cooling for a building," *Building Simulation,* vol. 8, no. 3, pp. 239-253, 2015.

[92] M. Sameti and F. Haghighat, "Integration of distributed energy storage into net-zero energy district systems: Optimum design and operation," *Energy,* vol. 153, pp. 575-591, 2018.

[93] "Suurstoffi ditrict energy system," [Online]. Available: https://www.suurstoffi.ch/gewerbeangebot/angebote/. [Accessed 10 10 2017].

[94] C. Milan, C. Bojesen and M. P. Nielsen, "A cost optimization model for 100% renewable residential energy supply systems," *Energy,* vol. 48, no. 1, pp. 118-127, 2012.

[95] V. Kuhn, J. Klemes and I. Bulatov, "MicroCHP: Overview of selected technologies, products and field test results," *Applied Thermal Engineering,* vol. 28, pp. 2039-2048, 2008.

[96] "Renewable Power Generation Costs in 2017," IRENA: International Renewable Energy Agency, Abu Dhabi, 2018.

[97] Q. Wu, H. Ren and W. Gao, "Economic Assessment of Micro-CHP System for Residential Application in Shanghai, China," Energy Procedia, 732-737, 2016.

[98] M. Sameti and F. Haghighat, "A two-level multi-objective optimization for simultaneous design and scheduling of a district energy system," *Applied Energy,* p. Article in Press, 2017.

[99] "https://www.confusedaboutenergy.co.uk/," [Online].

[100] K. M. Miettinen, Nonlinear multiobjective optimization, Kluwer Academic, 1998.

[101] S. Obara, "Equipment arrangement planning of a fuel cell energy network optimised for cost minimisation," *Renewable Energy ,* vol. 32, pp. 382-406, 2007.

[102] Z. Zhou, P. Liu, Z. Li, E. N. Pistikopoulos and M. C. Georgiadis, "Impacts of equipment off-design characteristics on the optimal design and operation of combined cooling, heating and power systems," *Computers and Chemical Engineering,* vol. 48, pp. 40-47, 2013.

[103] H. Ren, W. Gao and Y. Ruan, "Economic optimisation and sensitivity analysis of photovoltaic system in residential buildings.," *Renewable Energy ,* vol. 34, pp. 883-889, 2009.

[104] I. Staffell, "Purchase cost of condensing boilers in the UK," 2008.

[105] M. De Paepe, P. D'Herdt and D. Mertens, "Micro-CHP systems for residential applications," *Energy Conversion and Management ,* vol. 47, pp. 3435-3446, 2006.

[106] M. Sameti and F. Haghighat, "4th generation decentralized district energy system: development of an optimization model for design and planning," *Renewable Energy,* vol. 130, pp. 371-387, 2018.

[107] "https://www.suurstoffi.ch," [Online].

[108] R. M. Lazzarin and M. Noro, "Past, present, future of solar cooling: Technical and economical considerations," *Solar Energy,* p. https://doi.org/10.1016/j.solener.2017.12.055, Article in Press.